6-2014

A Physical and Mineralogical Analysis of Late Holocene Sand Deposits: A Case Study of Little Ice Age Coastal Change in the Shetland Islands, UK

Christopher Trent Halsted

A Physical and Mineralogical Analysis of Late Holocene Sand Deposits: A Case Study of Little Ice Age Coastal Change in the Shetland Islands, UK

Bates College Geology Department Thesis

Presented to the Faculty of the Department of Geology, Bates College,

in partial fulfillment of the requirements for the Degree of Bachelor of Science

by

Christopher Trent Halsted

Lewiston, Maine
April 7, 2014

Abstract

Late Holocene climate fluctuations resulted in pronounced coastal change across the North Atlantic. The transition between the stable Medieval Warm Period and the stormy Little Ice Age was associated with an increased north-south thermal gradient that led to a southward displacement of the polar atmospheric front and polar waters. The increased frequency and intensity of storms during the LIA resulted in inland sand transgressions that displaced communities across Europe and altered coastlines in the process.

A case study of this coastal change can be observed in the southern Shetland Islands, where extensive, thick deposits of sand stretch far inland. Within these sands are the buried remains of the township of Broo, which was abandoned in the midst of total inundation in the mid-18th century (Bigelow et al. 2005). The nearby Loch of Brow contains a distinctive, fine sand unit that has been hypothesized to be a result of the sand invasion event(s) that buried the township of Broo. Also within the study area are the Bay of Scousburgh and the Loch of Spiggie. 17th century maps show an inlet connecting the Loch of Spiggie to the ocean through the Bay of Scousburgh, but presently there is a low-lying land bridge separating the two. It has been hypothesized that the land bridge, as well as a sand unit found in the Loch of Spiggie, were created during a period of intense storminess within the LIA.

In order to test the hypotheses presented, sand samples were collected from around the study area and subjected to x-ray diffraction, grain size analysis, and grain surface morphology. XRD results established a mineralogic relationship between the Loch of Spiggie and the Bay of Scousburgh. These sites shared peaks in their diffractions that were missing in the Quendale sites and the Loch of Brow, simultaneously establishing a potential relationship between these sites as well. A trend of decreasing grain size and increasing sorting was observed between the Bay of Quendale and the Loch of Brow, suggesting a fining of sediment through aeolian transportation. This trend was not observed between the Bay of Scousburgh and the Loch of Spiggie, suggesting a more powerful transport mechanism. The grain surface morphology observations revealed that the sediment in the Loch of Brow had been in aeolian transportation for a long time before being subjected to a more forceful storm that carried it to its current location. At the Broo archaeological site, grains underneath thin organic horizons exhibited silica dissolution and precipitation, suggesting that the inundation of the site occurred in stages, with a strong storm depositing sand and a subsequent stable period enabling the growth of surface vegetation. Grains from the Loch of Spiggie showed textures associated with powerful subaqueous transportation. Together with the grain size analysis results, the sand unit in the loch appears to have been deposited as washover during a high-magnitude storm. This same sand invasion event appears to have created the land bridge that currently separates the Loch of Spiggie from the Bay of Scousburgh.

Acknowledgments

I have many people to thank for this opportunity and the final product that has resulted from it. There is no better place to start than with my advisor Mike Retelle. Mike introduced me to this project, and believed in me enough to suggest that I attempt to become a part of it. His advice, critiques, and assitance during this long process was invaluable, and through it all he displayed a patience the likes of which I have never witnessed before. Despite the pressures of being a department chair, Mike always found the time to sit down and talk about results, interpretations, or the Bruins. After working with him this year, I can say with the upmost confidence that Mike is most certainly not weak, nor a quitter.

I would also like to give a special thank you to Gerry Bigelow, without whom this research would not have been possible. My time working on the Shetland Islands Climate and Settlement Project has been one of the most memorable experiences of my life, and I cannot thank you enough for trusting me to take part in this endeavor. Every moment in Shetland was memorable; from the first day when you took me to the windiest spot in the area so I wouldn't fall asleep due to jetlag to our experience microwaving meals for almost a week straight. I wish you the best of luck in the continuation of this project.

I want to give a big thank you to everybody in the geology department here at Bates. In particular I want to thank John Creasy, who spent a lot of time during his last year as a professor helping me interpret and work through XRD and diffractograms. Bev, Dyk, Gene, and Alice, thank you so much for your support, critiques, and suggestions during our thesis meetings. Your interest and knowledge was invaluable during this process. Although not officially part of the geo department, I also want to thank Matt Duvall and Will Ash of the Bates College Imaging Center for their assistance and support.

I owe so much to my fellow geology seniors. What other questionably healthy young adults would stay up in Coram into the wee hours or take a serious interest into my research? Josh, Allie, Cam, other Cam, Saebyul, Sula, Tanner, Alec, Andrea, Megan, Sarah, and, of course, Ashley, you guys are the best. Watching the progression of your theses gave me more encouragement than you could possibly know, and I honestly can't put into words how grateful I am to have gone through this process with all of you.

Finally, I want to thank my friends and family. Although the majority of them contributed precisely nothing to the overall product, I could not have completed this thesis without my housemates. Through hiking trips, skiing, and aggressive MarioKart, you guys were the greatest stress relief I could have ever hoped for. To my family, I love you, and without you I would never have had the opportunity to participate in such an extraordinary project. Your support means the world to me, and I know you will be there for me in the coming years.

This study was made possible by the Bates College Department of Geology and funding from the National Science Foundation and the Bates College Student Research Fund.

Contents

Table of Figures

Introduction

1.1: Study Location and Previous Work

The Shetland Islands are the northernmost landmasses in the UK, forming an island archipelago that crosses the 60°N latitudinal line (Figure 1). The islands' narrow shapes and oceanic setting mean that all areas experience classic maritime climate, including suppressed seasonality. Shetland is located at the junction of the North Sea, the Norwegian Sea and the Atlantic Ocean. Its proximity to marine and atmospheric polar fronts causes the Shetland region to be very climatically sensitive (Birnie 1993). Its oceanic climate and high latitude means that Shetland has the highest monthly figures for humidity and the fewest hours of annual sunshine in Britain, leading to a short growing season (Birnie 1993).

Figure 1: The location of the Shetland Islands in relation to mainland UK, Scandinavia, and Iceland

Despite the hardships associated with living in Shetland, widespread evidence holds that the archipelago has been inhabited since at least the Neolithic period, with farming and herding settlements existing between 5000-4000 B.P. (years before present) (Bigelow et al. 2005). Due to the short growing season and oceanic climate, inhabitants of Shetland have always lived in a constant struggle against their local environment. The Shetland Islands Climate and Settlement Project (SICSP), a National Science Foundation-funded, multi-disciplinary project, is aimed at defining past, abrupt environmental changes and the subsequent human responses. The Quendale area was selected for SICSP research due to its large expanse of coastal sands, the largest in Shetland. It is known that a large township consisting of multiple farms was inundated by eolian sand in this location in the later seventeenth century A.D. (Bigelow et al. 2005). The township, called Broo, was owned by a branch of the Sinclair family and was one of the single most valuable properties in all of Shetland prior to its burial.

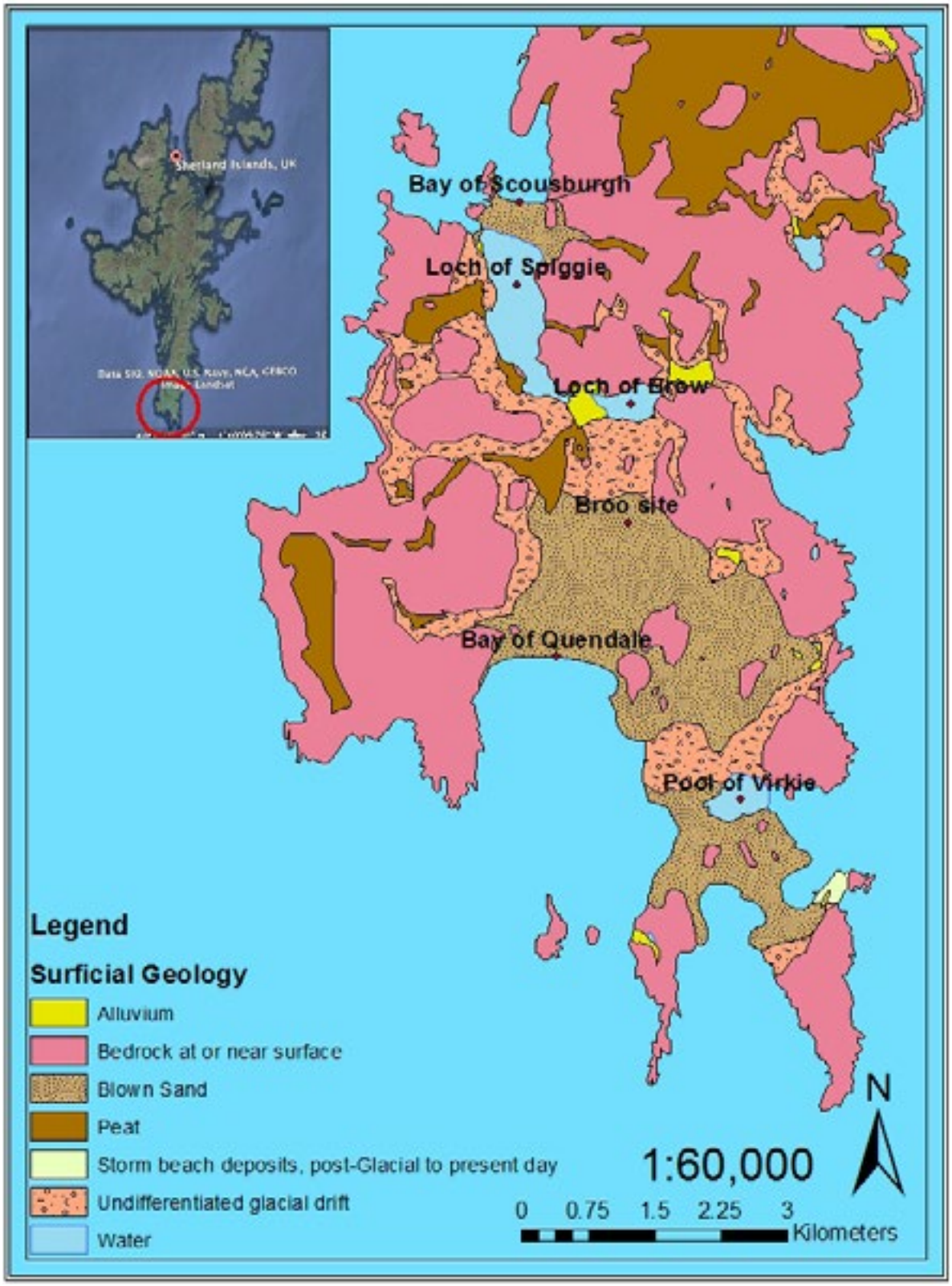

Figure 2: Surficial geology of the study area (Modified from Johnstone, 1978). The areas of focus in this study are labeled. In this study, the Quendale area refers to the area stretching from the Bay of Quendale north to the Loch of Brow while the Spiggie area stretches from the Bay of Scousburgh south the the Loch of Brow.

Historical records show that movements of sand onto the Broo lands began in the 1660s, and by the 1730s the lands no longer retained their taxable value or fertility (Bigelow et al. 2005). This inundation is just one example of sudden coastal sand blow events that have been recorded in this area of Shetland. The nearby Loch of Spiggie (Figure 2) hint at another such event. It appears to have once been connected by an inlet to the Bay of Scousburgh, but a low-lying sand bar now separates them.

Late Holocene coastal change is not unique to Shetland. Pronounced coastal change across the North Atlantic characterized the period from the mid-15th century to the mid-19th century, a period commonly referred to as the Little Ice Age (Clarke et al. 2002, Dawson et al. 2011, Lamb 1985, Lamb 1995). Sea-salt concentration studies performed on the GISP2 core from the Greenland ice sheet show a clear upwards shift around 1450 AD (Figure 3, Dawson et al. 2011). A proxy for storminess, the sea-salt concentration pattern indicates a transition from a more mild period known as the Medieval Warm Period to the stormy Little Ice Age. Despite their titles, the principle difference between the MWP and the LIA is not a marked change in temperature, but a difference in the atmospheric circulation of the northern hemisphere. Lamb (1985) argued that the transition between the MWP and the LIA was associated with an increased north-south thermal gradient across the North Atlantic. This led to a southward displacement of both the polar atmospheric front and polar waters. Lamb further explains that this displacement would provide a basis for severe storms not likely to be experienced during warmer climatic periods.

Examples of LIA coastal changes can be found across the North Atlantic. Dawson et al. (2011) describe increased winter storminess in the British Isles after AD 1420 that resulted in pronounced inland beach sediment transgressions. Dawson et al. (2011) also go over conclusions from Gilbertson et al. (1999) and Orford et

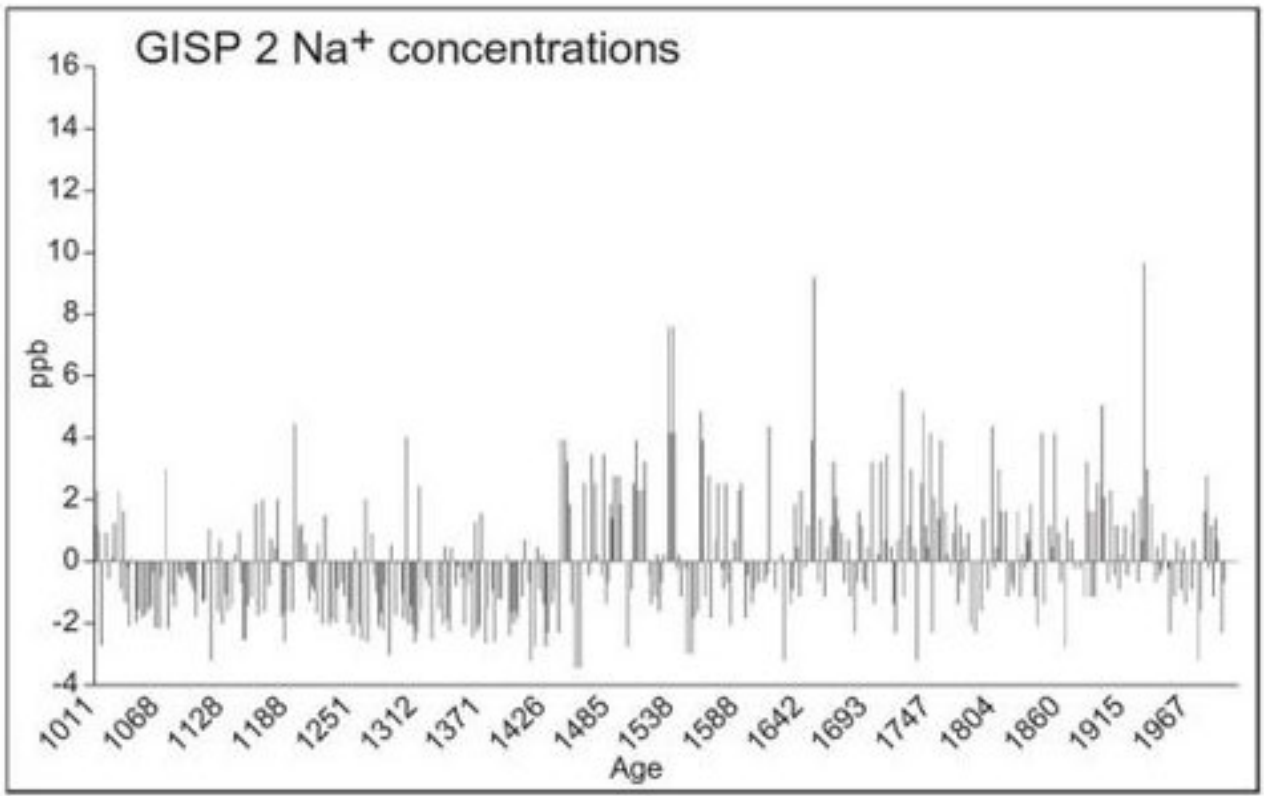

Figure 3: Sea-salt (Na^+) concentrations with relation to age from the GISP2 ice core, retrieved from the Greenland Ice Sheet (from Dawson et al. 2011).

al. (2000) describing LIA phases of sand movement in the Outer Hebrides and eastern England, respectively. Clarke et al. (2002) showed that the period from 1480 to 1750 AD was marked by accretion and reworking of sand bodies on the Aquitaine Coast in southwest France. North Atlantic coastal change has become associated with the Little Ice Age, and the Shetland Islands appear to be a case study of this change.

To research the historic sand movements in Shetland, an interdisciplinary team of SICSP project members, including researchers from Bates College, the University of Maine at Orono, the University of Southern Maine, the City University of New York, the University of Sterling, the University of Edinburgh, the University of Bradford, and the University of Glasgow, have employed a variety of techniques to gather data from the Sumburgh, Spiggie, and Quendale areas (all areas shown in Figure 2).

Alice Kelly, Joe Kelly, and Lee Sorrell from the University of Maine collected ground penetrating radar (GPR) profiles in 2011 using a low frequency (100 MHz) device. The GPR recorded stratigraphic profiles in the coastal dunes of the Quendale Links (Figure 2) and revealed significant dune morphology differences throughout the study site (Sorrell 2013). The following year, the same group obtained samples for Optically Stimulated Luminescence (OSL) dating. Their samples were taken from the base and top of the back side of the frontal dune at the Bay of Quendale. When excavating the frontal dune, the group "found barbed wire 1.5m below the surface. As barbed wire has been in use for only 145 years, this suggests that this part of the beach has rapidly accreted and has been active recently" (Sorrell 2013). Because this field work was done only last year, the results of the OSL dating have not been released yet. Further GPR work was done during the 2012 field season, including an investigation into the buried inlet that may have connected the Loch of Spiggie to the ocean (Sorrell 2013).

During the same field season (2012), a University of Southern Maine research team surveyed the dunes of the area using LiDAR in order to identify more structures that may be buried in the sand. David Sanderson, from the Scottish Universities Environmental Research Centre, and Gerald Bigelow collected OSL samples from the archaeological site in order to date the sand deposition events that occurred at the Broo township (Sorrell 2013). These OSL dates were recently processed and constrain the deposition of sand at the Broo site to a period between the mid-16th century and the mid-18th century (Kinnaird et al., 2014). 14th century sand was dated below the flagstones of the settlement, but the only significant accumulation to occur during the occupation of the site began in the mid-16th century. The sand used to obtain this date was sampled directly above the flagstones, marking the beginning of the sand blows during occupation. Paleoenvironmental data collected from the Lochs of Spiggie and Brow come in the form of sediment cores extracted by Jennifer Lindelof and Professors Michael Retelle and Beverly Johnson of Bates College. Both the Loch of Spiggie and Brow contain distinctive fine sand units of variable thickness located at approximately 15cm depth. In addition to these geomorphologic and sedimentary data collection methods, students and researchers from Bates College have been conducting an archaeological excavation of the Broo site itself for several years through college-sponsored academic trips.

1.2: Geologic Setting

The bedrock geology for the project study area can be seen in Figure 4. The general geologic history for this area begins with the deposition and metamorphism of a precambrian metasedimentary base of the Clift Hills Division, formed in the Scottish Caledonides of the Caledonian orogeny. The Spiggie intrusive complex, a coarse-grained, acid igneous formation, intruded between the Silurian and Devonian, covering the entire study area except for Fitful Head (Figure 4). A quartzite sandstone unit commonly called the Old Red Sandstone was then laid down unconformably on this granite intrusion on the eastern side of the Quendale/Dunrossness region (Figure 4) (Brown 1984b, Mykura et al. 1976). Detailed descriptions of the bedrock units follow.

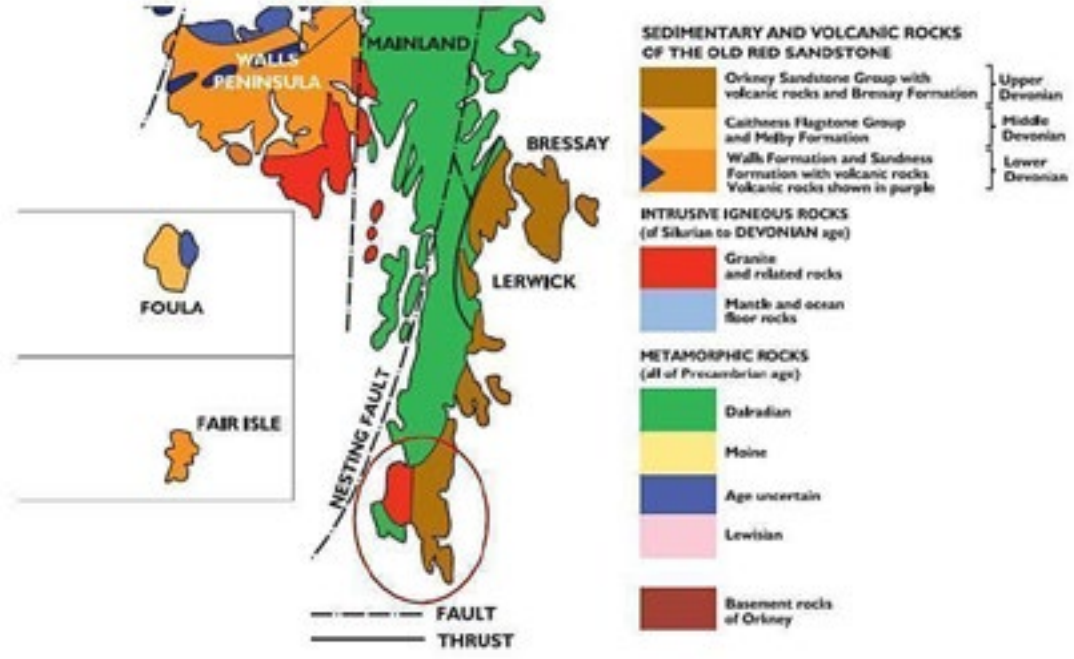

Figure 4: Simplified bedrock map of the southern Mainland (Modified from McKirdy, 2010). The study area is circled in red.

Clift Hills Division (Part of the Dalradian metamorphic group)

Fitful Head (green peninsula in the study area in Figure 4) is the only location within the study area where Precambrian metasedimentary bedrock is exposed. The majority of the Fitful Head peninsula belongs to the Dunrossness Phyllitic Group, which is a part of the Clift Hills Division. The phyllites in this group are uniform in texture and composition and are characterised by abundant muscovite, chlorite and chloritoid (Mykura et al. 1976). The closely related Dunrossness Spilitic Group crops out on the western cliffs of Fitful Head. This group contains metamorphosed lavas and pyroclastic rocks with the original textures well preserved (Mykura et al. 1976). These units were formed in the Caledonian Orogeny, which occurred from the Ordovician to the early Devonian, roughly 490-390 mya.

The Spiggie Intrusive Complex

The western side of the study area (Figure 4), which includes the Loch of Spiggie and the Bay of Scousburgh, is composed of a coarse-grained acid igneous intrusion of Silurian to Devonian age called the Spiggie Intrusive Complex (Brown 1984b). This complex consists mostly of granodiorite and porphyritic ademellite. Monzonite, pyroxenite and serpentine are also present, but in limited localities. The order of intrusion for this complex is as follows: 1. Ultrabasic rocks, 2. Monzonite and related rocks, 3. Granodiorite and porphyritic adamellite (Mykura et al. 1976). In the study area, the only ultrabasic rock present is a 350m wide serpentinite band along the margin of the complex at Scousburgh. The monzonite and related rocks in the study area consist of monzonite outcrops alongside the serpentinite at Scousburgh and strips of hornblende-rich rock at the edge of the complex at Quendale. The rest of the Spiggie area is made up of granodiorite and porphyritic adamellite (Mykura et al. 1976).

At its contact with the Dunrossness Phyllitic Group, the Spiggie Intrusive Complex displays extensive contact metamorphism effects. At Scousburgh, newly formed minerals include garnet, andalusite, sillimanite, kyanite, chloritoid and staurolite (Mykura et al. 1976). Mykura et al. (1976) suggested that the thermal metamorphism in this area took place in at least two stages separated by a period of deformation during which a strain-slip cleavage developed.

Old Red Sandstone

On the eastern side of the study area, quartzite sandstone unconformably rests on the Spiggie Intrusive Complex (Figure 4) (Mykura et al. 1976). This sandstone, commonly called the Old Red Sandstone, contains clasts of volcanic rocks and have been dated to the high Middle Devonian. Mykura et al. (1976) interpreted the Old Red Sandstone as a number of lithological facies which interdigitate with each other. They further explain that the sandstone was likely laid down on an east-south-east sloping bed. The exposed sequences, which can be seen at Sumburgh Head, consist of cross-bedded sandstones with thin bands of sun-cracked siltstone and mudstone. Interbedded with these are fairly thin but widespread lenses of conglomerate (Mykura et al. 1976).

1.3: Quaternary History of Shetland

Glacial History:

The glacial history of Shetland has been reconstructed primarily from striae observations along with interpretations of stoss and lee features on ice-moulded bedrock. Provenance studies of surface erratics and the clastic components of glacial diamects were additionally compiled in order to form a more complete picture. Mykura (1976) stated that Shetland must have been covered by ice during every glacial maxima of the Pleistocene, but that the majority of the glacial deposits present today are attributed to the last (Devensian) glacial episode. Despite the availability of glacial indicators, the exact Devensian glaciation pattern in Shetland is debated.

Peach and Horne (1879) suggested an initial glaciation involving ice from Scandinavia flowing over Shetland from the northeast. This ice experienced diversion to the northwest by a confluent Scottish ice sheet (Figure 5a). During deglaciation, a local ice cap was established that flowed radially off the land (Birnie 1993). Mykura (1976) has stated that this ice-flow model has not been substantiated.

Hoppe (1972) agreed with Peach and Horne (1879), concluding that Shetland was overridden by a Scandinavian ice sheet during maximum Devensian glaciation (Mykura 1976). This conclusion was reached based on the fact that north-east and south-east striae can be found on Bressaay and Weisdale Hill, respectively (Figure 5b). This indicates ice movement following Peach and Horne's (1879) pattern of easterly flow deflected by a confluent Scottish ice sheet.

Flinn (1983), on the other hand, concluded that any glaciation of Shetland by Scandinavian ice must have predated the last glaciation. A radially flowing local ice cap throughout the last glaciation was the proposed model instead (Figure 5d). Flinn stated that eastern ice may have been carried across the Norwegian Sea to a position near Shetland, but it never flowed over the islands.

Mykura (1976) used these conclusions to form his own Devensian glaciation model (Figure 5c). Based on the available evidence, Mykura (1976) agreed with Flinn's concept of a local ice cap during the Devensian maximum. Mykura, though, suggested that the Scandinavian ice sheet interacted with this local ice cap, deflecting around it to the north and south (Figure 5c).

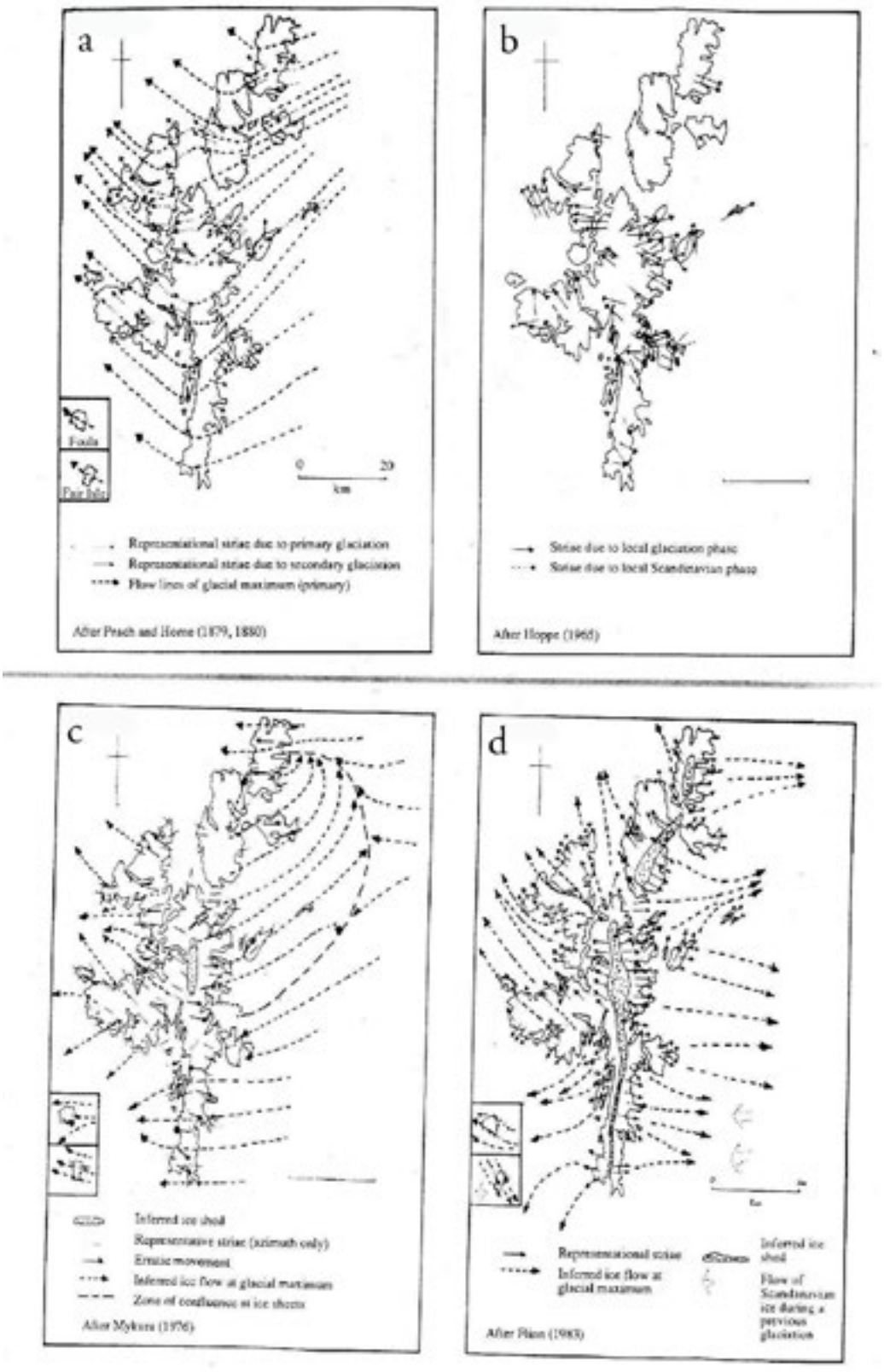

Figures 5a-d: Proposed Pleistocene glaciation models for Shetland (from Birnie 1993)

Sea Level Changes:

During the Holocene, Shetland experienced fluctuating sea levels. Submerged peat beds and the local traditions of submergence in historic times have been used to estimate the changes in sea level. Birnie (1993) suggested that Shetland initially experienced isostatic uplift associated with the decay of the Late Devensian ice mass, with relative sea level falling until 13,000 BP. Sea level then rose continuously, standing at approximately -65m at 10,000 BP, -10m at 5000 BP and reaching the present level at 3,000 BP.

Mykura (1976) described peat found at 8.9m below the current high-water mark with a 14C date ranging from 5455-6970 BP. This indicates that sea level must have been at least 9m lower than present 5500 BP.

1.4: Surficial Geology of Shetland

An overview of the surficial geology of the study area can be seen in Figure 2. Exposed or nearly exposed bedrock is present over large areas of the south Mainland, particularly at Fitful Head and around the Loch of Spiggie. Almost all of the areas close to the coast are exposed bedrock, the ocean having stripped away any overlying sediment. Extensive, thick peat deposits are found in this area, with thicker deposits occurring on Fitful Head and near the Lochs of Spiggie and Brow.

The Quendale Links, stretching upwards from the Bay of Quendale, are composed of blown sand which is covered with marram grass (Figure 6). This blown sand extends to the south and to the east, covering much of the

Figure 6: View of the Quendale Links. Photo was taken looking north from the top of the foredune backing the Bay of Quendale. The sand patch in the foreground is the result of artificial sand extraction that went towards building the nearby airport runway.

Sumburgh area (Figure 2). Blown sand is also present between the Bay of Scousburgh and the Loch of Spiggie. As there are no major rivers in Shetland, alluvial deposits are limited to a few small localities, with two of the larger deposits located right around the Loch of Brow (Johnstone 1978) (Figure 2). The remaining area within the study site is composed of undifferentiated glacial drift.

1.5: Climatology of Shetland

The Shetland Islands are narrow, with few sites more than 5km from the sea. The islands therefore have a maritime climate, with lower seasonality than one might predict and very windy conditions year round. Shetland is located at the junction of the North Sea, the Norwegian Sea and the Atlantic Ocean. The North Atlantic Current and the Shelf Edge Current pass between Shetland and the Faroe Islands (Figure 7). These currents are extremely warm and saline, tempering Shetland's climate (Bigelow et al. 2005). As previously mentioned, this oceanic climate and latitude gives Shetland the highest monthly figures for humidity and the fewest hours of annual sunshine in Britain (Birnie 1993).

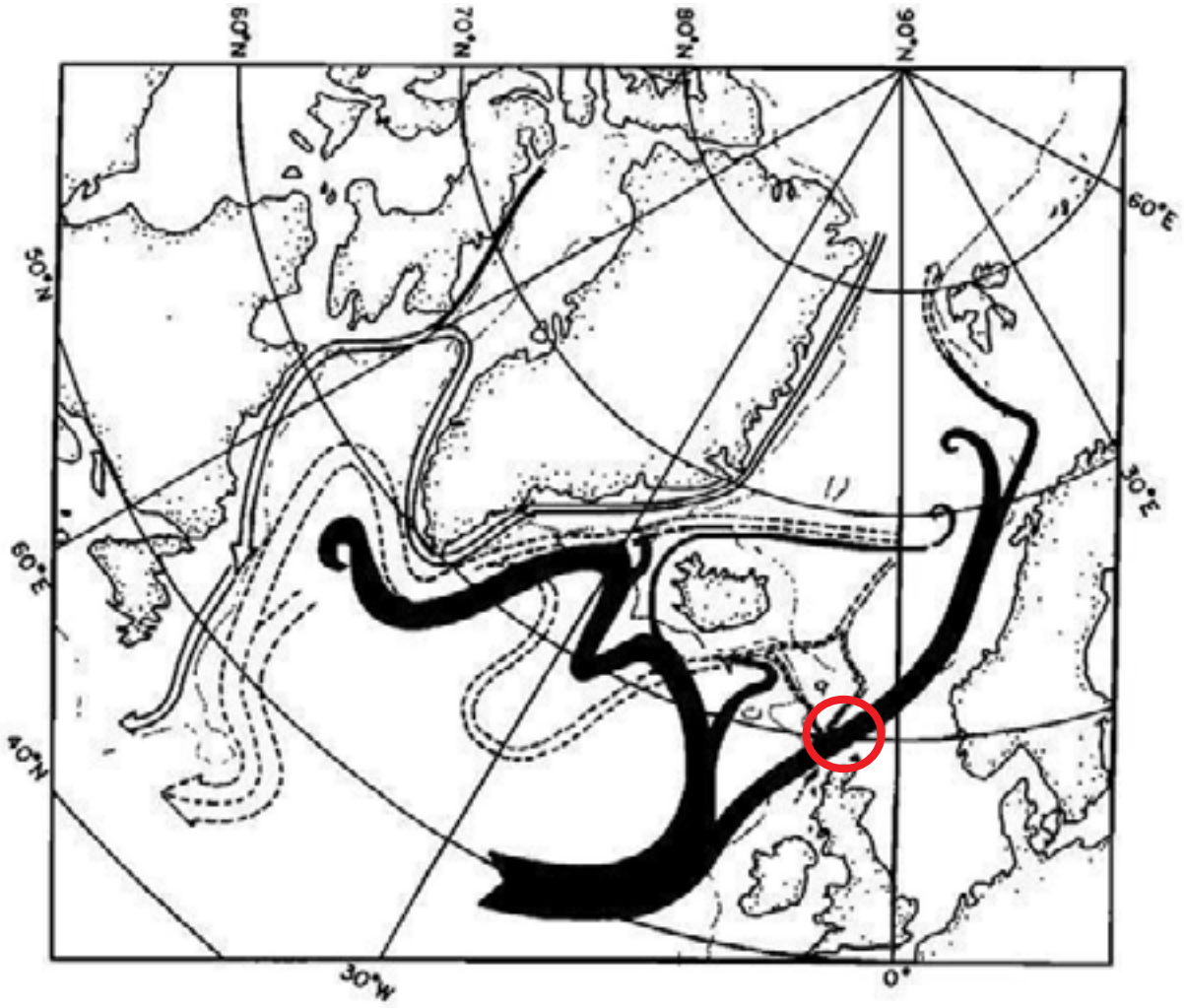

Figure 7: Dominant currents in the North Atlantic. Shetland is located in the red circle. Warm (<4°C) currents are depicted as solid black arrows, with curled ends indicating sinking. Open arrows indicate cold water currents, with light and dense overflows denoted with solid and dashed arrows, respectively (Dickson & Brown 1994)

Shetland is strongly affected by the North Atlantic Oscillation. Dawson et al. (2004) described the NAO as a 'see-saw' in winter air temperatures between Greenland and northern Europe, Shetland included. When mild winters occur in Greenland, more severe winters occur in northern Europe, and vice versa. The interannual variability of the Icelandic flow atmospheric pressure cell is responsible for this 'see-saw'. When westerly winds in the North Atlantic are weak, a blocking ridge of high pressure is created across the eastern Atlantic which results in higher air temperatures across western Greenland (Figure 8). This ridge advects cold, polar air from the Arctic across Europe.

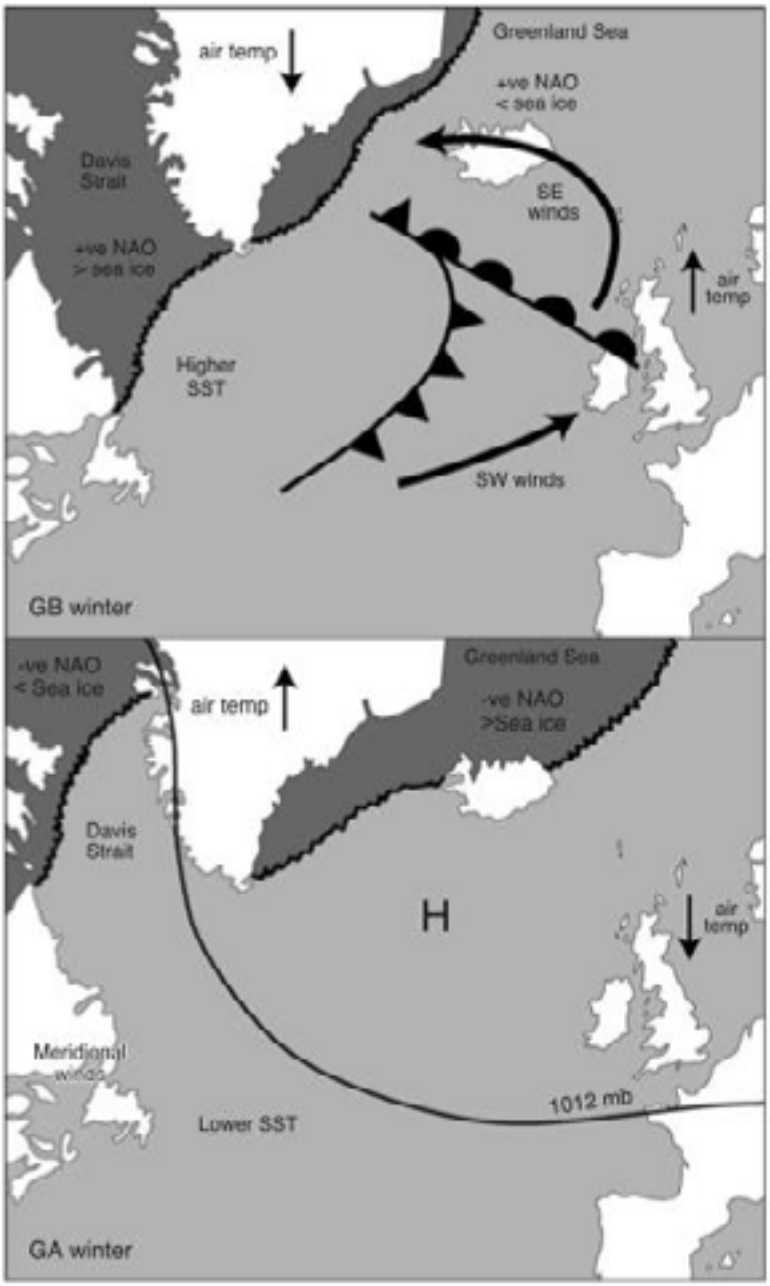

Figure 8: Schematic illustration of the North Atlantic Oscillation. Top: Positive NAO index characterized by warm winters in northern Europe and severe winters in Greenland. Bottom: Negative NAO index characterized by severe winters in northern Europe and warm winters in Greenland (Dawson et al. 2004)

When the westerly winds are strong, this ridge is absent and northern Europe receives warmer air following the Gulf Stream. Polar air from the Arctic is pushed south to Greenland and causes a more severe winter (Figure 8). This interannual variation is reflected in the NAO index, which is based on an analysis of a time series of monthly air pressure differences between Iceland, the Azores and Lisbon. Dawson et al. (2004) associated a negative NAO index with warm Greenland winters and severe northern European winters. A positive NAO index, on the other hand, produces severe Greenland winters and warm northern European winters.

Luterbacher et al. (2002) estimated the monthly (1659-present) and seasonal (1500-1658) NAO index through time using instrumental data and proxy predictors (Figure 9). They found that the NAO index swings from positive to negative frequently, with only a few periods of stability, positive or negative (observe the negative decade around 1640 and the positive decade around 1730 in Figure 9).

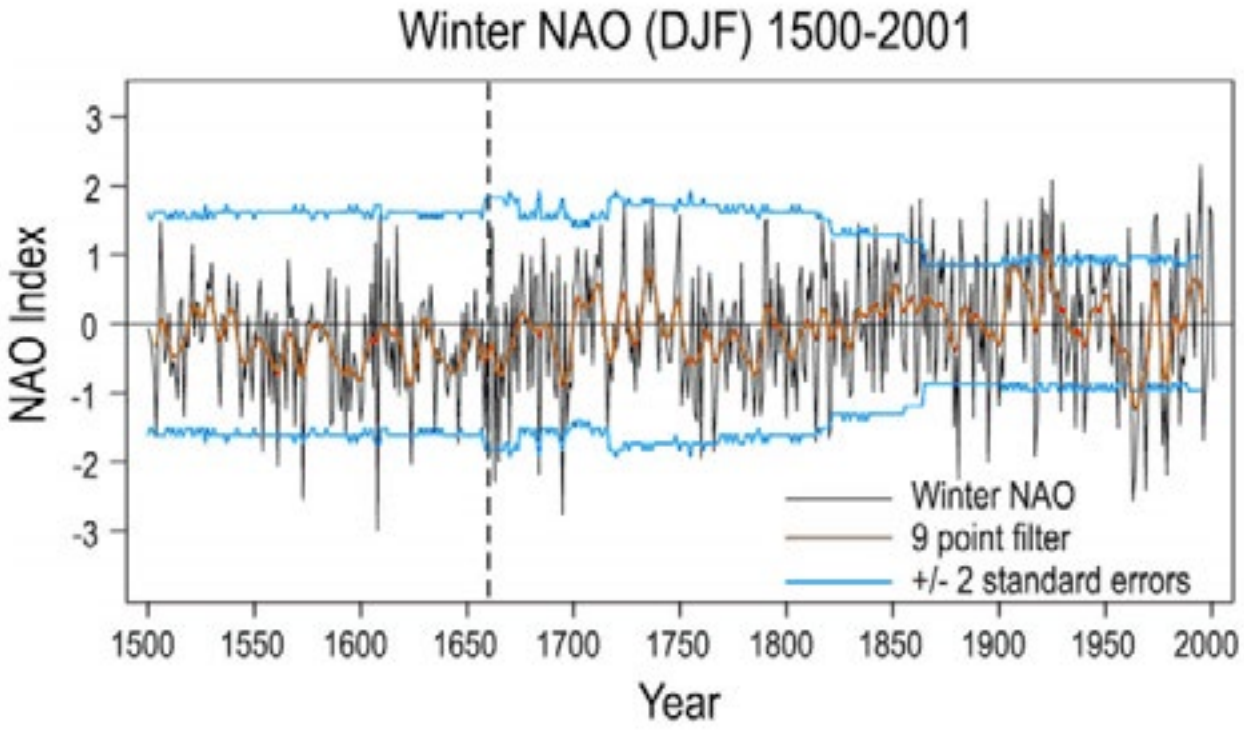

Figure 9: Winter NAO index reconstruction from 1500 - Present using instrumental data and proxy records. Luterbacher et al. (2004)

Procter et al. (2000) used annual organic matter bands on stalagmites as a proxy for annual precipitation in northern Scotland. Because stalagmite growth rate is controlled by precipitation, a large stalagmite could contain over 1000 years of high-resolution precipitation records. A banded stalagmite from a cave in NW Scotland was used to provide a 1100 year precipitation record which can be used to infer paleo-precipitation in Shetland (Figure 10) The record shows a major shift in precipitation around the 17th century, as the precipitation went from one of the lowest recorded levels to one of the highest.

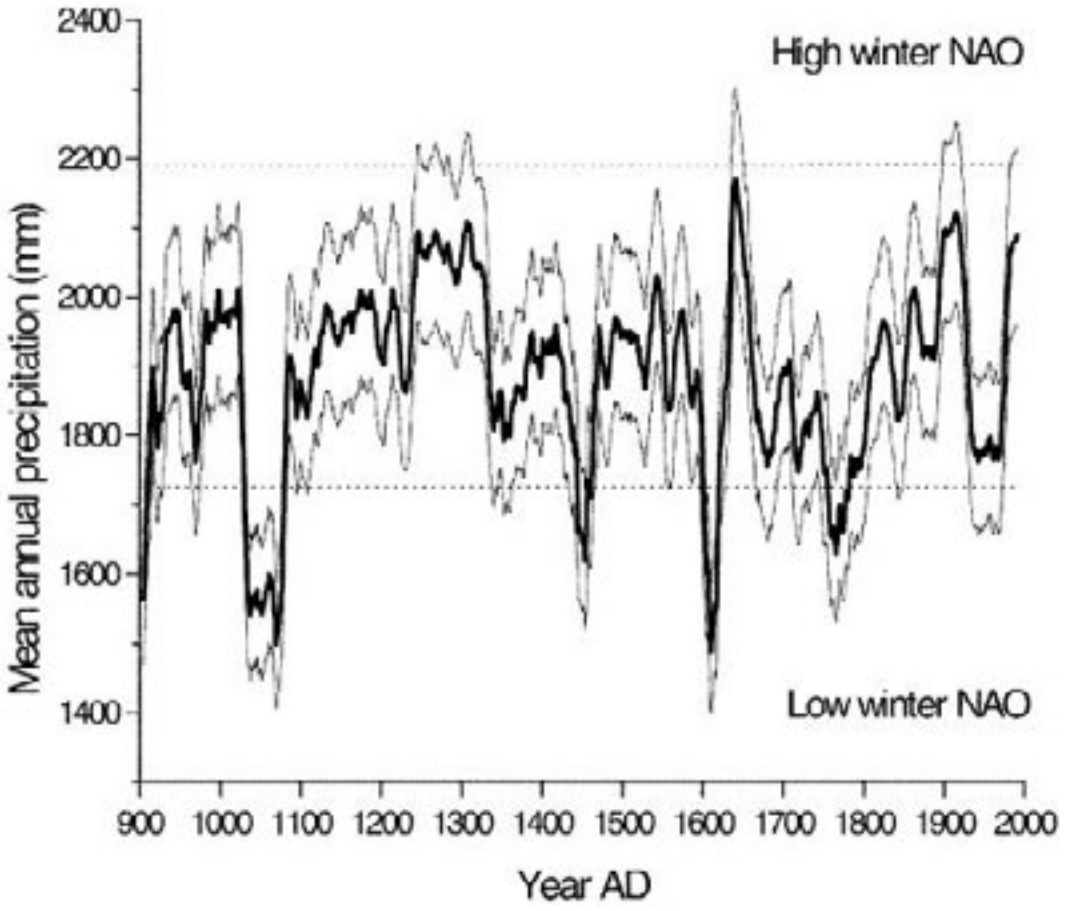

Figure 10: Reconstructed mean annual precipitation record from a banded stalagmite (Procter et al. 2000). Horizontal dotted lines show the 2 standard deviation range of mean annual precipitation recorded in the period of instrumental observations (1879-1993)

1.6: Summary and Purpose

The Shetland Islands are located in a climatically sensitive area of the Northern Atlantic. Their latitudinal position and proximity to the warm, saline North Atlantic Current and Shelf Edge Current result in a short, wet growing season. This short, but powerful, growing season has been enough to sustain a consistent population on the islands since Neolithic times. This is not to say that inhabitants have lived in comfort; life in Shetland has always been a perpetual struggle against the cold, windy local environment. This struggle has been amplified at times in the past due to abrupt, devastating environmental changes which have tested the hardiness of the Shetland residents. The onset of the Little Ice Age was marked by a sharp increase in storminess across the North Atlantic, subjecting Shetland to more frequent, severe storm events. This increase in storminess was likely amplified by regular swings in the North Atlantic Oscillation which gave rise to severe winters across northern Europe, shortening the already narrow growing season (Figure 8). Additionally, anomalous swings in precipitation could indicate periods of increased storminess that could blow sand inland on a large scale (Figure 10). The precise combination of winds and precipitation that trigger and sustain sand blows in Shetland is not known, but this study forms part of the larger effort to define the forcing factors behind sand mobilizations on different scales.

Members of the Shetland Island Climate and Settlement Project, through funding from the National Science Foundation, aim to identify these past environmental changes and log the subsequent human responses. From the data gathered, several hypotheses have been proposed to explain the sand deposits observed around the Quendale and Spiggie areas. While the sand that buried the Broo site clearly came from the nearby Bay of Quendale, the pacing and extent of this deposition unknown. Based on their GPR profiles of coastal dunes, Joe and Alice Kelly have hypothesised that more than one sand invasion event occured in the Quendale area, with confidence that a single event is an unlikely model for the observed dune stratigraphy (Climate Change Institute 2013). At the Loch of Spiggie, Gerald Bigelow, along with the Kellys, hypothesized that an inlet once connected the it to the ocean. Bigelow based this hypothesis on Willem Blaeu's 1654 map of Shetland (Blaeu 1654), which shows an inlet between Spiggie and the Bay of Scousburgh. Joe and Alice Kelly researched this hypothesis further with their GPR profiles of the low-lying land bridge. Based off of their profiles, they support the hypothesis for a buried inlet (Climate Change Institute 2013). In this study, I will be continuing research into these two hypotheses as well as investigating two additional hypotheses related to the Lochs of Spiggie and Brow that have been proposed by Gerald Bigelow, Michael Retelle, and myself. The first of these hypotheses relates the observed sand unit in the Loch of Spiggie to the burial of the proposed inlet that connected the Loch of Spiggie to the ocean. We believe that the sand mobilization event(s) responsible for the burial of the inlet also created the sand unit in the Loch of Spiggie, essentially continuing its mobilization farther inland. The second additional hypothesis centers on the sand unit observed in the Loch of Brow. The source of this sand is unclear, as it is nearly equidistant from the Bays of Scousburgh and Quendale. Our initial hypothesis states that this unit is composed of wind-blown sand from the Bay of Quendale, but the presence of Scousburgh sand in Brow remains a possibility.

To test these hypotheses, I will be utilizing physical and mineralogical analyses in an attempt to reveal more information about the pacing of sand invasion events as well as trace the origin of sand units observed in the Lochs of Spiggie and Brow. The results from these analyses will be placed in context with the current suite of collected data in order to accurately reconstruct the series of events that led the landscapes we observe in the Quendale and Spiggie areas today.

Methods

2.1: Field Methods

Sand Samples were taken from the following locations (Figure 2):

- Bay of Quendale (east and west dunes plus beach)
- Bay of Scousburgh (east and west dunes plus beach)
- Pool of Virkie
- Broo archaeological site
- Transect from the Bay of Quendale to the Broo site (Figure 11)
- Transect from the Bay of Scousburgh to the Loch of Spiggie
- Cores from the Lochs of Spiggie and Brow that contain sand units beneath an upper organic-rich silt layer
- Till samples

Figure 11: Transect from the foredune of the Bay of Quendale to the Broo archaeological site. The transect is approximately 1.2 km in length. The yellow stars are locations where samples were taken.

At each sample site observations and descriptions were recorded in a field notebook and photos were taken using a digital camera. If needed, a shovel was used to dig into dunes or soft sediment to expose fresh strata. The samples were taken with a small hand shovel and then tagged and bagged for transport to Bates College.

2.2: Laboratory Methods

Several analyses were performed on the sand samples at Bates College during the summer and fall of 2013. Before a sample was used for any of the analyses, it was thoroughly washed. Deionized water was poured over the sand, covering it completely, and the sample was stirred using a glass rod. The water, along with any organics or non-sediment it picked up, was then carefully decanted out. The sample was then put in a drying oven set at 100°C until it was fully dried. If a sample contained a large volume of organic matter, it was first covered with hydrogen peroxide and placed on a hot plate until any observable reaction ceased. The hydrogen peroxide strips the organic matter from the sand grains, allowing it to then be decanted out of the sample. The sample is then washed with deionized water, decanted, and allowed to dry. After washing, the samples were usually subsampled in order to make them available for multiple analyses. The analyses performed included grain size analyses, x-ray diffraction, and grain surface morphology.

Grain Size Analysis:

Grain size analyses (GSA) were performed on almost every sample. Before the analysis, the sample in question is weighed and subsampled if needed. A sample of 50-100g is ideal for a GSA, so taking a representative subsample of the larger samples was necessary. After being weighed, the sample is poured into a dry sieve stack running from -1.0Ø to +4.0Ø, with bin increments of 0.5Ø. After 10-15 minutes in a shaker, the sieve stack is removed and the sediment captured in each bin is weighed.

The measured bin weights were converted into weight percent of the total sample and were then plotted onto a cumulative weight percent curve. This curve can be used to calculate a suite of analytical statistics as described by Folk (1974). The statistics used in my analysis include mean grain size, median grain size, mode grain size, and inclusive graphic standard deviation, a measure of sorting.

X-Ray Diffraction:

X-Ray Diffraction (XRD) was used to identify the mineralogical composition of the sand samples. Every mineral has a unique mineralogical structure, and incident x-rays will reflect off of these structures in equally unique patterns (Figure 12). An x-ray diffractometer operates on this principle, firing x-rays from a range of angles onto a sample and then interpreting the resulting pattern of scattered x-rays.

Before the analysis can be run, samples were first run through a Frantz magnetic separator set at 0.8 amps, which parted the sand into two sub-samples in an attempt to separate quartz and felspars from heavier minerals. Once the sand was separated, the subsamples were put into a Spec ball mill, which turned the sand into a fine powder which was then mounted in a circular holder. The most essential part of mounting the rock powder was ensuring that the sample had a completely flat surface, as it eliminated the possibility of false reflections. Once mounted in a holder, the sample was put into a Rigaku MiniFlex II X-Ray Diffractor and the sample was analyzed from 10-50° 2theta.

After the diffractor completed its run, a diffractogram was produced which showed the intensity of return signals at every angle. These diffractograms were put through a whole pattern fitting software, but the complexity of the samples did not allow for accurate results using this method. Many of the minerals suggested by the software did not make any sense in the context of the study location, and results were generally inconcsistent. We attempted to perform manual peak searches which were then complemented by a whole pattern fitting, but

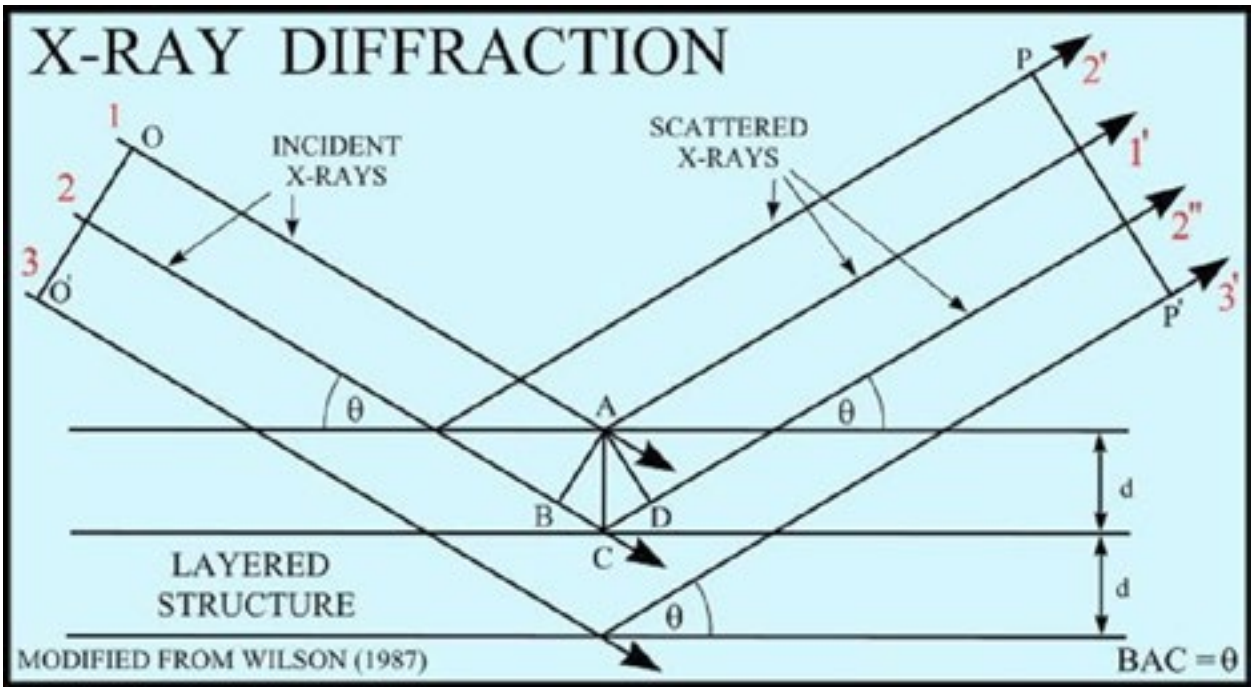

Figure 12: A schematic diagram illustrating the principles behind X-Ray Diffraction. Source: Ross (2000)

similar problems resulted from this method as well. Instead, the diffractograms were analyzed manually, with emphasis placed on the comparison between samples from different locations. Manual analysis began by using Jade 9 mineral analysis software to identify potential minerals in the samples with special focus on peaks present in one sample, but missing from others. This was complemented by comparing pure mineral diffractograms to the peaks observed in the sample diffractograms to make matches. Finally, the potential minerals were noted and then confirmed by visually identifying them under a microscope.

Grain Surface Morphology:

Due to its ability to resist both mechanical and chemical weathering, quartz has become a ubiquitous mineral in sand found around the world. Analysis of quartz grains from various sedimentary environments has revealed that mechanical abrasion and chemical solution do in fact modify the surface of quartz grains at a microscopic level, resulting in unique microtextures that can be used to recreate the transportation and deposition history of a single grain. (Bull and Morgan, 2006, Costa et al., 2013, Costa et al., 2012, Hellend et al., 1997, Kenig, 2006, Krinsley, 1968, Mahaney, 1990, Marshall et al., 2012, Narayana et al., 2010, Walley and Krinsley, 1974). Krinsley (1968) defined three broad categories, glacial, littoral, and aeolian, that encompass the microtextures observed from many sedimentary environments and processes. The cross-cutting relationship of surface microtextures allows for a reconstruction of the transport histories of sediment samples. An unofficial fourth category, chemical weathering, can provide information on the duration of deposition and what the surface environment was like above the grain.

In this study, a JEOL JSM-7100FLV scanning electron microscope (SEM) was used to achieve an excellent level of focus and detail at extremely high magnification. To prepare for this analysis, 10-15 quartz grains were selected from the sample in question. This was achieved using a 20x magnification microscope to observe the sample and a wet, fine brush to remove the grains without disturbing their surface. The grains were then mounted to an SEM specimen stub and coated with gold in a vacuum evaporator directly from above while the sample was being slowly rotated. This coating made the grains a better conductor for the electron beam, allowing the grains to be observed in better detail under higher magnification.

Glacial features:

The glacial category encompasses all textures derived from glacial transportation or incorporation into a glacial sediment such as till (Krinsley, 1968). Quartz grains that have been transported by glacial means are generally very angular, with a large number of conchoidal fractures and large-scale breakages resulting from forcefull interaction with grains of many different sizes (Figure 13) (Krinsley, 1968, Mahaney, 1990, Hellend et al., 1997, Bull and Morgan, 2006). Glacial movement imparts pressure on grains, and crushing and grinding features are commonly observed (Figure 14). The fractures and breakages derived from glacial environments come in a variety of sizes and generally have high relief due to a lack of physical or chemical weathering. Some edge abrasion or subaqueous textures can be imparted on glacial grains if they have experienced glacio-fluvial transport. In areas with warm-based glaciers, these weathering patterns can be quite common, as meltwater channels can act as powerful subaqueous environments.

Subaqueous/Littoral features:

In this study, the littoral category defined by Krinsley (1968) has been rebranded as subaqueous. Subaqueous environments include littoral, fluvial, and lacustrine, as well as any associated environments such as glacio-fluvial. Grains that undergo subaqueous transport frequently collide with other grains, resulting in numerous

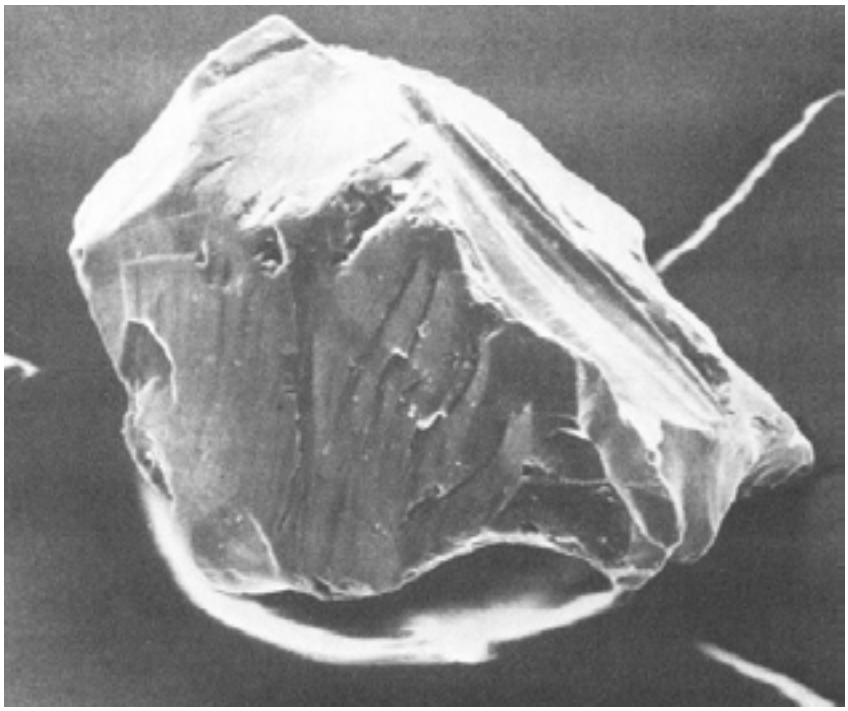

Figure 13: A quartz grain that has experienced glacial transportation (from Krinsley (1968). Note the angularity, high relief, and lack of extensive weathering.

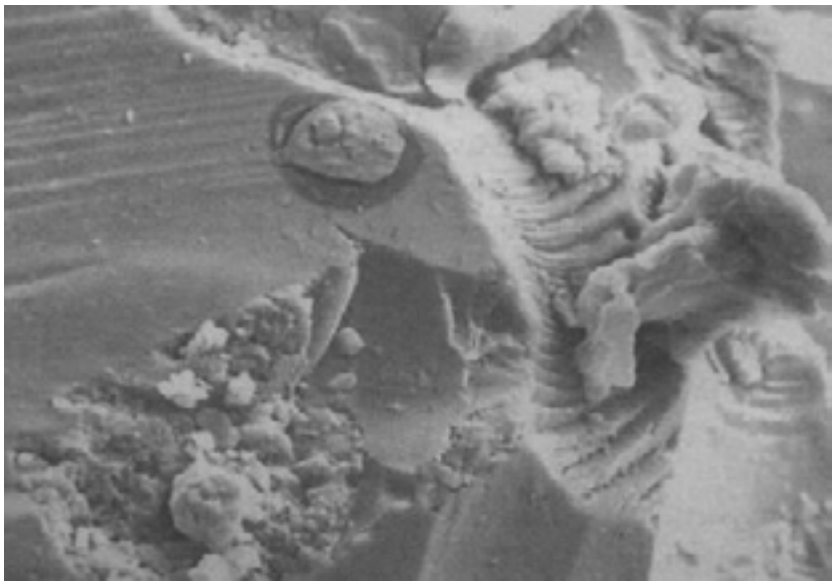

Figure 14: Grinding and crushing features derived from glacial transport (from Bull and Morgan, 2006).

impact features which can be seen on the grain's surface (Figure 15). The size and shape of these impact features depends upon the force of collision and the shape of the impacting grains. These percussion marks range from small pits obseved on otherwise smooth surfaces (Figure 15) to large, star-shaped fractures (Figure 16).

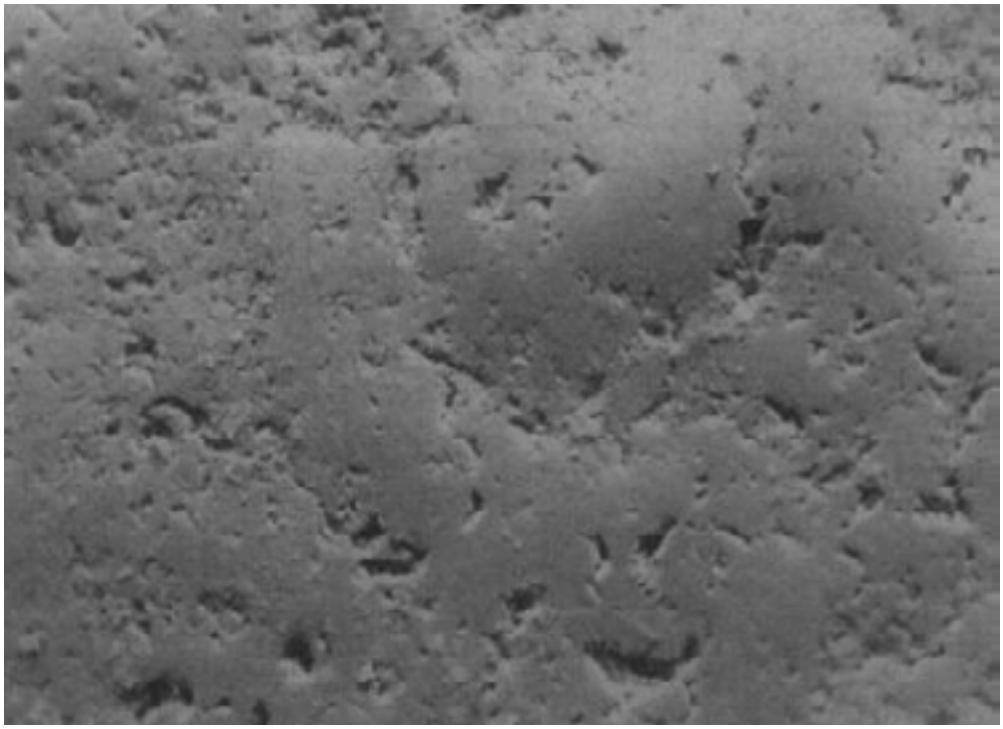

Figure 15: Subaqueous impact features (from Bull and Morgan, 2006)

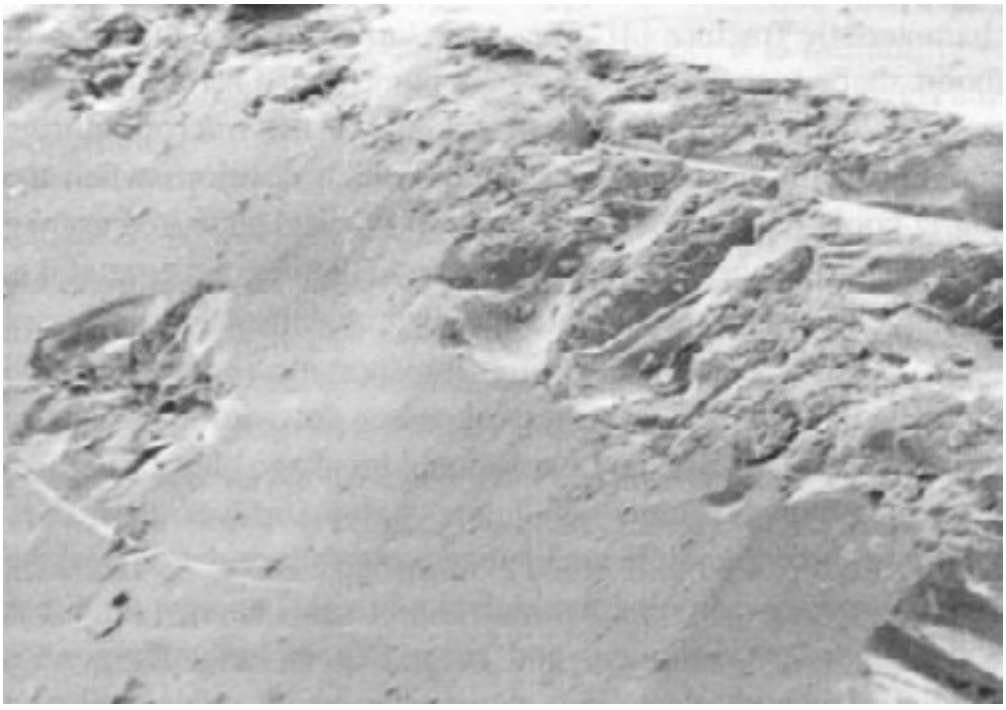

Figure 16: Quartz grain exhibiting a star fracture (left-center) and blocky edge abrasion. The blocky edge abrasion seems to override previously-existing platey edge erosion (from Bull and Morgan, 2006)

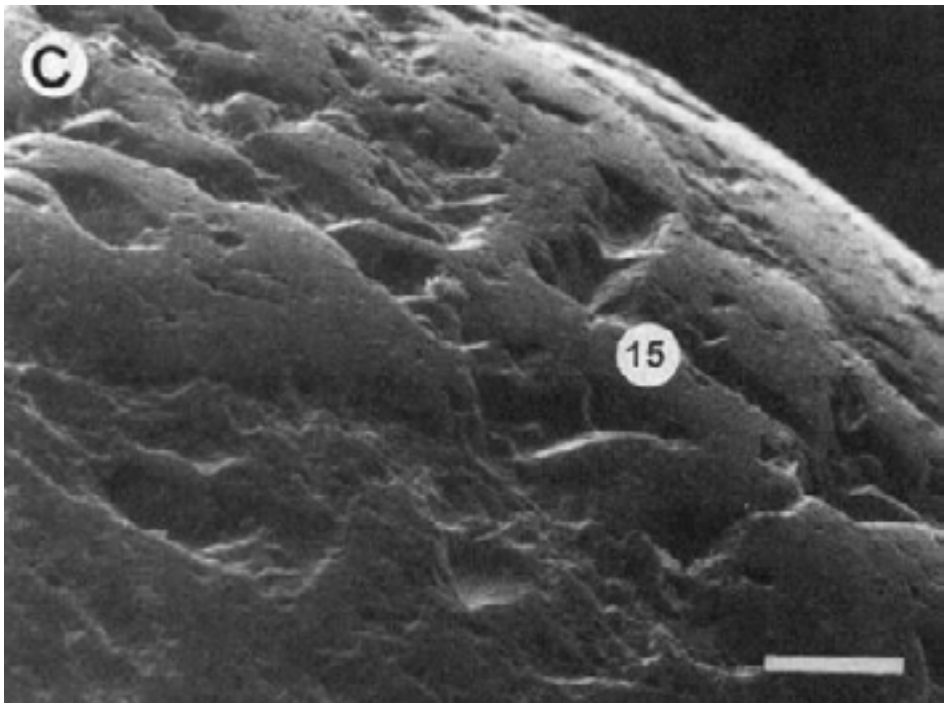

Figure 17: Example of subaqueous pitting superimposed on a surface smoothed by water action (from Hellend et al., 1997)

Edge abrasion is also an indicator of subaqueous transport or deposition. Edge abrasion can be platey or blockey (Figure 16), with blocky edge abrasion indicating more powerful transport. The weathering action of flowing water creates a smoother surface than grains that have been exposed to aeolian transport. Impact marks are superimposed on this smooth surface, but it is usually still visible between the impacts (Figure 17).

Aeolian features:

The transportation of quartz grains by wind exposes them to frequent, persistent grain collisions that can have extensive weathering effects. A wide variety of aeolian impact features have been documented (Costa et al. 2013, Kenig 2006, Krinsley 1968, Marshall et al. 2012), ranging from upturned plates and platey textures (Figure 19) to conchoidal fractures and even large-scale breakages. Marshall et al. (2012) demonstrated that these features are derived in differing energy regimes, and their distribution can indicate the strength of the wind that transported the grains (Figure 18). Aeolian impact textures can be differentiated from subaqueous textures by the absence of smooth surfaces. The frequency of collisions results in a surface composed almost entirely of upturned plates (Figure 19) or which shows a general roughness in appearance. The frequency of collisions also results in extensive edge abrasion. This abrasion is usually platey in

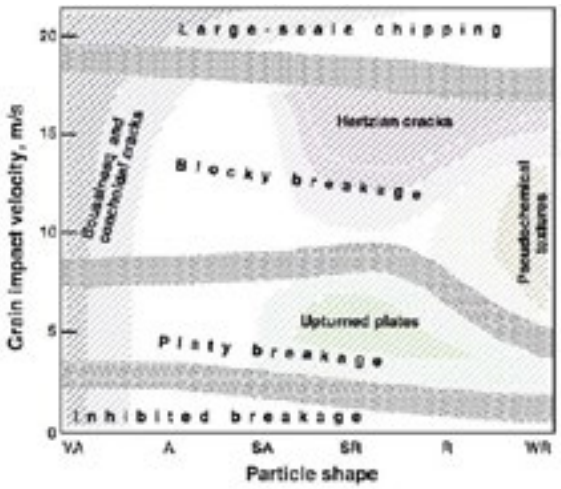

Figure 18: Aeolian impact textures oberved for grains of different angularities travelling at increasing speeds (from Marshall et al., 2012)

appearance (Figure 20), but can take on a blocky texture if winds are strong. This high rate of weathering can be used to infer the maturity of a quartz grain. Grains that have recently been eroded out of a parent rock or glacial sediment are typically very angular, with many fresh fractures and high relief. As a fresh grain is subjected to aeolian transport, its relief lowers and it loses angularity. The fresh, fractured surfaces become rougher and

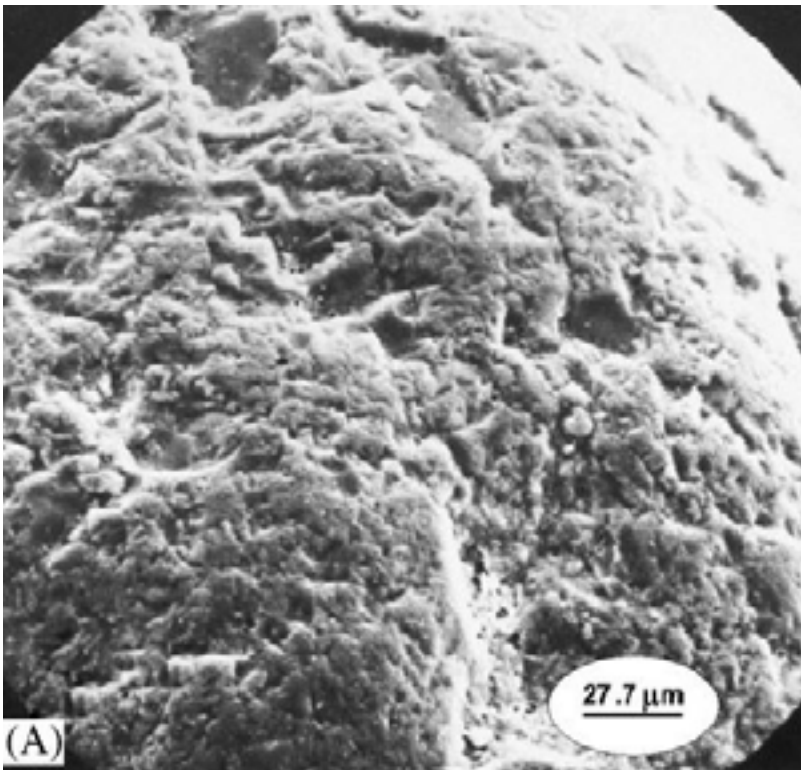

Figure 19: Upturned plates and an overall platey surface derived from aeolian transportation. Note the lack of smooth surfaces.

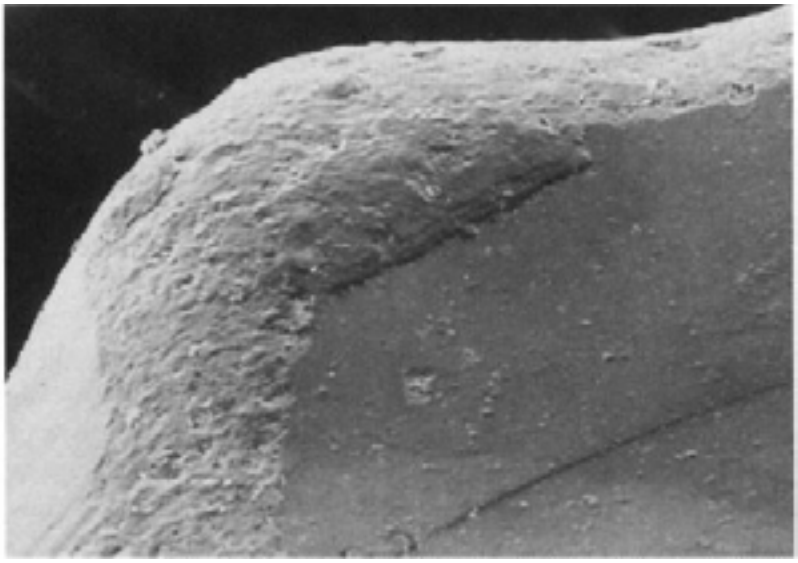

Figure 20: The beginning stages of platey edge abrasion. The lack of weathering on other surfaces indicates that this is a relatively fresh grain that has only recently experienced aeolian transportation

the fractures themselves tend to flatten out. As a result of quartz's innate ability to resist weathering, this process takes time, and only grains that have been in a dune-like aeolian environment for an extended period are well-rounded with a completely rough surface. Sometimes, though, this process of gradual weathering is interupted by a particularly strong storm which imparts fresh fractures on the grain's surface. By analyzing the relationships between these surfaces, it is possible to tease out the transportation and depositional history of any quartz grain.

Chemical Textures

The introduction of vegetation and organic matter following deposition can further alter the surface of a quartz grain. If the environment into which a quartz grain is deposited remains stable, a vegetation layer may form at the surface. An increased number of organic acids are introduced to the surface environment through the process of pedogenesis, and infiltrating water becomes more acidic (Bull and Morgan, 2006). Quartz

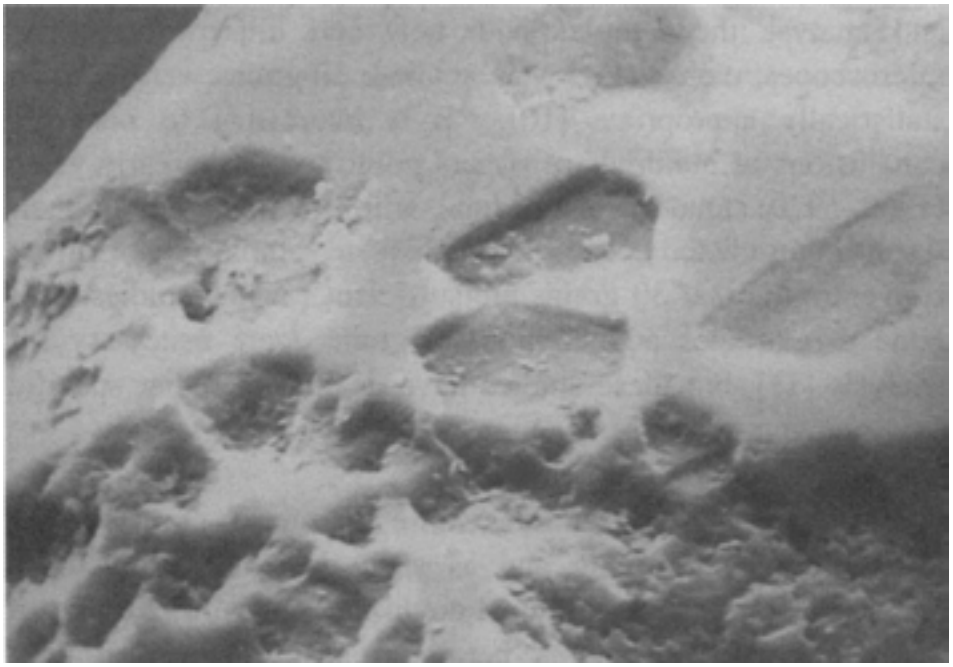

Figure 21: Extensive silica precipitation observed on a quartz grain

residing in the more acidic subsurface experiences silica dissolution and subsequent re-precipitation across its surface (Figure 21). Silica dissolution commonly occurs in pre-existing pits, where acidic water can collect and remain in place. Precipitation, on the other hand, can cover large areas, appearing as a smooth cover over rough features (Figure 21). The extent of silica dissolution and precipitation can be used as an indicator of time spent under vegetation.

Results

Due to the importance of spatial relationships in this study, the results are presented based on sample locations. Within each location section, the results of each analysis are shown.

Grain Surface Morphology Labelling System

The individual grain surface morphology results are given for each sample site below, but the results can be difficult to interpret, so a labeling system was constructed to ease viewing. Many textures were observed over the expanse of the study area (Table 1). Some textures can be recieved in multiple environments, but those unique to certain methods of transportation or deposition are labeled as such.

Mechanically-derived textures	Chemically-derived textures (post-deposition)
1. Conchoidal fractures	13. Silica dissolution
2. Blocky breakage	14. Silica precipitation
3. Platey edge abrasion	15. Secondary mineral growth
4. Blocky edge abrasion	
5. Meandering ridges (aeolian)	
6. Star fractures (subaqueous)	
7. Complete grain breakage	
8. Platey impact textures (aeolian)	
9. Subaqueous impact textures (subaqueous)	
10. Grinding and crushing (glacial)	
11. Mechanical V-shaped pits (subaqueous)	
12. Fractured plates	

Table 1: Observed microtextures on quartz grains. Textures unique to certain environments are labeled

Pool of Virkie

Grain Surface Morphology

The Pool of Virkie can be thought of as a control environment for analysis of grain surface morphology. The Pool of Virkie is a littoral environment with a complete absence of water during low tide. Therefore, the sand within the pool is subject to both subaqueous and aeolian transportation.

The Pool of Virkie grains are sub-angular to sub-rounded (Figure 22). Unsurprisingly, they display an abundance of physical weathering textures. Textures unique to subaqueous or eolian transport are present in tandem on these grains. Where fractures have occured recently, and the surface is relatively fresh, subaqueous textures can clearly be seen. Eolian textures tend to override all other features, though, and on more weathered areas of the grains they are the dominant texture. The fractures and complete grain breaks seem to vary in age, with some displaying extensive weathering in the form of edge abrasion and platy textures, and others appearing almost fresh, with only subaqueous pitting visible on their surface. This indicates a consistent renewal of large-scale fractures and breakages with persistent weathering.

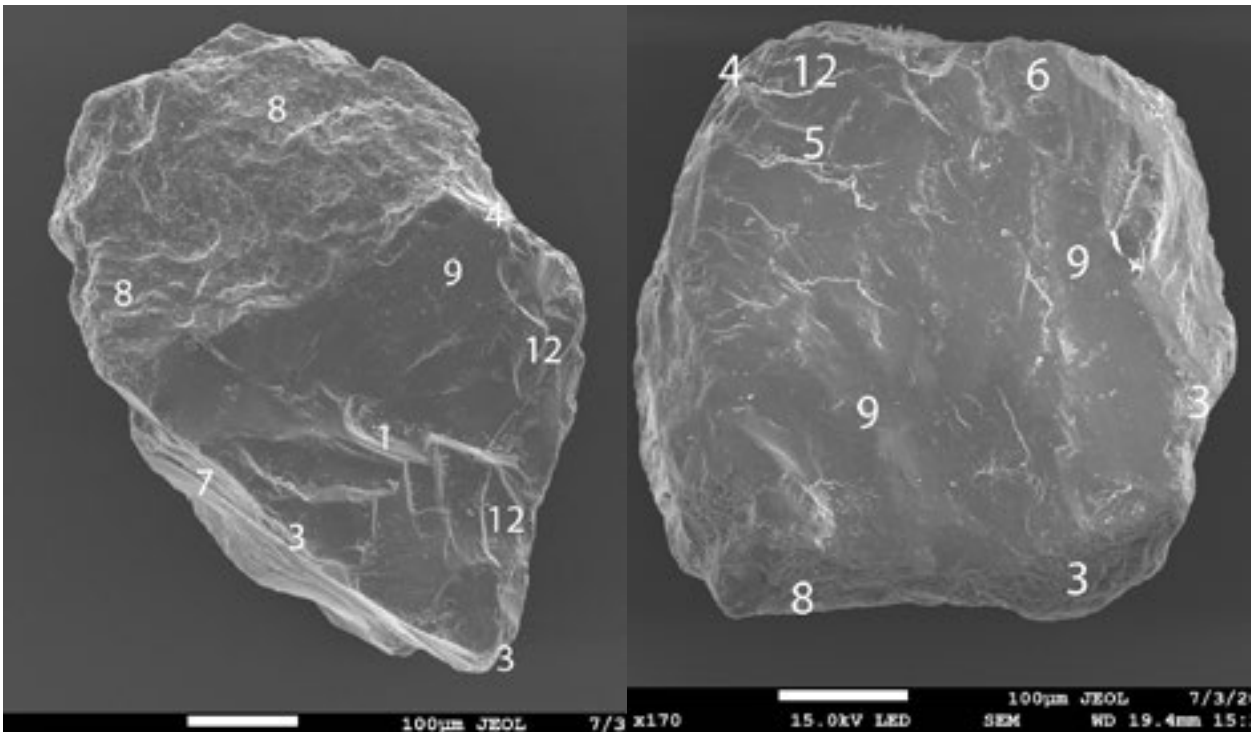

Figure 22: Quartz grains from the Pool of Virkie.

Till Samples

Several till samples were taken from various locations in the study area (Figure 2) and subjected to XRD and grain surface morphology. Due to the unsorted, chaotic nature of till, grains size analyses were not performed, as no useful information would be obtained.

X-Ray Diffraction

The till sample run through a powdered x-ray diffraction came from an outcrop located on the eastern side of the Bay of Scousburgh. This sample was not magnetically separated, and the resulting diffractogram with interpreted minerals can be seen in figure 23. Quartz and albite, ubiquitous minerals throughout the study area, are present. These minerals hold little informative value and are not going to receive a lot of attention in this study. Minerals of interest in the till sample include muscovite, chloritoid, enstatite, and a serpentine mineral. Muscovite, a phyllosilicate minerals belonging to the mica group, shares several peaks with quartz but can be identified by its peak just before 18º 2theta (Figure 23). Muscovite was also visually confirmed in the till sample. Chloritoid is an orthosilicate mineral of metamorphic origin with outcrops recorded on the Mainland of the Shetland Islands (mindat.com, 2014). An unspecified serpentine mineral was also identified in the till samples. Kaolinite and cronstedtite, both serpentine minerals, share almost every peak in their diffractions, making the distinction between the two very difficult. Visual identification suggests kaolinite as the mineral present in the till, but further research needs to be done before confirming this result. Three unidentified peaks were present in the till diffraction, indicated by question marks in figure 23. A search/match function using Jade 9 software did not produce any conclusive results, and manual searching for matching peaks proved equally futile. These peaks represent one, if not more, unidentified minerals present in the till samples.

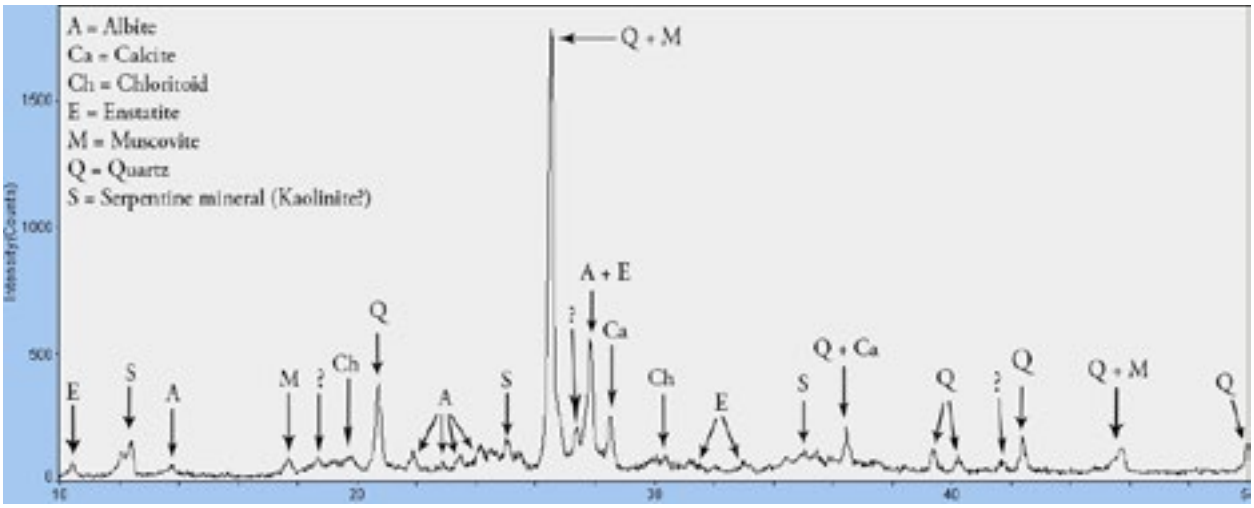

Figure 23: Diffractogram from a till outcrop located next to the Bay of Scousburgh

Grain Surface Morphology

The grains from till samples show a surprising amount of weathering (Figures 24a-e). Platey textures can be seen on large areas of the surface of these grains, smoothing out some older fractures and breakages. Viewing these platey textures is made somewhat more difficult by the presence of large amounts of debris which cling to the grains even after thorough washing. This debris is likely the remnants of the fine-grained matrix in which the grain was once imbedded. Looking past the debris unveils a surface with a mixture of rough, platey surfaces and smooth, fractured surfaces. The grain in figure 24a is one of the more fractured grains found in the till samples. The surface is almost entirely covered with conchoidal fractures of various sizes, with few areas displaying weathering of any kind. Contrasting this is the grain in figures 24b-c. This grain has no visible fresh fractures, only the weathered remnants of older fractures. This grain comes from a till that is directly overlain by a soil layer, and chemical weathering can be seen on large areas of the grain's surface (Figure 24c). Silica dissolution pits are complimented by extensive silica precipitation in these areas. The grain in figures 24d-e is representative of most of the till grains. It shows a more even distribution of fresh fracture surfaces and platey, weathered textures. Interestingly, the locations containing fractures displayed an incredible complexity, with evidence of many impacts occuring in roughly the same area (Figure 24e).

Quendale Transect (Includes the Bay of Quendale)

X-Ray Diffraction

The magnetically-susceptible fraction from the foredune of the Bay of Quendale (Figure 11 for location) can be seen in figure 25, while the non-magnetically-susceptible fraction can be seen in figure 26. Ignoring quartz and albite, the magnetically-susceptible fraction contained muscovite, chloritoid, enstatite, and a serpentine mineral. Like the till samples, identifying the exact serpentine mineral in the sand was difficult, but kaolinite is the most likely candidate. The Quendale samples contained an unknown peak, indicating the presence of an unidentified mineral remaining to be found in the sample.

The non-magnetically-susceptible fraction (figure 26) contained far fewer minerals than the magnetically-susceptible fraction. Quartz and albite appear in this fraction as well, but are joined by calcite. There are some

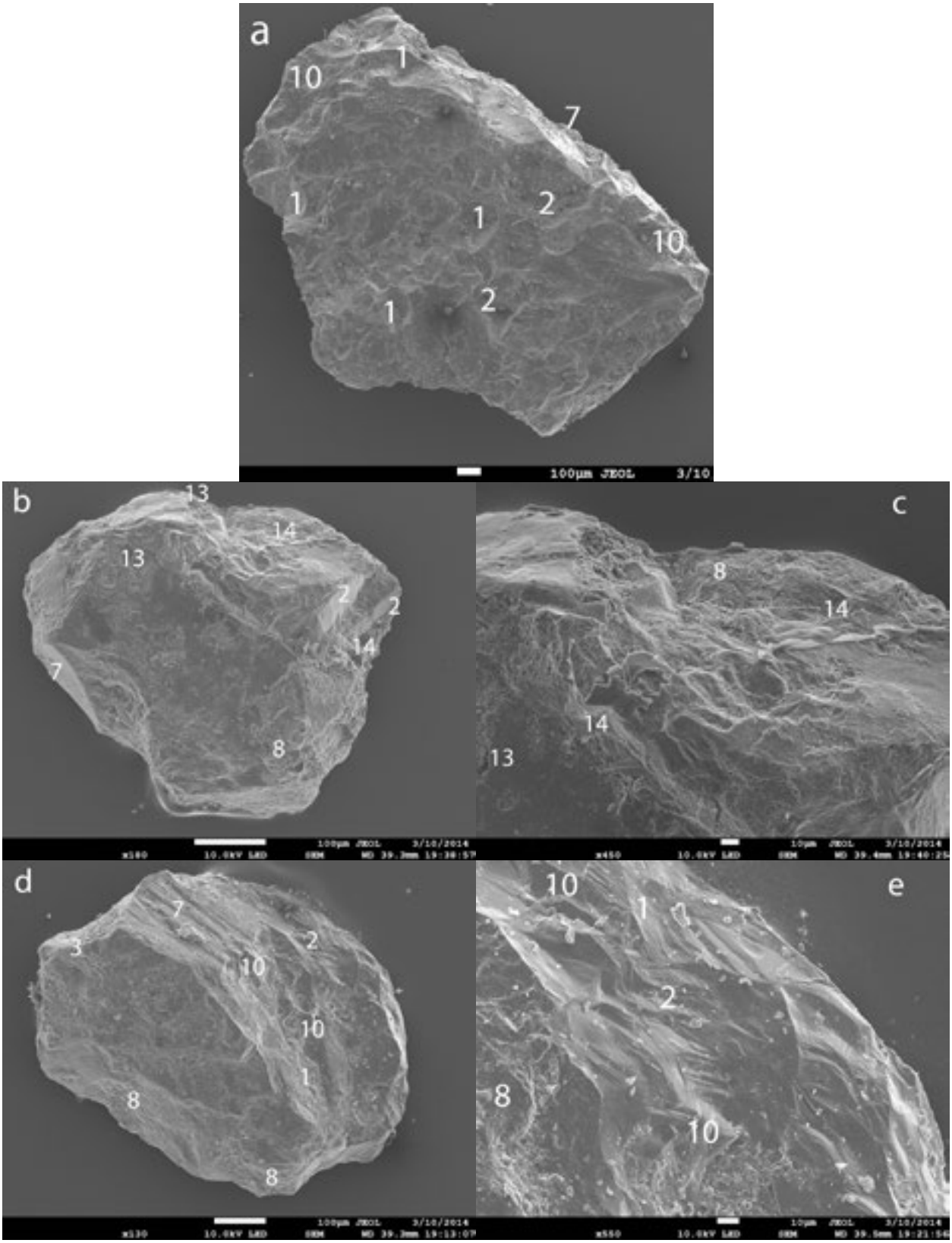

Figure 24a-e: Quartz grains from till outcrops around the study area. (a) is from a till outcrop located on the eastern shore of the Bay of Scousburgh, while (b) - (e) are from till outcrops found to the west of the Quendale Links (see figure 2).

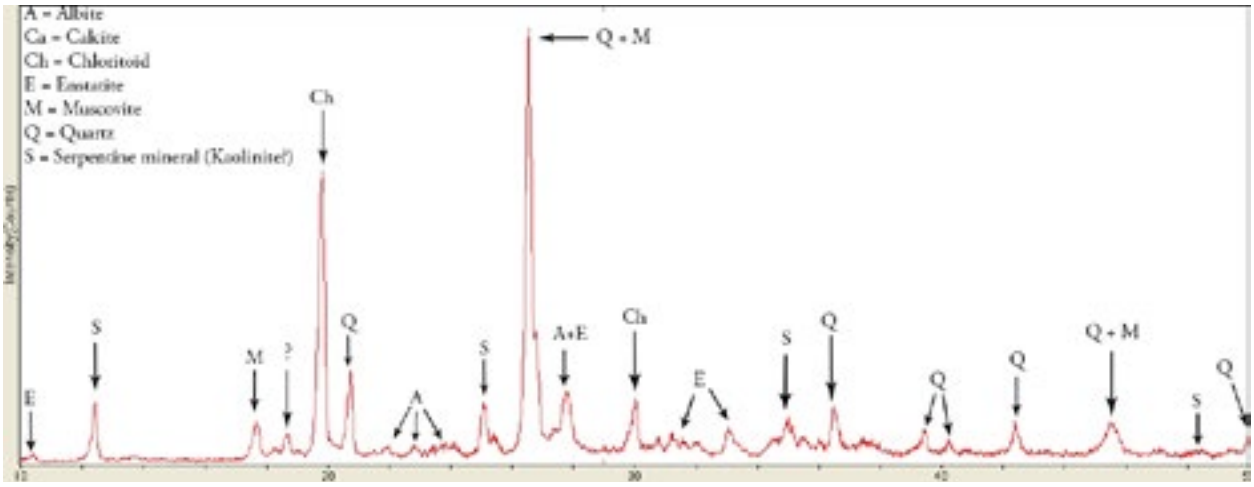

Figure 25: Diffractogram from the magnetically-separated portion of sand taken from the first stop of the Quendale transect. Identified minerals (as well as unidentified peaks) are labelled.

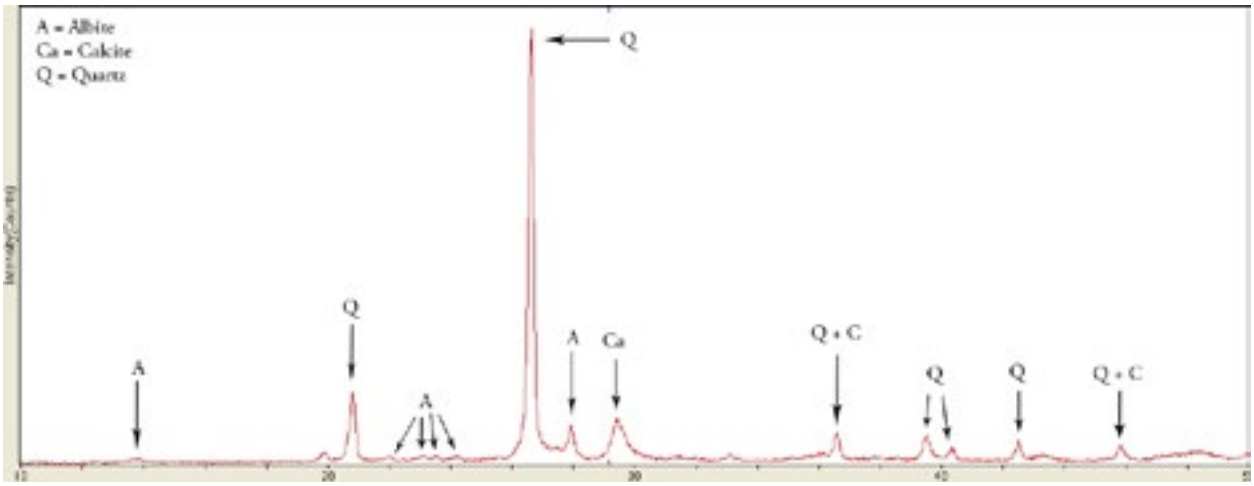

Figure 26: Diffractogram from the non-magnetically-susceptible portion of sand taken from the first stop of the Quendale transect. Identified minerals are labelled.

small bumps present in the diffractogram that could signify the presence of another trace mineral. These bumps are miniscule, though, making confident identification based soley on their presence difficult.

Grain Size Analysis

Several grain size distributions for the Bay of Quendale can be seen in figures 27a-c. A steady increase in grain size can be observed as one moves from surf to beach to dune at the Bay of Quendale. The distribution curves are fairly normal, with slight skews towards smaller grain sizes. Additionally, the western side of the Bay of Quendale contains smaller grains on average than the eastern side (Figure 28). For the Quendale transect the mean grain size values are very consistent, falling in a range of 0.26-0.30mm (Figure 28). This consistency in grain size contrasts the decrease in sorting with distance inland that can be observed in the inclusive graphic standard deviation results (Figure 29). While this decrease in sorting is relatively small between QT-1, -2, and

-3, QT-4 displays a value of 0.70Ø, almost 0.20Ø higher than the other transect stops.

This decrease in sorting can be better seen through histograms displaying the grain size distibution of each stop (Figures 30a-j). Note the subtle decrease in sorting as one moves from QT-1 to QT-3. At QT-4, however, there is a prominent decrease in sorting as both fine silts and coarse gravel increase their presence.

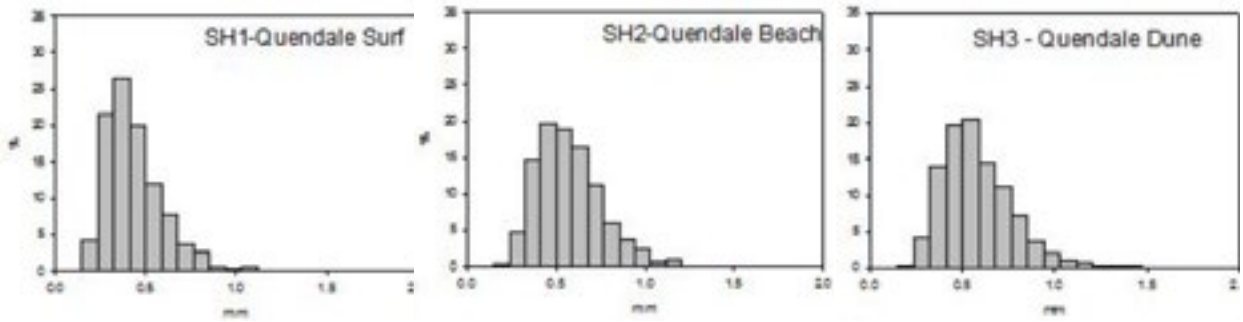

Figures 27a-c: Grain size distibution results for the Bay of Quendale surf, beach, and dune. Results were obtained by Michael Retelle using a camsizer grain analyzer

Figures 28: Average mean grain sizes (in mm) for the Bay of Quendale, the Quendale Transect stops, and the Broo archaeological site.

Figure 29: Average inclusive graphic standard deviation values (in units phi) for the Bay of Quendale, the Quendale Transect, and the Broo archaeological site. Note: lower values indicate better sorting.

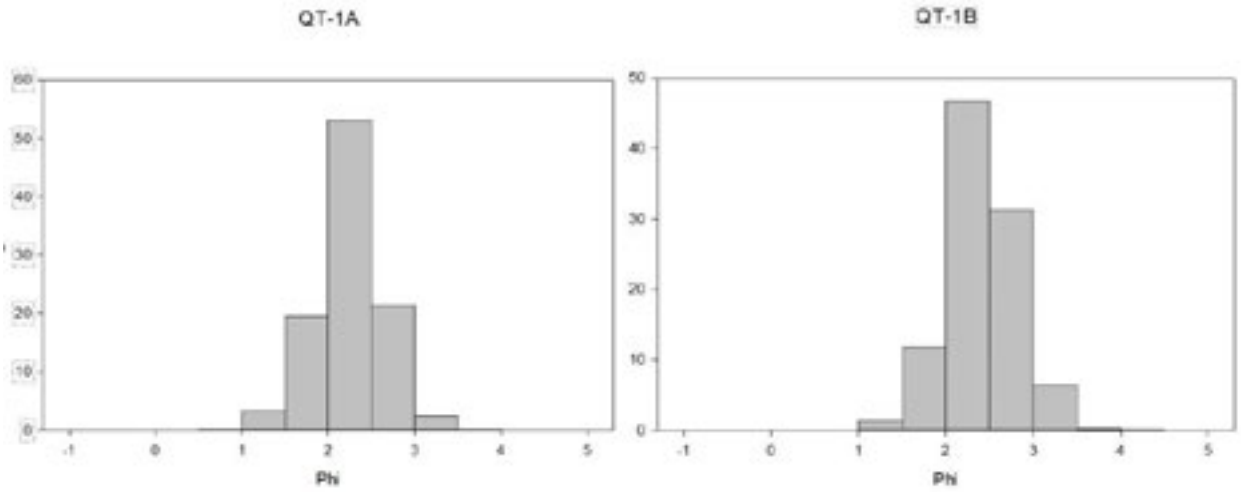

Figures 30a & b: Grain size distributions (in units phi) from the Quendale transect. Both (a) and (b) are from the first stop of the transect (see figure 11 for location)

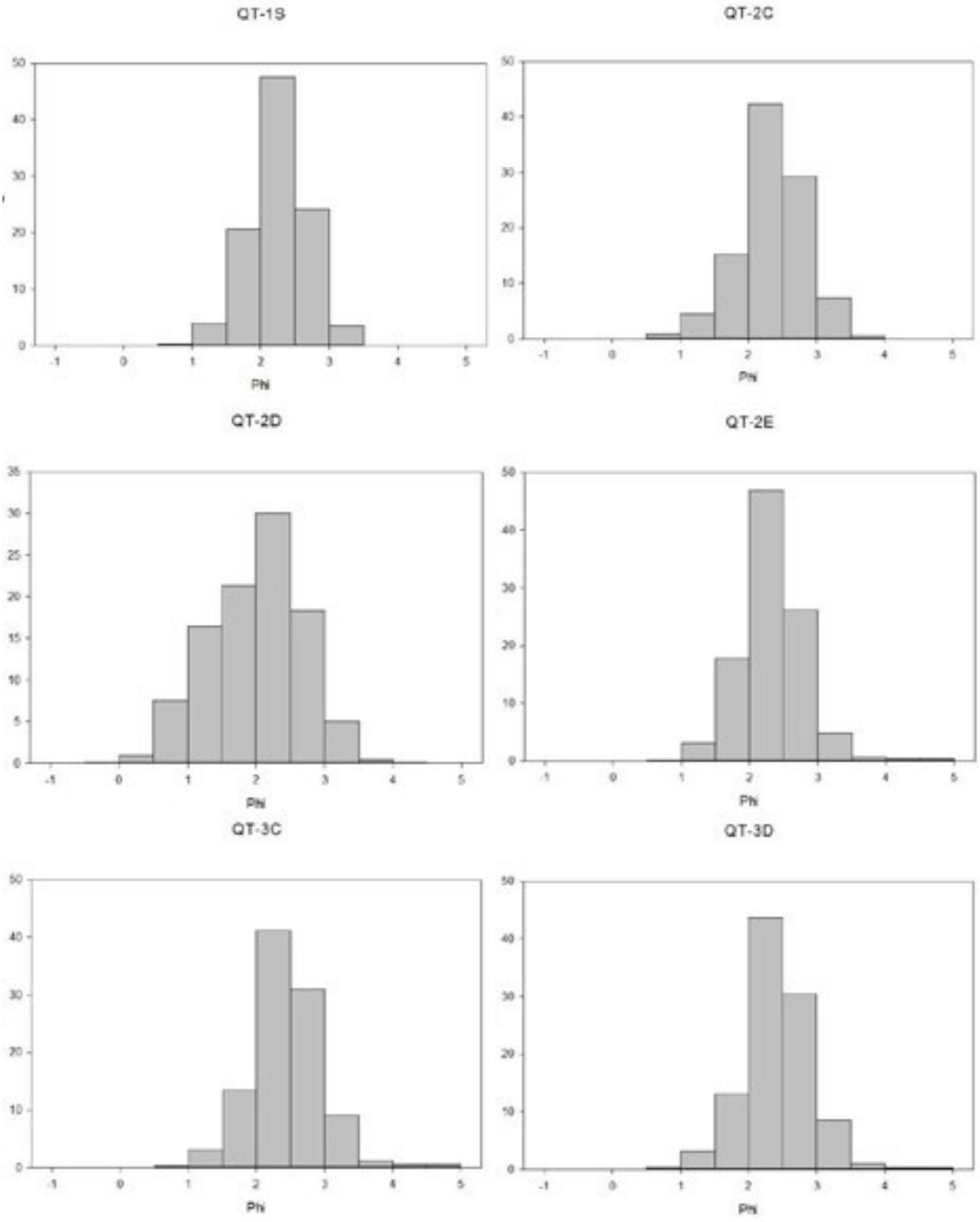

Figures 30c - h: Grain size distributions (in units phi) from the Quendale transect. (c) is from the first transect stop, while (d) - (f) are from the second. (g) and (h) are from the third transect stop (figure 11 for location)

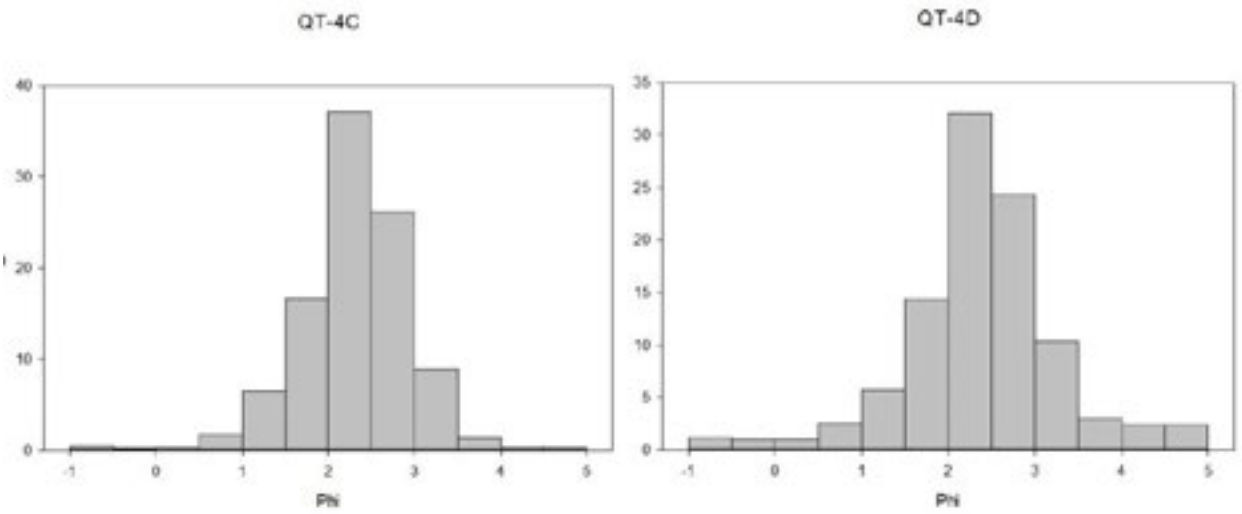

Figures 30i-j: Grain size distribution (in units phi) for Quendale Transect stops. (i) and (j) are from the fourth transect stop (see figure 11 for location).

Grain Surface Morphology

The grains from the Quendale Transect display extensive physical weathering in the form of platey textures, subaqueous impact features, conchoidal fractures, blocky breakage, blocky and platy edge abrasion, and other impact features (Figures 31a-e). The grains from QT-1 are, on average, sub-angular, while grains found futher inland are sub-rounded or even rounded. The conchoidal fractures and blocky breakages seen on QT-1 grains are the freshest of all the sampled stops, but even these exhibit edge abrasion (Figures 31a-b). Fractures and breakages from other stops do not appear fresh and display extensive weathering, losing their overall shape. Most of the grains contain at least some subaqueous impact surfaces with extensive pitting and some larger, star-shaped fractures (Figure 31a-e). Limited chemical weathering can be seen on the transect grains, and those displaying it are found near the surface, close to vegetation. The grains from QT-4 are the most weathered of all the grains (Figure 31e). They have a rough, platey surface across the entire grain and do not contain any fresh conchoidal fractures. These grains are also more rounded than the other grains, illustrating the degree of weathering they have experienced.

Broo Archaeological Site

X-Ray Diffraction

The Broo sample run through a powdered x-ray diffraction is from layer B-8, one of the lowest in the stratigraphic sequence. The diffraction results from the magnetically-susceptible fraction can be seen in figure 32, while the non-magnetically-susceptible fraction is shown in figure 33. The magnetically-susceptible fraction contained the ubiquitous quartz and albite in addition to muscovite, chloritoid, enstatite, and a serpentine mineral. Kaolinite and cronstedtite, both in the serpentine group, share peaks in the observed range, making absolute identification using the diffractogram futile. Visually, kaolinite appears to be present in the sample, but more mineralogic work needs to be done to confirm this. An unknown peak was present in the magnetically-susceptible Broo samples, indicating the presence of an unidentified mineral.

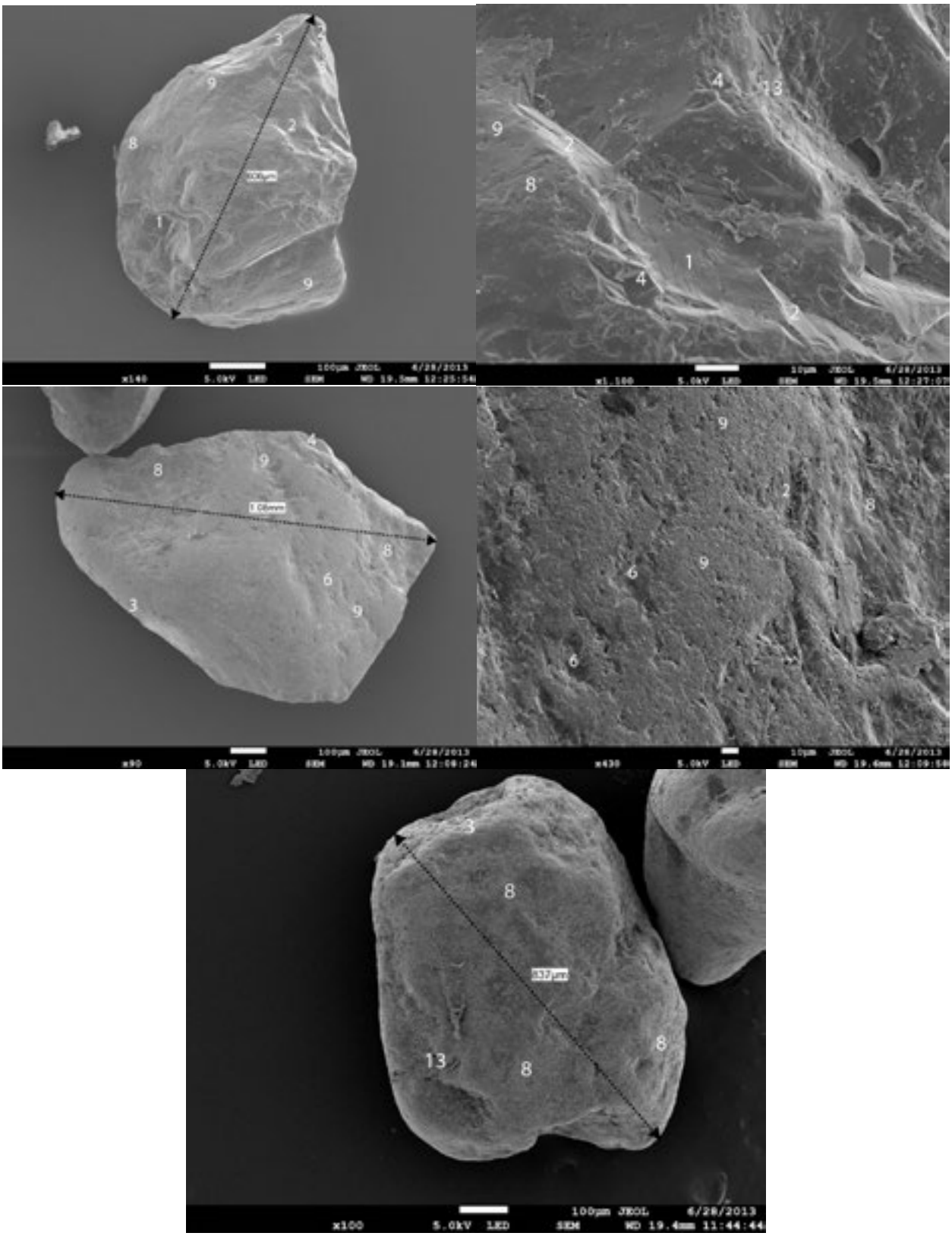

Figure 31a-e: Representative quartz grains from the Quendale transect. (a) is from the first stop, while (b) is a closer look at the northeastern part of the grain. (c) is from the second stop, and (d) is a zoomed in look at the southeastern portion of the grain. (e) is from the fourth transect stop.

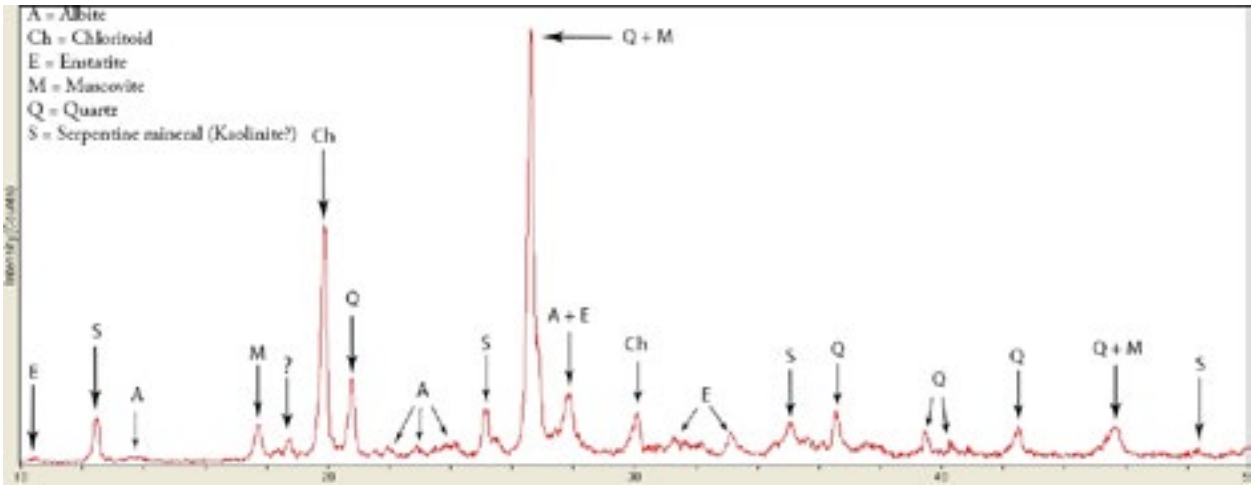

Figure 32: Diffractogram from the magnetically-susceptible fraction of sample B-8, from the Broo Site

The non-magnetically-susceptible fraction of sample B-8 contained calcite in addition to the ubiquitous quartz and albite. Calcite shares two peaks with quartz within the scanning range, and has only one individual peak (Figure 33). This peak is small in the Broo sample, potentially indicating a reduced volume of calcite compared with other samples. Several small bumps were unidentified, but their small stature makes concrete identification difficult.

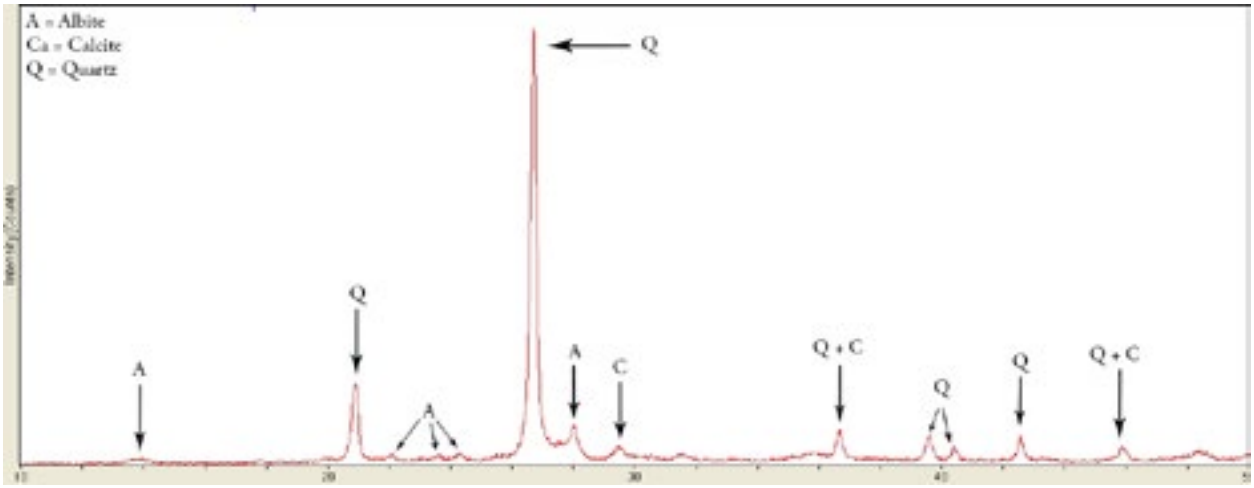

Figure 33: Diffractogram from the non-magnetically-susceptible fraction of sample B-8, from the Broo site

Grain Size Analysis

The averaged grain size analysis results for the Broo archaeological site can be seen in figures 28 and 29, but the numerous observed sand units make the average values poor indicators of grain sizes and sorting at the site. Instead, the statistics of each layer were calculated and can be observed in Figures 34a and b. Almost all of the layers on the western side of the site have an inclusive graphic standard deviation value between .44Ø and .55Ø, but layer B-1B is an outlier with a value of 0.70Ø (Figure 34a). The mean grain sizes of the western Broo layers can be seen in Figure 10. B-1B is again an outlier with the largest grains of all the layers (Figure 34b). B-1A

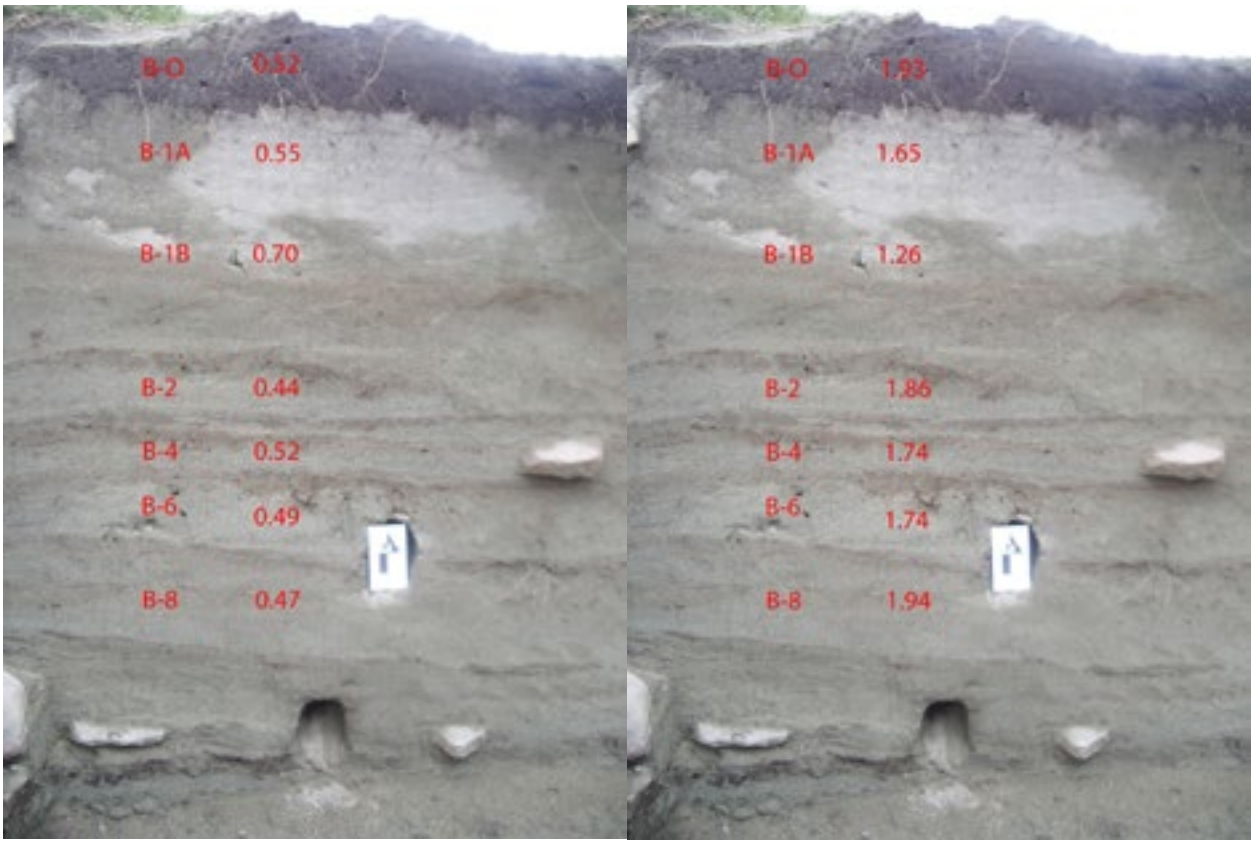

Figure 34a and b: (a) Inclusive graphic standard deviation values (in units phi) for the observed layers on the western side of the Broo archaeological site. (b) Average mean grain sizes (in units phi) for the observed layers on the western side of the Broo archaeological site. Note: The absent layers (B-3, B-5, B-7) contained too little sediment to reliably perform grain size analysis using a sieve.

contains the second-coarsest grains, but they are still nearly four-tenths of a phi unit finer on average than the grains of B-1B. The rest of the layers contain mean grain sizes between 1.74Ø and 1.94Ø.

Two sand samples from a previous survey of the Broo site (Lindeloff 2012) were run through a camsizer in order to get a very accurate measurement of the grain size distribution. The results for these samples, taken from 36-41 and 87-90 cm in depth, can be seen in figures 35a and b, respectively. These samples show a mode of 0.3-0.4 mm with a negative skew.

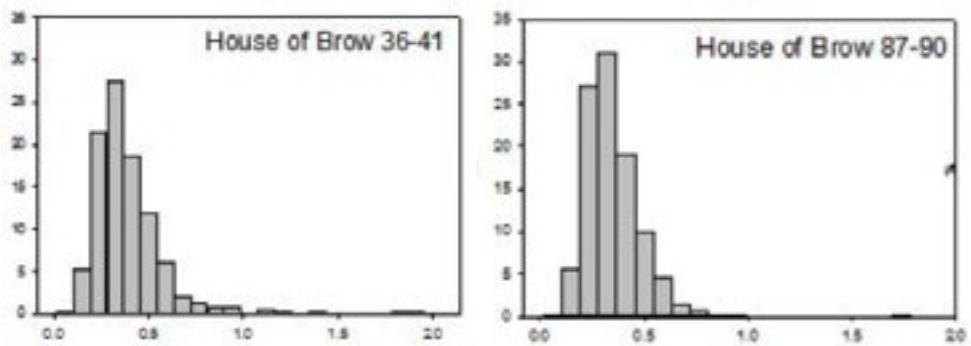

Figures 35a and b: Grain size distributions (x-axis in mm) for two depths at the Broo archaeological site. Grain size analysis performed by Michael Retelle using a camsizer grain size analyzer.

Grain Surface Morphology

Overall, the grains from the Broo site are sub-angular to sub-rounded (Figures 36a-f). They are almost ubiquitously covered in platey surface textures, with few smooth, pitted surfaces visible. Fresh conchoidal fractures or breakage blocks are rare. Most former fractures have been weathered and rounded, losing their angularity to edge abrasion and gaining platy textures on their surfaces. Large scale breakage plates can be seen on some of the grains (Figure 36b), but these breakage plates are older features, as evidenced again by edge abrasion and pitting on their surface. Figure 36b shows one of the more angular and fractured grains observed from the Broo samples. This grain contained several observable conchoidal fractures and breakage blocks. All of these have experienced some degree of edge erosion. A large-scale grain breakage was observed, with minimal edge erosion, indicating violent transportation in the recent history of this grain. The majority of the grains did not contain these recent fractures, and instead appeared similar to the grain in figure 36c. Small amounts of chemical weathering in the form of silica dissolution and precipitation can be seen on most of the grains (figure 36f). This weathering is present not only in layers closer to the surface, but in layers such as B-6, more than a meter below the surface. The silica observed on these grains is limited in its coverage, with only small areas displaying these textures.

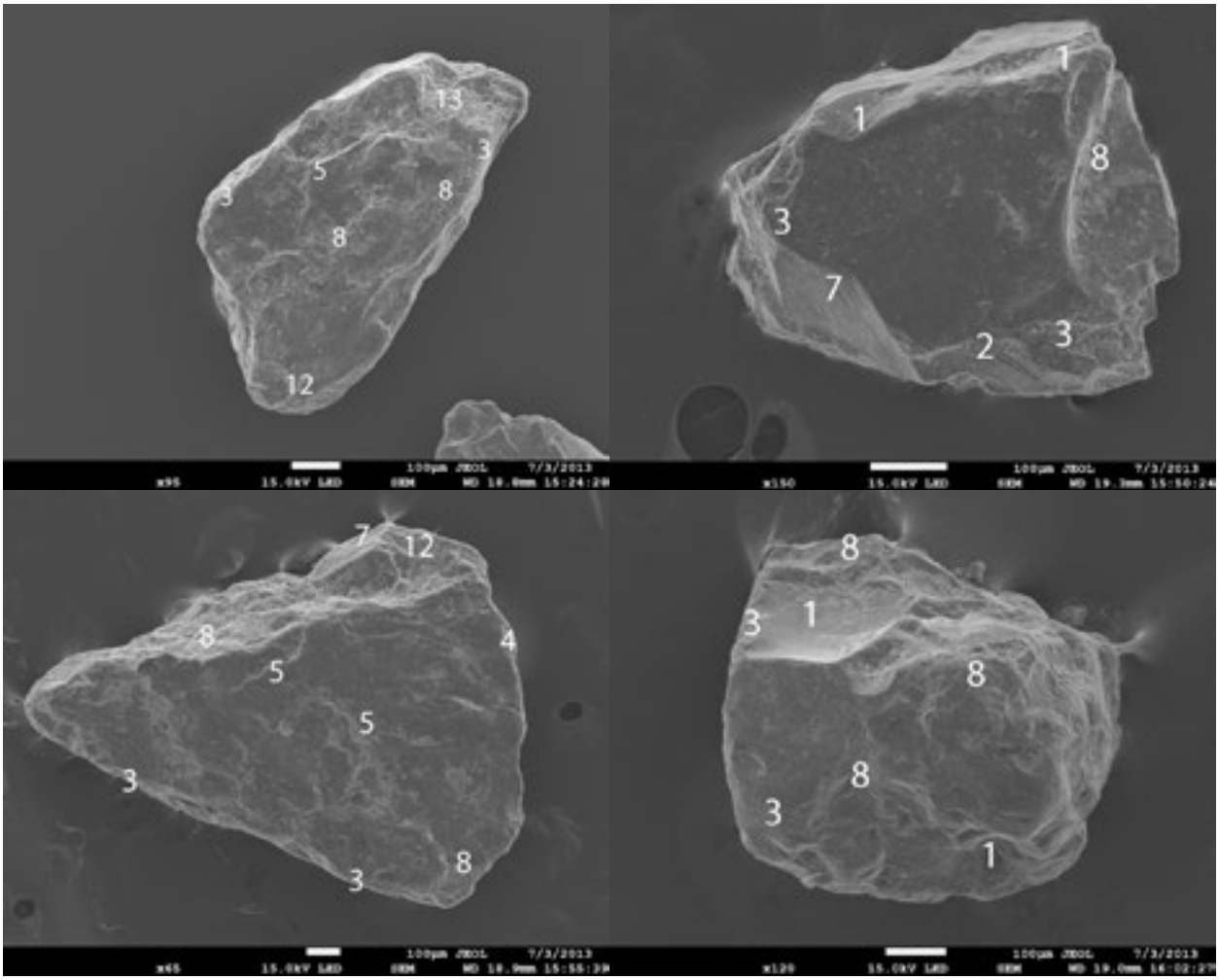

Figures 36a-d: Representative quartz grains from the Broo archaeological site. (a) and (b) are from B-1A, the layer directly under the surface organic layer. (c) and (d) are from B-1B, the layer with anomalous grain size analysis results that underlies B-1A (figures 33a and b for locations)

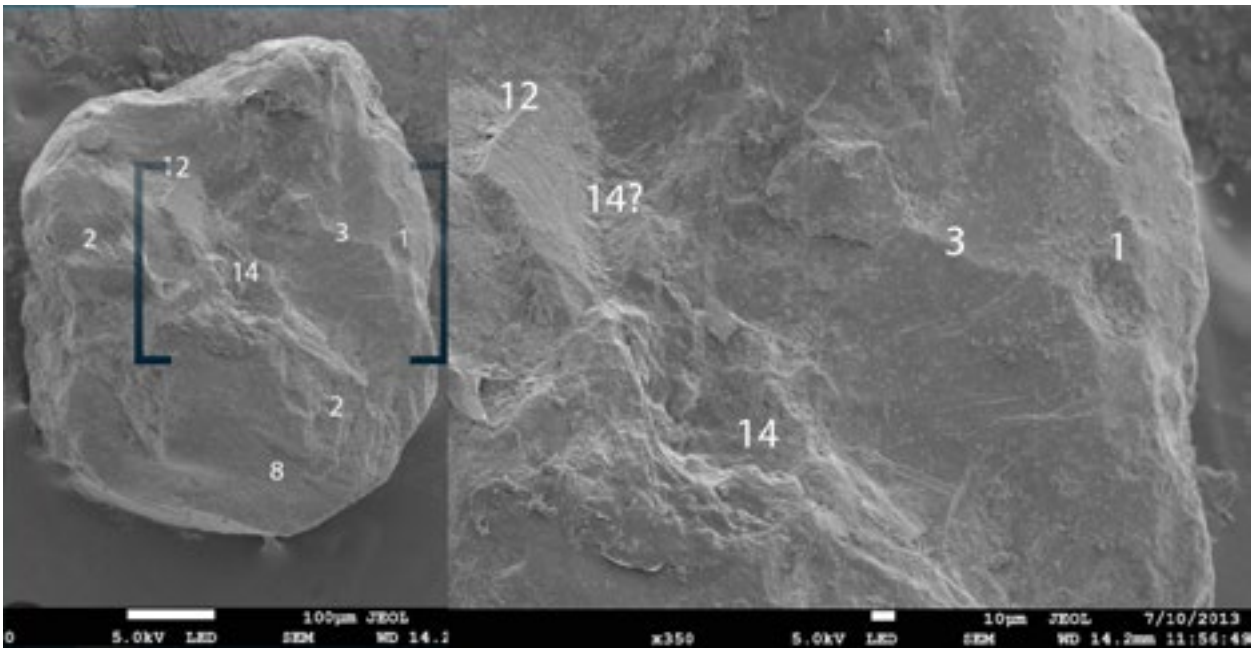

Figures 36e and f: Representative quartz grain from the Broo archaeological site. (e) is from B-6, while (f) is a closer look at the bracketted area in (e) (Figures 33a and b for location).

Bay of Scousburgh

Grain Size Analysis

Figure 50 shows the grain size relationships between the east and west sides of the Bay of Scousburgh. The bay has moderately-well sorted sand with a sorting value that does not change dramatically between from east to west. The mean and median grain size values, though, register a difference in size of 0.08mm between the eastern and western sides of the bay, with the eastern side having the larger grains. The western side of the Bay of Scousburgh contains the smallest mean and median grain sizes in the entire study area.

A more detailed grain size distribution for the Bay of Scousburgh can be seen in figure 37. Obtained by Professor Michael Retelle using a camsizer, this negatively-skewed distribution shows that the Scousburgh sands have a mode grain size of 0.2-0.3 mm. This distribution is similar to those seen at the Bay of Quendale and the Broo site.

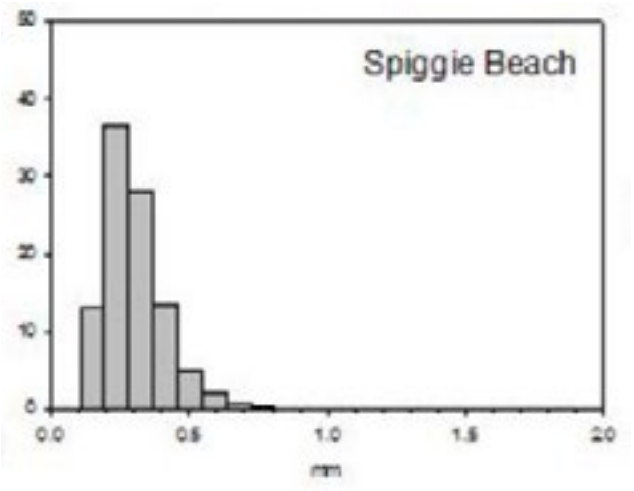

Figure 37: Grain size distribution at the Bay of Scousburgh obtained by Michael Retelle using a camsizer

X-Ray Diffraction

The magnetically-susceptible fraction of a sand sample taken from the foredune at the Bay of Scousburgh can be seen in figure 38. This fraction contained muscovite, chloritoid, enstatite, and a

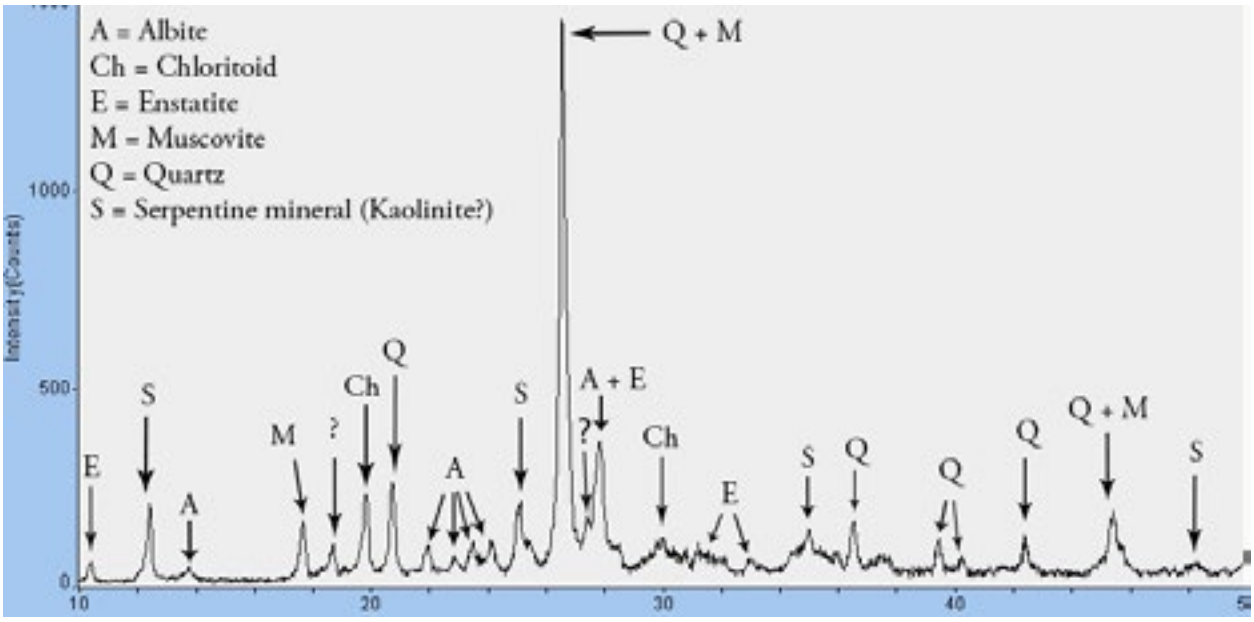

Figure 38: Diffractogram from the magnetically-susceptible fraction of a sand sample taken from the foredune backing the Bay of Scousburgh

serpentine mineral in addition to quartz and albite. Two unidentified peaks were present in this fraction of the Scousburgh sample. The unknown peak at around 27.5º 2theta matches a peak that belongs to kyanite (see figure 39), but no other kyanite peaks are present in this fraction. One or more unidentified minerals are present in this sample, and more mineralogic work needs to be done in order to extract the exact mineralogy.

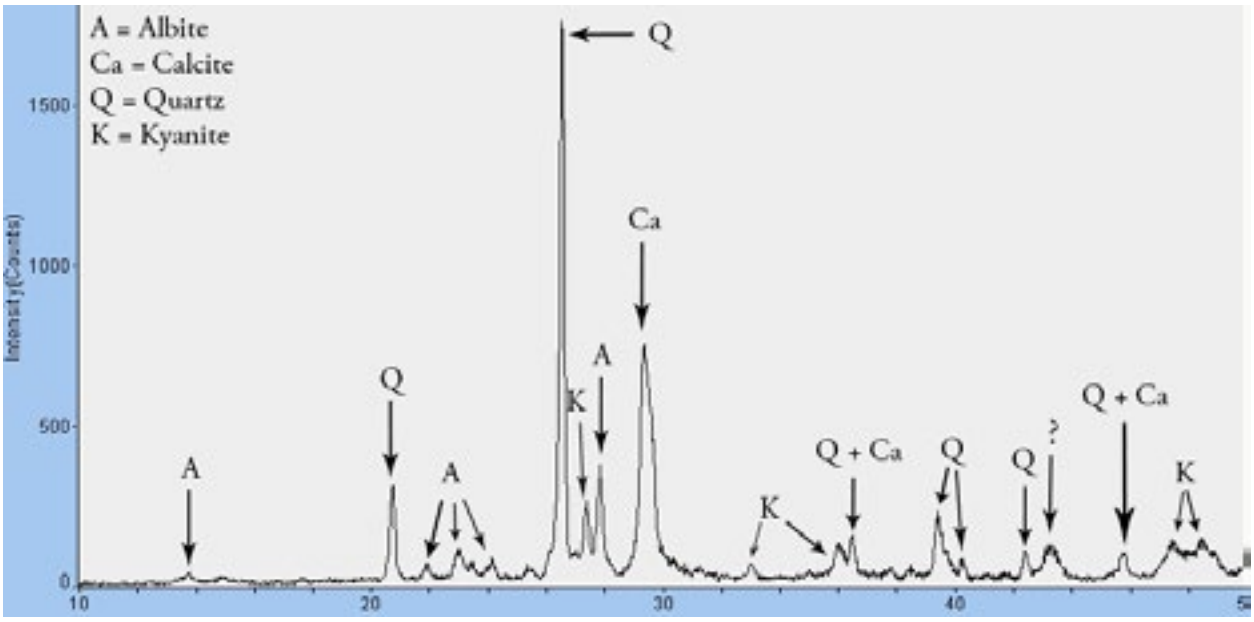

Figure 39: Diffractogram of the non-magnetically-susceptible fraction of a sand sample taken from the foredune backing the Bay of Scousburgh

The non-magnetically-susceptible fraction of the Bay of Scousburgh sample can be seen in figure 39. In addition to quartz, albite, and calcite, this sample contained kyanite, a metamorphic silicate formed under moderately-high pressure. The presence of kyanite at the Bay of Scousburgh was visually confirmed.

Grain Surface Morphology

Grains from the foredune backing the Bay of Scousburgh were analyzed for grain surface morphology. Overall, these grains display angular shapes, with relief ranging from moderate to high (Figures 40a and b, respectively). Edge abrasion can be seen on most of the fractures and breakages, but some are fresh with defined edges. The edge abrasion is of the platey and blockey varieties, while most of the overall surface textures are platey. On some grains, grinding and crushing can be seen. The presence of grinding and crushing features combined with the angularity that many of these grains display suggests that they were recently weathered out of a glacial sediment.

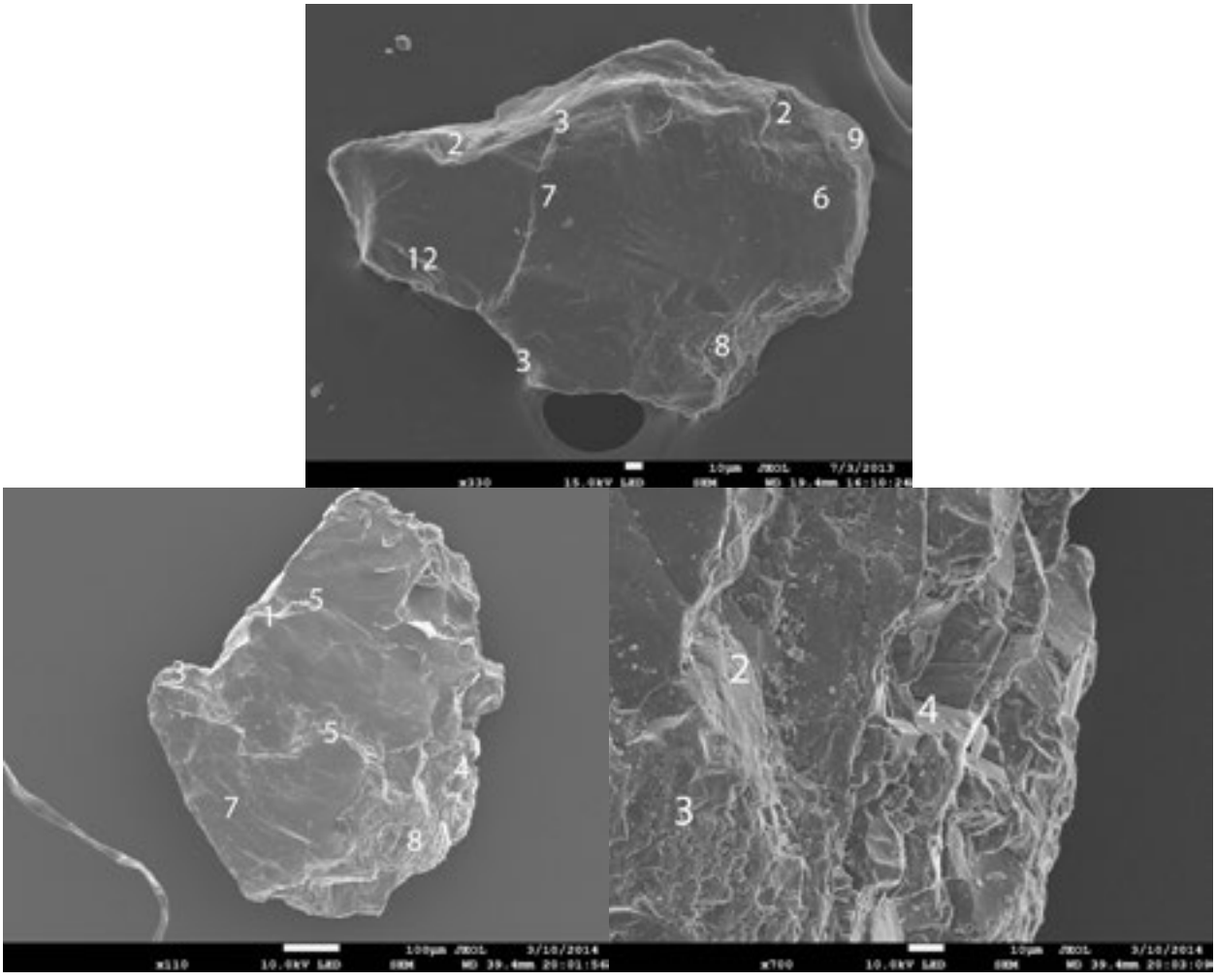

Figure 40a - c: Representative quartz grains from the Bay of Scousburgh. (c) is a closer look at the bracketted area in (b)

Spiggie Land Bridge

X-Ray Diffraction

Powdered x-ray diffraction was performed on a sample from a depth of about 40 cm on the Spiggie land bridge The diffractogram from the magnetically-susceptible fraction can be seen in figure 41, while the diffractogram from the non-magnetically-susceptible fraction can be seen in figure 42.

Besides quartz and albite, the magnetically-susceptible fraction contained muscovite, enstatite, chloritoid, and a serpentine mineral (Figure 41). One clear peak was not identified, indicating the presence of an unknown mineral in the sample. The non-magnetically-susceptible fraction contained calcite and kyanite in addition to quartz and albite (Figure 42). This fraction also contained an unidentified peak, this one located around 43° 2theta. This peak could indicate the presence of yet another unknown mineral in the sample.

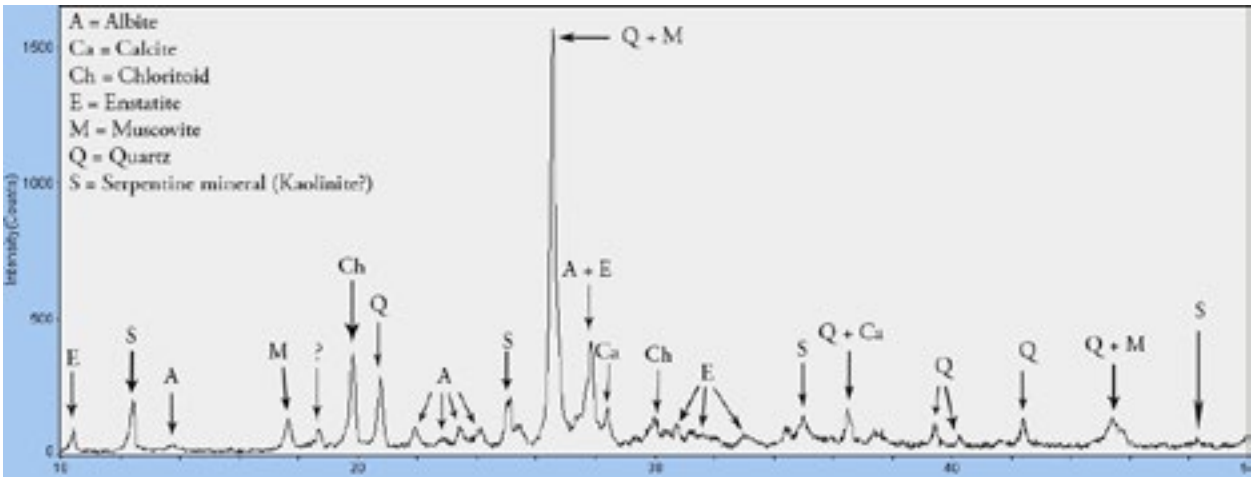

Figure 41: Diffractogram from the magnetically-susceptible fraction of a sand sample taken from the land bridge separating the Loch of Spiggie and the Bay of Scousburgh.

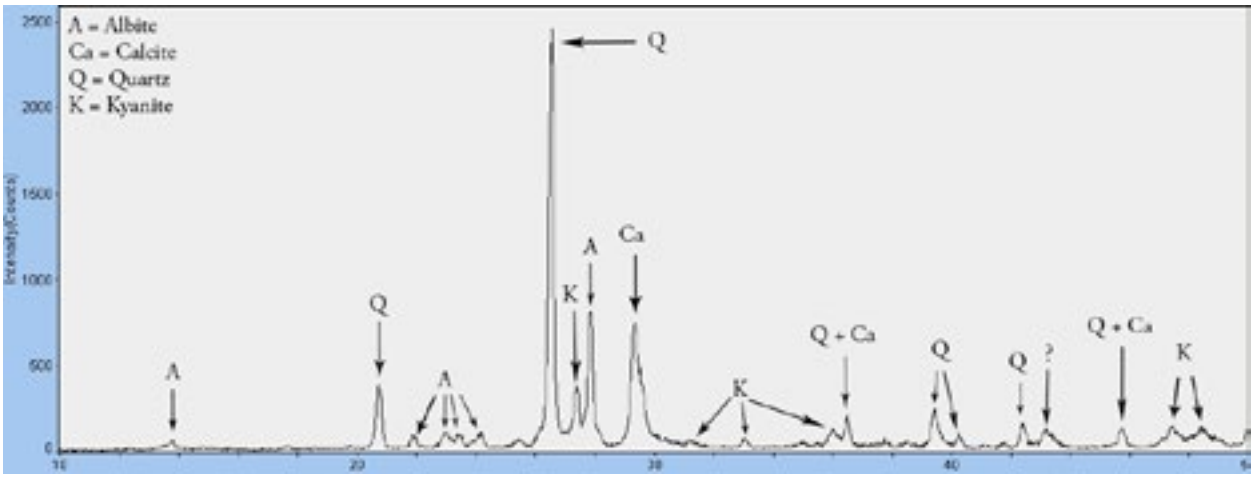

Figure 42: Diffractogram from the non-magnetically-susceptible portion of a sand sample taken from the land bridge separating the Loch of Spiggie and the Bay of Scousburgh

Grain Surface Morphology

The Spiggie land bridge was sampled at two depths. The analysis of surface grains was complemented by an analysis of grains from 40 cm in depth. Quartz grains from the surface or near-surface were generally angular in overall shape with a combination of weathered and fresh surfaces (Figures 43a - g).

Figure 43a shows one of the more angular grains from the surface of the land bridge. An older, large-scale grain breakage can be seen on this grain, but it has been weathered to a rough, low-relief feature. A zoomed-in view of one of the more recent large-scale blocky breakages can be seen in figure 43b. Small pits, as well as a large star fracture, that indicate subaqueous transport disrupt the smoother fracture surface. Both blocky and platey edge abrasion are present on this portion of the grain.

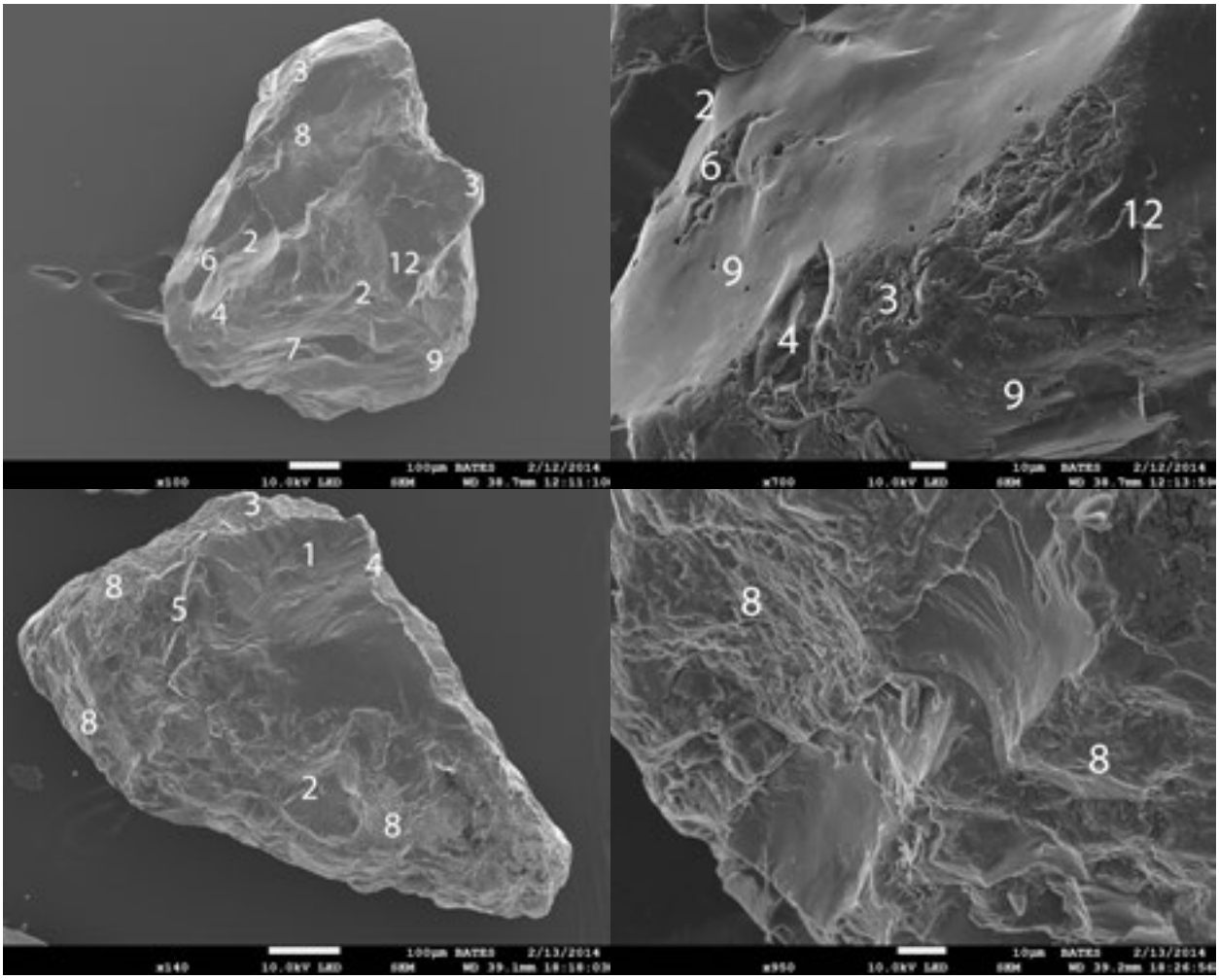

Figure 43a-d: Representative quartz grains from the surface of the land bridge separating the Loch of Spiggie and the Bay of Scousburgh. (a) and (c) are grains from the surface ofthe land bridge, while (b) and (e) are closer looks at specific textures on (a) and (c), respectively.

Other grains from the Spiggie land bridge are more weathered than the grain in figure 43a. Figure 43c shows one of the more intensely weathered grains from the surface of the Spiggie land bridge. The majority of this grain

is covered with a platey, aeolian surface texture. Interupting these textures, though, are some recent fractures and breakages. The largest of these comes in the form of a large conchoidal fracture occupying the northern area of the grain. Several other breakages exist, one of which is featured in Figure 43d. This image clearly shows the temporal relationship between the platey textures and the more recent fractures. It appears as if the edge of another grain scraped along the surface with enough force to gouge out the trench observed in the image.

The grains from 40 cm depth on the land bridge showed more extensive weathering than the grains found at the surface (Figures 43e-g). The grain in figure 43e illustrates this with a surface covered with a mixture of platey and subaqueous textures. Extensive edge abrasion has smoothed out the more angular features on the grain, giving it a rounder overall shape. The grain in figure 43g shows one of the more angular grains found at this depth. Despite the angular overall shape, significant edge abrasion is present.

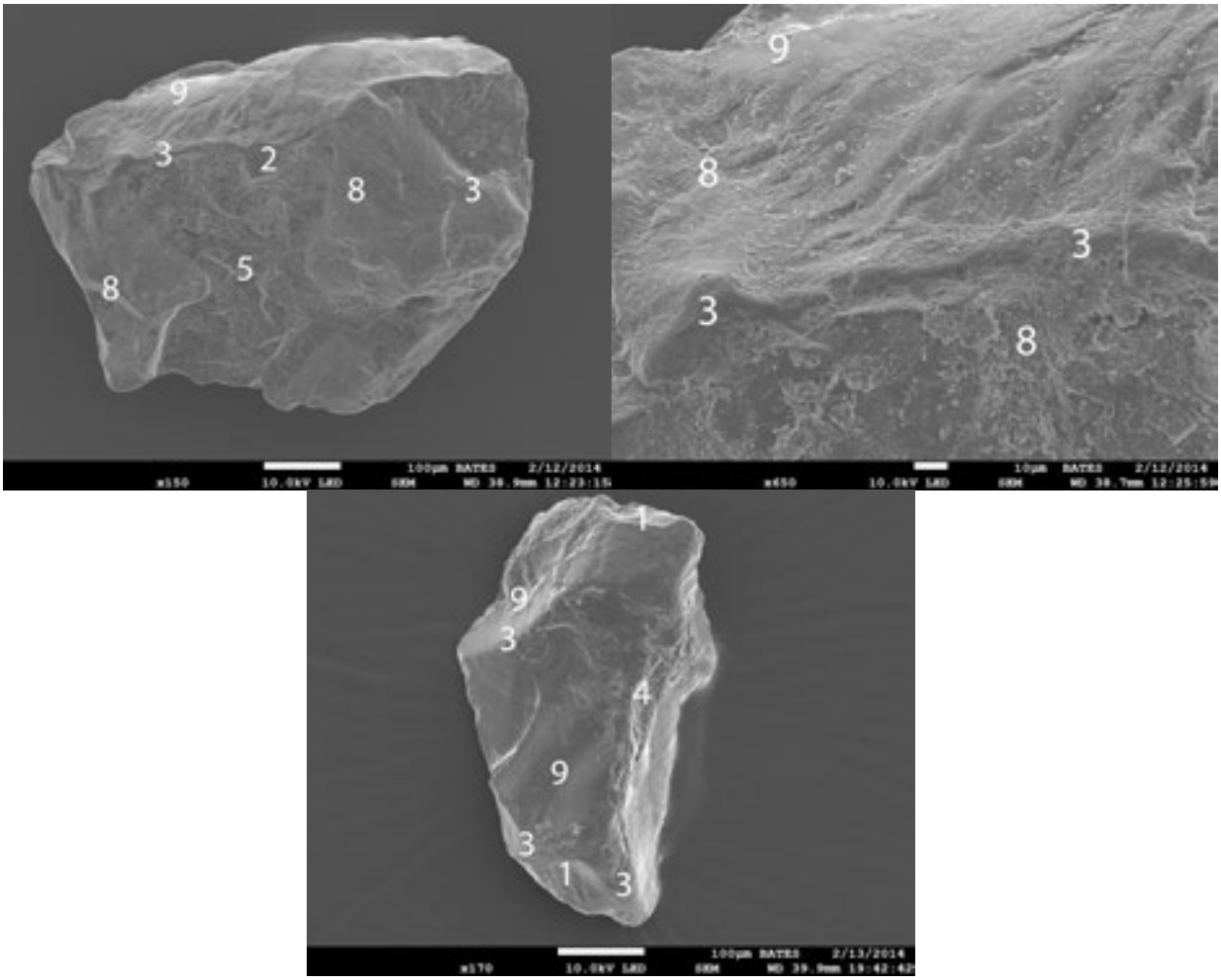

Figure 43e - g: Representative quartz grains from 40cm deep in the land bridge separating the Loch of Spiggie and the Bay of Scousburgh. (f) is a closer look at the area marked with a "3" in the northwestern section of the grain in (e)

Loch of Spiggie

Three cores from the Loch of Spiggie were collected during a previous field session by Jennifer Lindelof and Professors Michael Retelle and Beverly Johnson of Bates College. Sand units devoid of organic matter appeared in every core (Lindelof 2012). These sand units usually contained shell fragments and overlaid a dark grey coarse grained diamicton. The sand units were sampled and subjected to every analysis performed in this study.

X-Ray Diffraction

Because the sand samples obtained from the Loch of Spiggie core were only a 2 ccs in total volume, a magnetic separation was not performed. The resulting fractions would have been too small in volume to execute a powdered x-ray diffraction, so the sample was put through this analysis as a whole. The resulting diffractogram and interpreted minerals can be seen in figure 44. Besides quartz, the Loch of Spiggie sample contained muscovite, chloritoid, and a serpentine mineral. As with most of the other sites, this serpentine mineral is believed to be kaolinite, but further work needs to be done to confirm this. There was one peak in the Loch of Spiggie sample that caused confusion. This peak, located at approximately 27.5° 2theta, matches a kyanite diffraction peak, but none of the other kyanite peaks are present. Another, unidentified mineral may be present in the Loch of Spiggie samples.

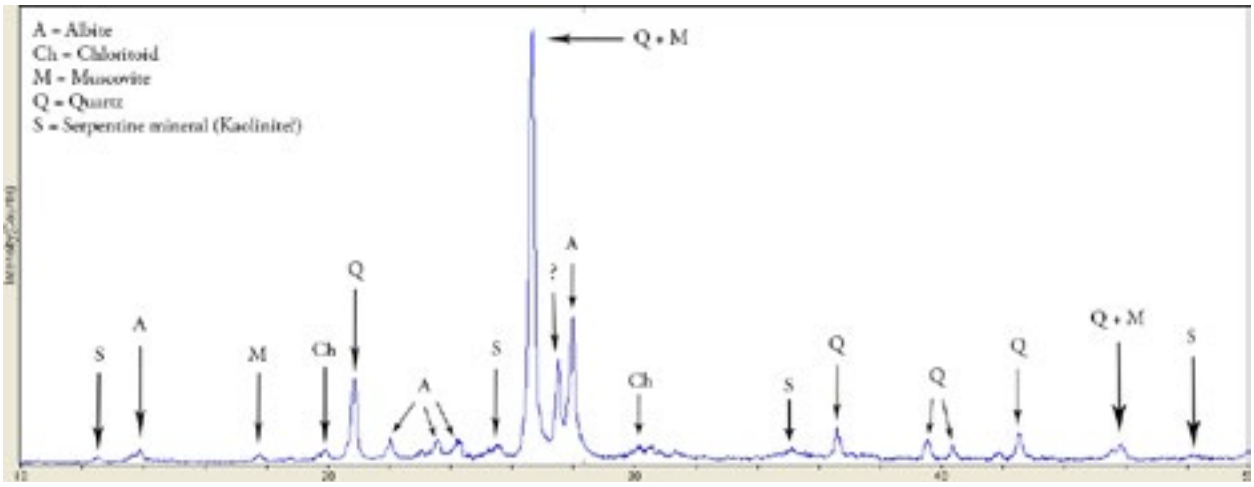

Figure 44: Diffractogram from a sand unit found in the Loch of Spiggie.

Grain Size Analysis

Samples from the Loch of Spiggie sand unit were too small to perform a seive grain size analysis. Instead, a camsizer was used to analyze the grain size distribution in the cores (Figure 45). The Loch of Spiggie sand has a mode of 0.2-0.3 mm with a negatively skewed distribution. The distribution is similar in appearance to that of the samples from the two bays and from the House of Broo.

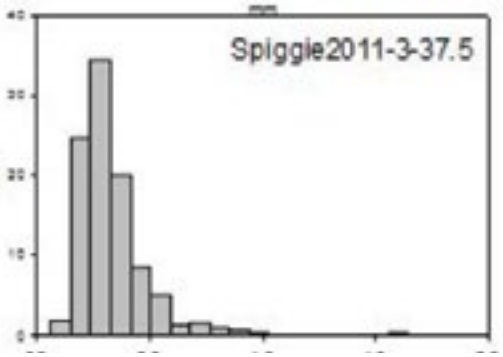

Figure 45: Grain size distribution for a sand unit found in the Loch of Spiggie. Results were produced by Professor Michael Retelle

Grain Surface Morphology

The grains from the Loch of Spiggie varied in their appearance, with overall shapes ranging from very angular (Figure 46e) to sub-angular (Figure 46a) and with differing degrees of weathering present. Only one of the sampled grains had an absence of fresh fractures (Figure 46a). This grain exhibited the highest degree of weathering observed in the Loch of Spiggie grains. The surface of this grain displayed a mixture of eolian and subaqueous impact textures. Every other grain from the Loch of Spiggie contained at least one fresh fracture with minimal edge abrasion. Six of the nine grains had a mixture of fresh, fractured surfaces and rougher, weathered surfaces (example in Figures 46c and e). The temporal relationships between these textures seem to vary from grain to grain. Figure 46c shows a grain with a surface primarily composed of fresh fractures. In a couple of locations, though, platey textures derived from eolian transport seem to have eroded these fresh surfaces. On other grains, such as the grain in Figure 46e, fractures appeared to have developed after the platey textures. Some of the fractures on these grains are located in a generally weathered region of the grain, but they themselves are smooth and fresh. This indicates that the fractures formed recently, removing a platey surface in the process. The occasional presence of star fractures on these grains indicates that they were put through extensive subaqueous transport at some point in their history.

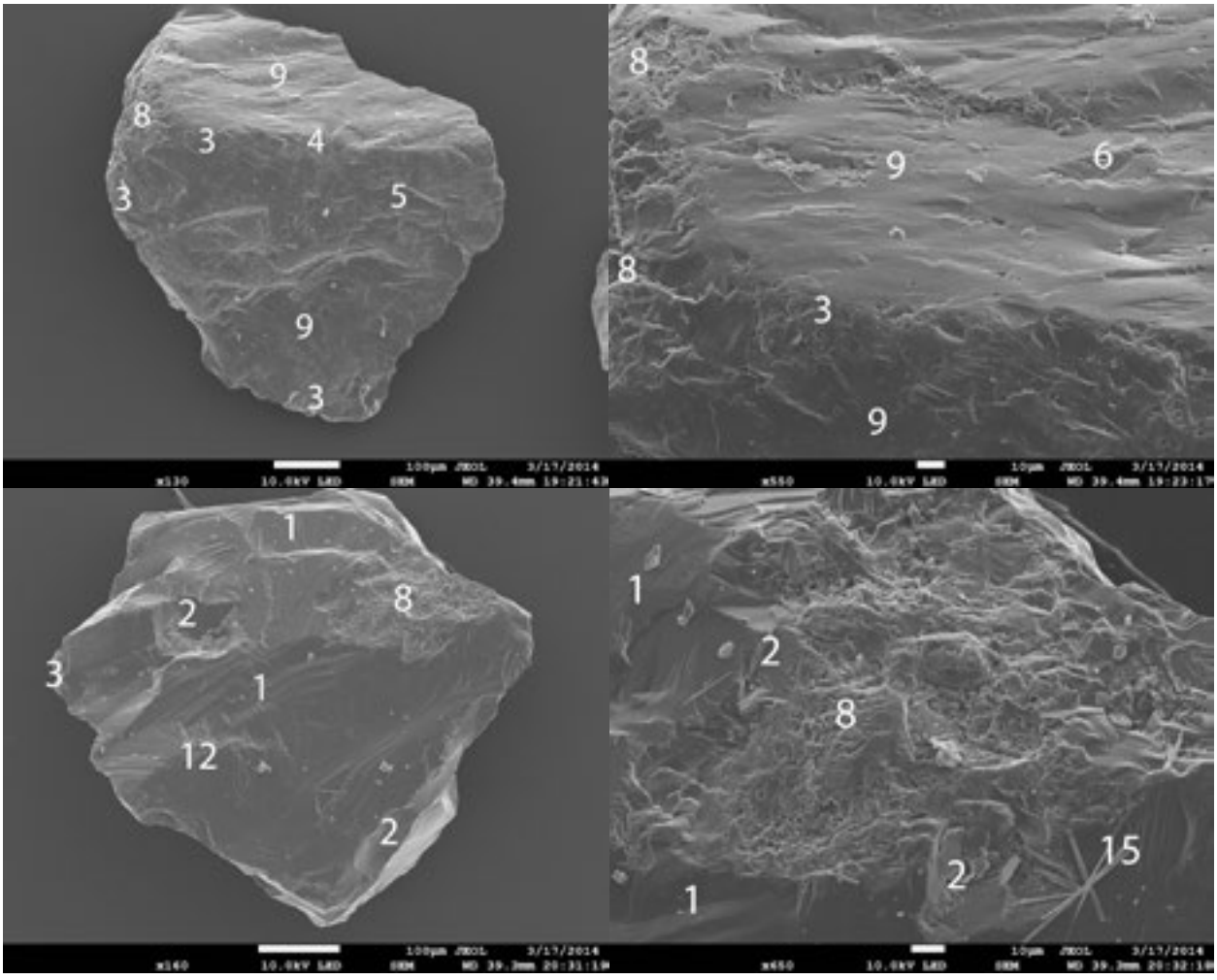

Figure 46a-d: Quartz grains from the Loch of Spiggie. (a) is the most weathered of the sampled grains, with (b) providing more detail on the surface. (c) is one of the most fractured grains found in the Loch of Spiggie, and (d) is a zoomed in image of an area that has experienced what appears to be extensive aeolian weathering

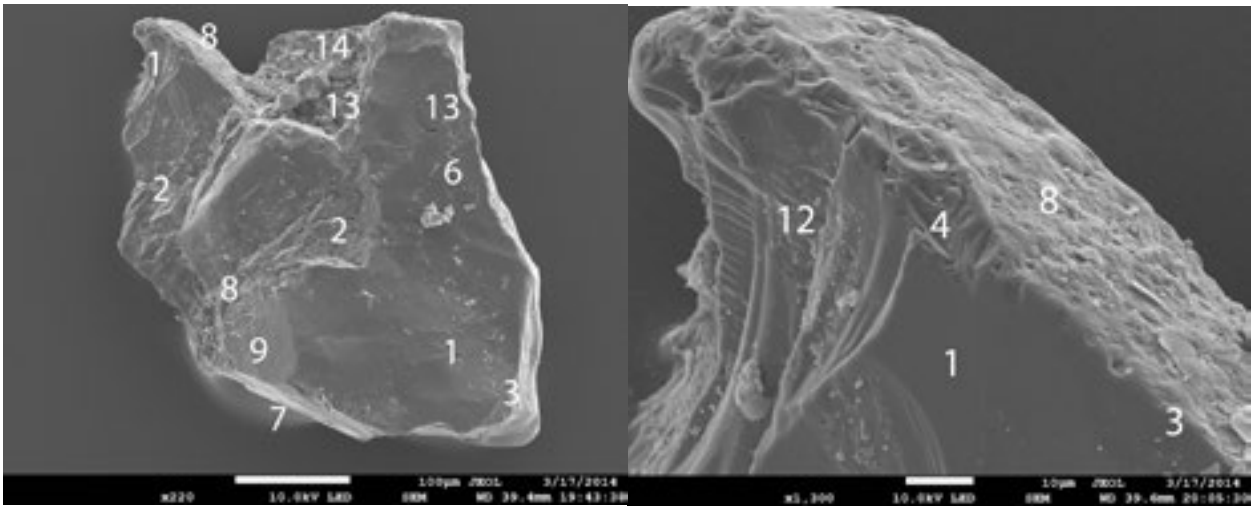

Figure 46e - f: Representative quartz grains from the Loch of Spiggie. (e) is a representative grain from the Loch of Spiggie, angular but with areas displaying clear aeolian weathering.

Loch of Brow

Five cores from the Loch of Brow were collected during a previous field session by Jennifer Lindelof with Professors Michael Retelle and Beverly Johnson of Bates College. A sand unit containing narrow organic bands and surrounded by an upper organic-rich silt layer and a lower gyttja unit was observed in four of the five cores (Lindelof, 2012). This sand unit was sampled and subjected to every analysis performed in this study.

X-Ray Diffraction

Like the Loch of Spiggie, the samples collected from the Loch of Brow sand unit were too small to magnetically separate prior to performing powdered x-ray diffraction. The diffractogram obtained from running the whole sample can be seen in figure 47. The sand in the Loch of Brow contained muscovite, chloritoid, and a serpentine mineral in addition to quartz and albite. There were no major unidentified peaks in the Loch of Brow sample, and there almost no background noise, leading to a conclusive identification.

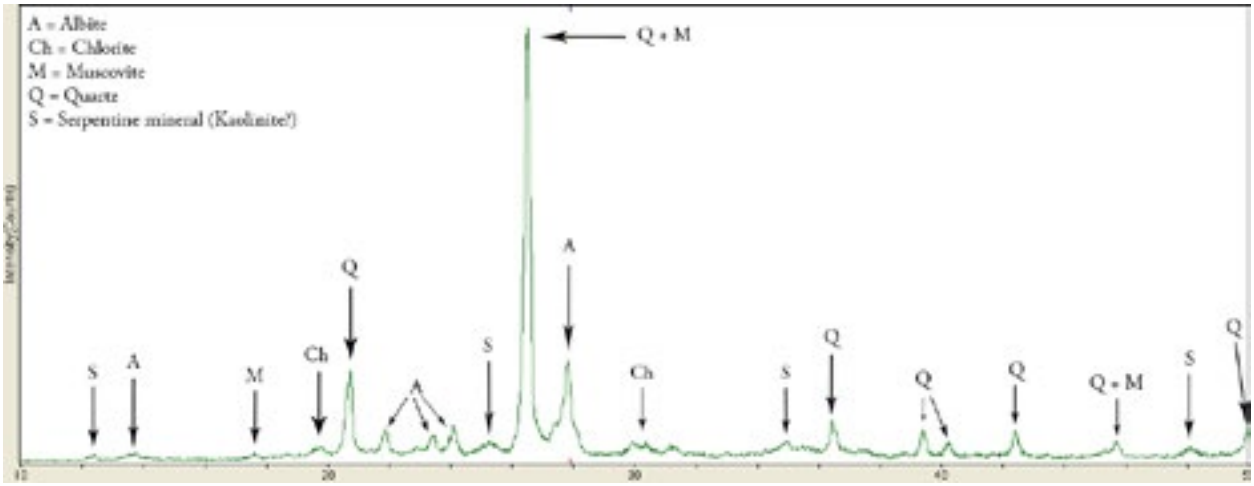

Figure 47: Diffractogram from a sand unit found in the Loch of Brow

Grain Size Analysis

Samples from the Loch of Brow sand unit were too small to perform a seive grain size analysis. Instead, a camsizer was used to analyze the grain size distribution in the core (Figure 48). The Loch of Brow has the finest grains and the highest degree of sorting of any location in the study area. The mode is in the 0.1-0.2 mm grain size range, and there is almost no skew to the distribution profile. The standard deviation is very low, illustrating the high degree of sorting observed in the Loch of Brow.

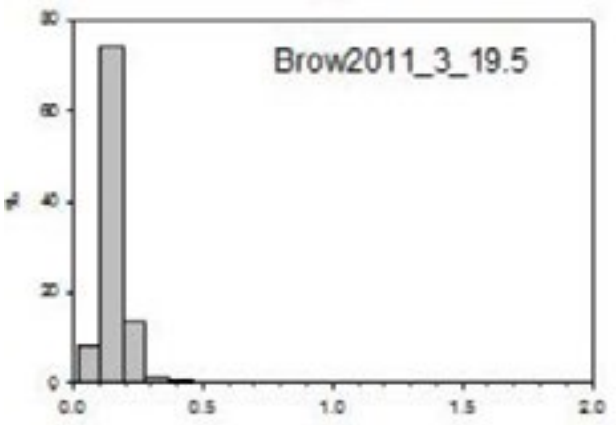

Figure 48: Grain size distribution from the Loch of Brow. Results were obtained by Professor Michael Retelle using a camsizer.

Grain Surface Morphology

The grains from the Loch of Brow (Figures 49a - f) were significantly more weathered than the grains from the Loch of Spiggie (Figures 46a - f). The freshest, most fractured grain from the Loch of Brow can be seen in Figure 49a. The majority of the surface of this grain is a smooth, fresh, fractured surface. It is only in the eastern hemisphere of this grain that weathering can be seen. The weathering comes in the form of platey impact features and limited chemical dissolution/precipitation (Figure 49b). No other grain from the Loch of Brow sample comes close to this degree of fresh fracturing, and I am considering it an outlier. The most weathered grain from the Loch of Brow is visible in Figure 49c. This grain displayed no fresh conchoidal fractures or breakages of any kind. Overall, it has a sub-rounded shape and is covered with a platey surface texture. Although this is the most intensely weathered grain found in the sample selection, many grains displayed weathering close to this degree. On every grain, the weathering came in the form of platey surface textures (Figures 49d and f) and, to a more limited degree, chemical weathering in the form of silica dissolution and precipitation. The majority of the grains from the Loch of Brow sand unit are similar in appearance to the grain visible in Figure 48e. Their surfaces are covered in a platey surface texture which is interupted in some areas by fresh conchoidal fractures. These conchoidal fractures are clearly recent features derived from large impacts which likely occured shortly before deposition.

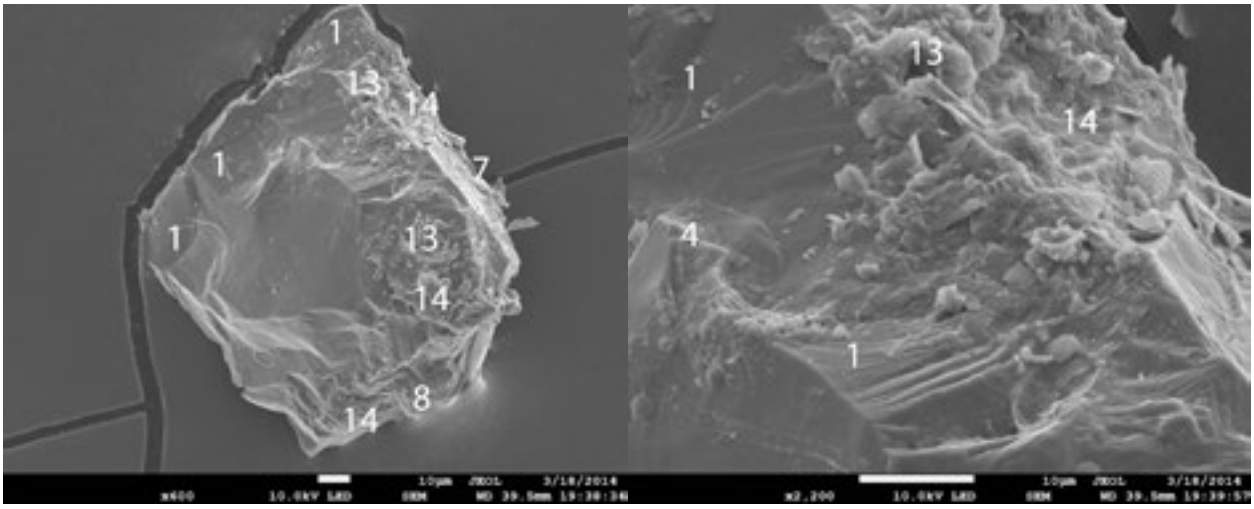

Figure 49a & b: Quartz grains from the Loch of Brow. (a) is the freshest, most fractured grain found in the Loch of Brow. (b) is a closer view of the northwestern area of the grain in (a)

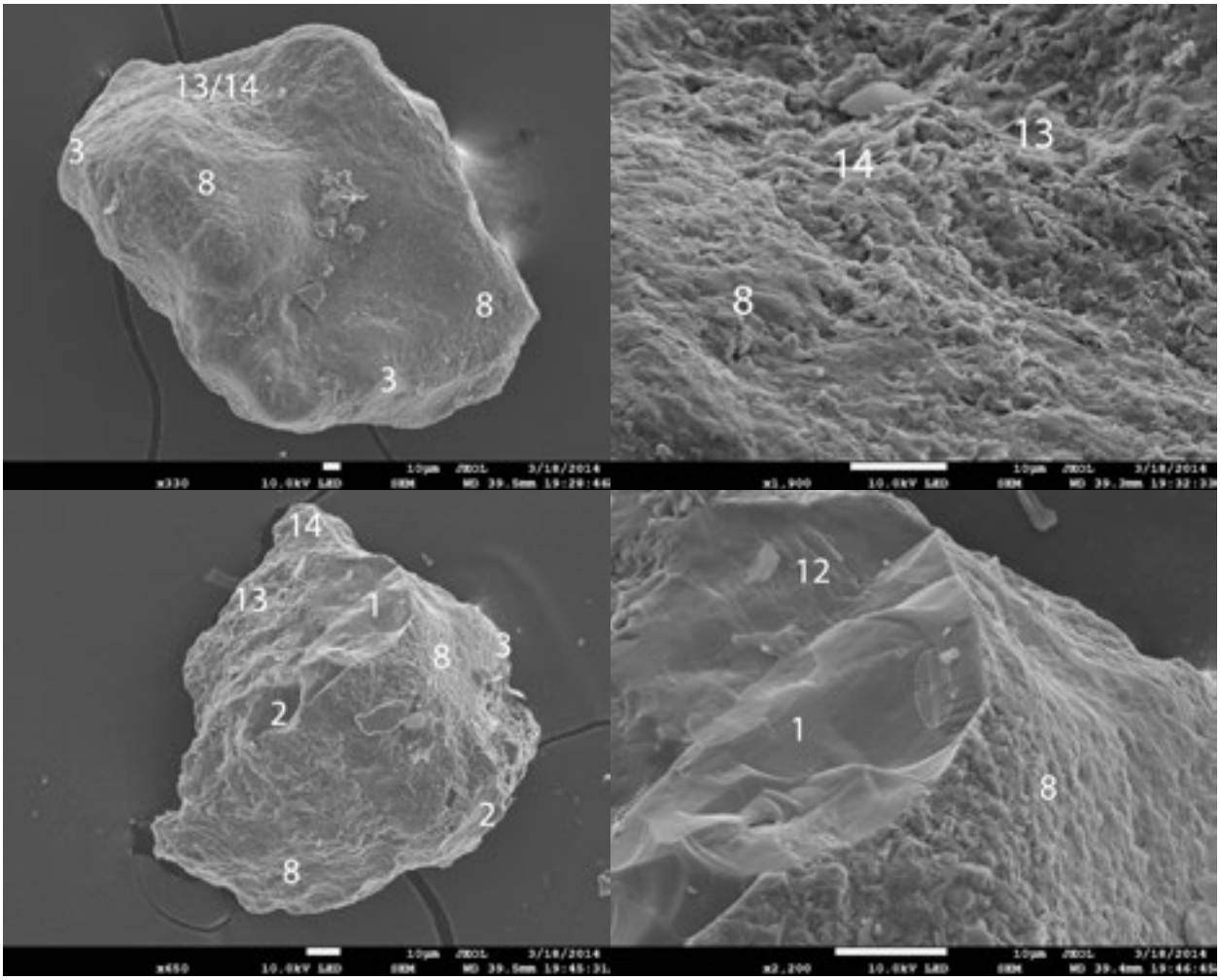

Figure 49c - f: Quartz grains from the Loch of Brow. (c) is the most weathered grain observed in the Loch of Brow, with a complete absence of fresh fractures. (d) is a close up of the northern area of the grain in (c). (e) is a representative grain from the Loch of Brow, weathered but with one or two fresh fractures. (f) is a closer look at the fracture in (e).

Generalized Grain Size Results

In order to observe larger-scale patterns in grain size distribution, figure 50 was created. The averaged mean grain size results (in mm) are shown in yellow, while the inclusive graphic standard deviation values (in mm) are shown in red. On average, the Pool of Virkie contains the largest grains, while the western side of the Bay of Scousburgh has the smallest. The eastern side of each bay contains coarser grains than the west side, with a lower standard deviation.

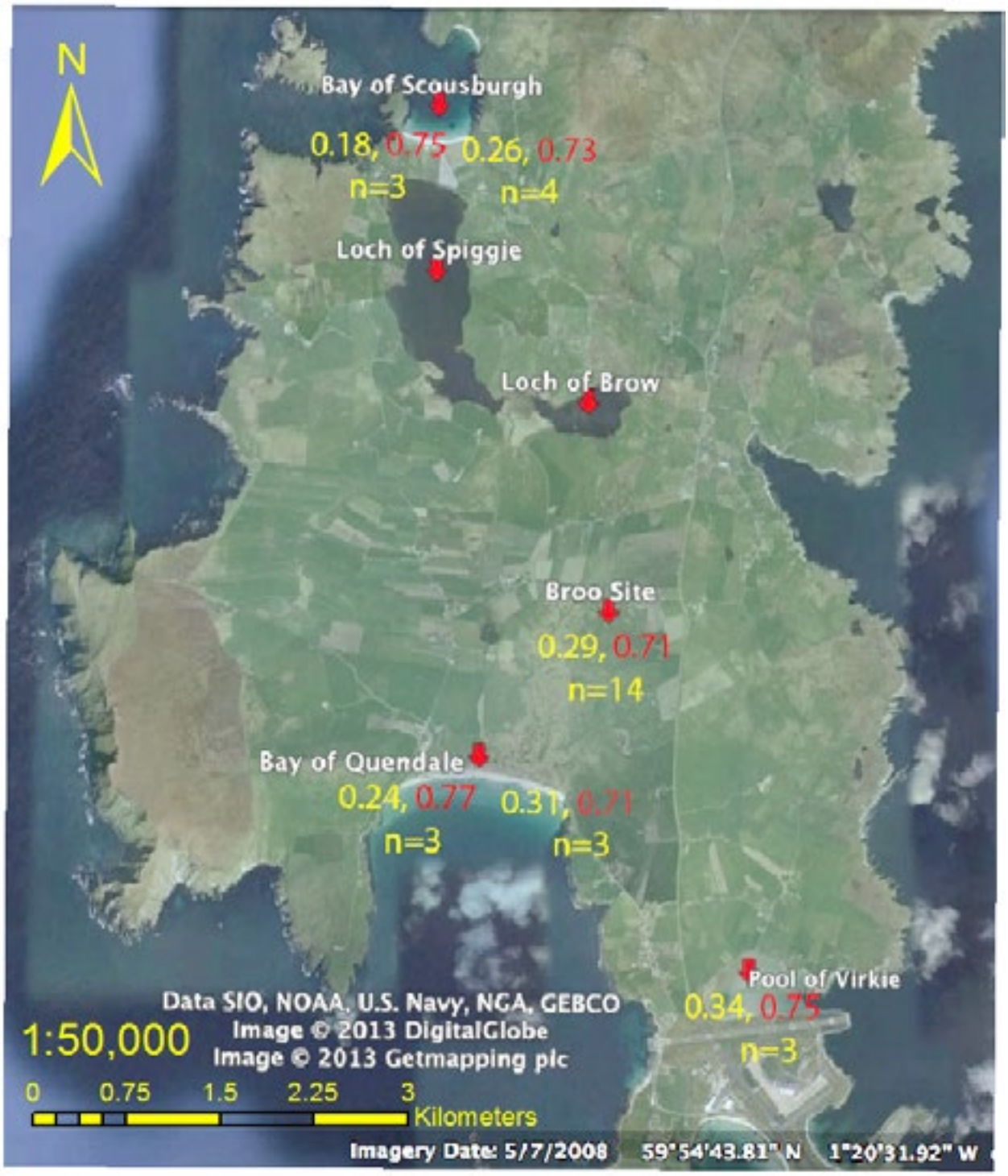

Figure 50: Generalized grain size analysis results for the entire study area. Averaged mean grain size results (in mm) are in yellow, while the inclusive graphic standard deviation results are in red.

Discussion

Mineralogical Comparisons

Bays of Quendale & Scousburgh

The two main sources of sand in the study area, the Bay of Quendale and the Bay of Scousburgh, were compared in order to get a sense of the overall mineralogy of the area. In figure 51, the magnetically-susceptible portions of each sample are presented, while figure 52 shows the non-magnetically susceptible portion of each sample. In each figure, the Bay of Quendale diffractogram is red, while the Bay of Scousburgh diffractogram is blue.

Quartz and albite appear in abundance in both samples, adding an element of difficulty to the identification of other accessory minerals present. It is apparent that the magnetic separation was not entirely effective. This could be the result of several factors, including a non-effective amperage or a flow of sediment that was too fast, all of which are based in human error. However, the inclusion of quartz and feldspar appears in all samples, enabling the reliable comparison of diffractograms.

The magnetically-susceptible fractions from the Bay of Scousburgh and the Bay of Quendale appear nearly identical (Figure 51). The intensity of some peaks vary (see the chloritoid peaks in figure 51), but no peaks appear in only one sample. Accessory minerals shared between the two locations include muscovite, chloritoid, enstatite, and a serpentine mineral. Currently, there is one unidentified peak shared between the diffractograms (Figure 51), indicating the presence of an additional mineral in the samples. This unidentified peak is present in both the Bay of Quendale and Bay of Scousburgh samples, though, and therefore holds no value as a provenance marker.

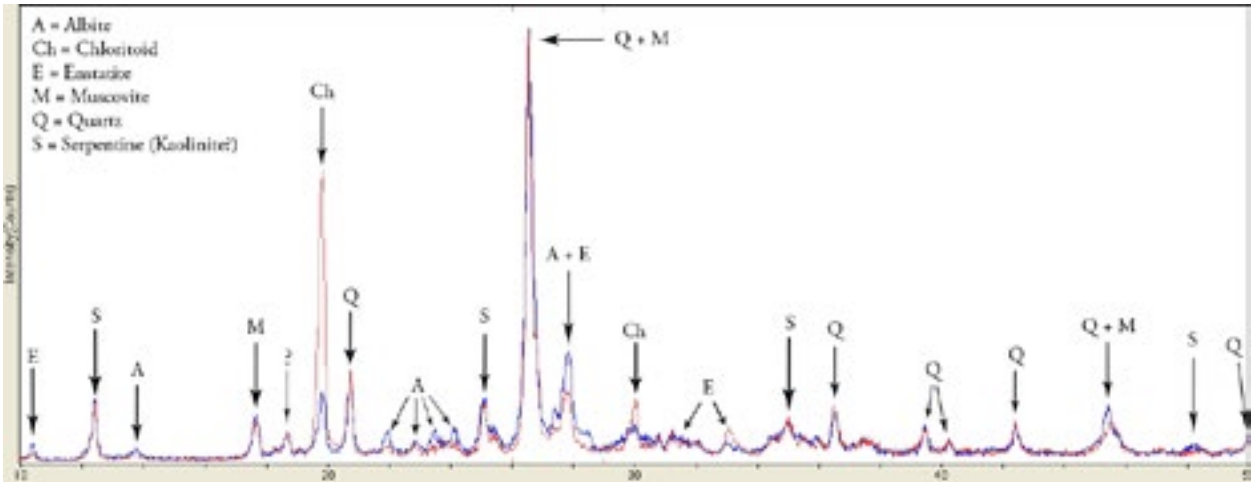

Figure 51: Comparison of the magnetically-susceptible portions of sand from the Bay of Quendale and the Bay of Scousburgh. The diffractogram from the Bay of Scousburgh is blue while the Bay of Quendale diffractogram is red

In the non-magnetically-susceptible portion of the sands (Figure 52), there are some mineralogical differences between the Bay of Quendale and the Bay of Scousburgh. Both samples contain quartz, albite, and calcite, but there are several peaks present in the Bay of Scousburgh sample that do not appear at the Bay of Quendale. Marked in blue, the majority of these peaks have been attributed to kyanite. There still exists a peak in the

Scousburgh diffractogram that is unaccounted for and it is possible that one or more of the kyanite peaks is shared with this unidentified mineral, making its identification more complicated. The presence of kyanite along with the lone unidentified peak in the Bay of Scousburgh samples provides a distinction from the Bay of Quendale that allows provenance tracing to be performed in the study area.

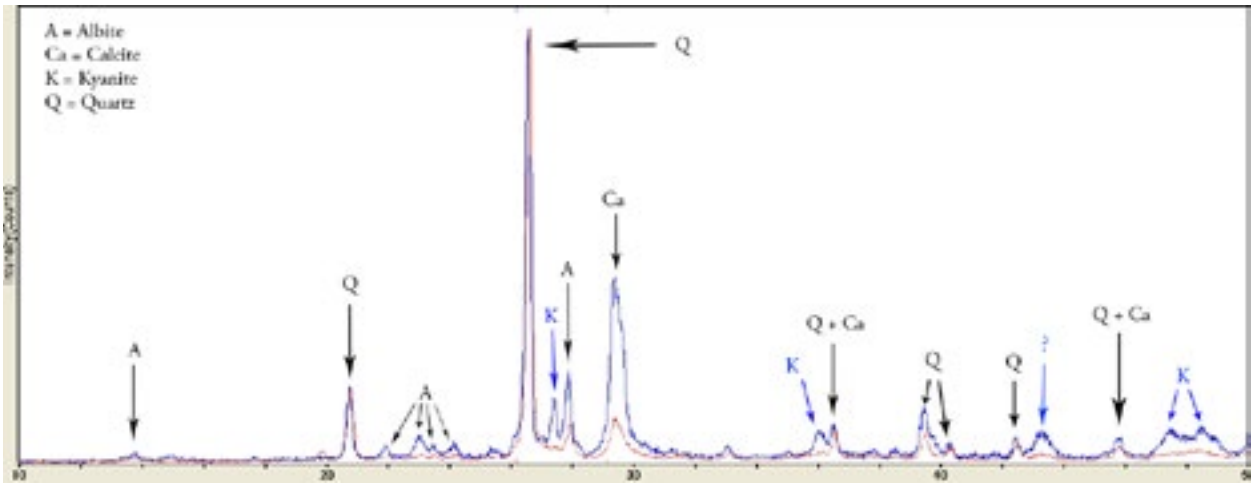

Figure 52: Comparison of the non-magnetically-susceptible portions of sand from the Bay of Quendale and the Bay of Scousburgh. The diffractogram from the Bay of Scousburgh is in blue while the Bay of Quendale is in red. Peaks unique to one diffractogram are labeled in its color.

Lochs of Brow & Spiggie

A comparison between the diffractograms from the Lochs of Brow and Spiggie can be seen in figure 53. In this comparison, the diffractogram from the Loch of Spiggie is blue while the Loch of Brow diffractogram is green. The diffractograms are similar in appearance and show that many of the accessory minerals observed in the bay samples travelled together to the lochs. The only minerals lost during transport appear to be enstatite, kyanite ,and the mineral(s) responsible for the unidentified peaks in the magnetically-susceptible fraction of the bay

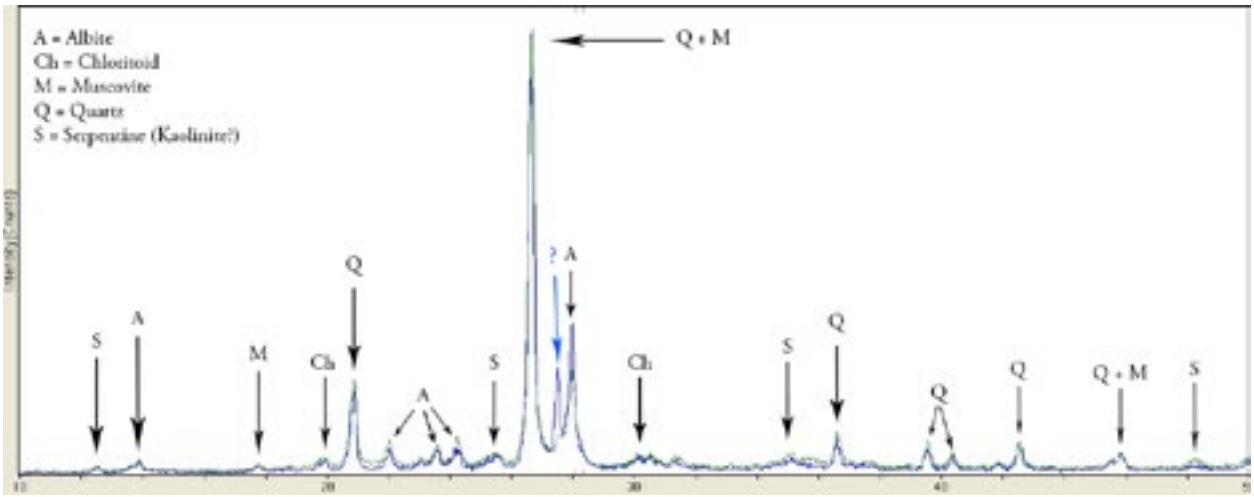

Figure 53: Comparison of the diffractograms from the Lochs of Spiggie and Brow. Note that the Loch of Spiggie diffractogram appears as a hazy gray while the Loch of Brow diffractogram is a solid white

samples (Figure 51). Additionally, calcite is not present in the loch samples, as it most likely dissolved out of the sand in the more organic-rich environments within the lochs.

There is only one peak that the loch samples do not share (blue label in figure 53). This peak, found only in the Loch of Spiggie samples, coincides with a kyanite peak, but the other kyanite peaks are not present. Looking at figure 52, other kyanite peaks can be seen in the Bay of Scousburgh samples, but these peaks do not appear in the Loch of Spiggie samples. The mineral responsible for this peak remains a mystery, but this particular peak is shared only between the Bay of Scousburgh and the Loch of Spiggie. The absence of this peak in the Loch of Brow suggests that the sand unit contained in its cores does not trace its origins to the Bay of Scousburgh. The more likely origin for this sand is the Bay of Quendale, which does not contain either kyanite or the peak located just before 28° 2theta.

The mineralogical evidence presented adds weight to the hypothesis that the sand unit in the Loch of Spiggie was created during a sand invasion event in the Bay of Scousburgh. The evidence also suggests that the sand unit found in the Loch of Brow originated at the Bay of Quendale. These hypotheses, as well as the others presented in this thesis, are explored further in the following sections, where the results from physical analyses are discussed in two general areas. As mentioned in the introduction, the Spiggie area encompasses the Bay of Scousburgh, the Loch of Spiggie, and a low-lying land bridge separating them (figure 2). The Quendale area stretches from the Bay of Quendale to the Loch of Brow and includes the Quendale links and the Broo archaeological site (figure 2).

Spiggie Area

Grain Size Analysis

The Loch of Spiggie had sand with similar grain sizes and sorting values as the sand from the Bay of Scousburgh (Figure 54a & b). There is only a slight difference in the grain size distribution profiles of the Bay of Scousburgh and the Loch of Spiggie, with the loch exhibiting a slightly more negative skew than the bay. The slight fining observed between the Bay of Scousburgh and the Loch of Spiggie suggests a powerful transport mechanism, one that would carry more than just the fine portion of the sand from the Bay of Scousburgh.

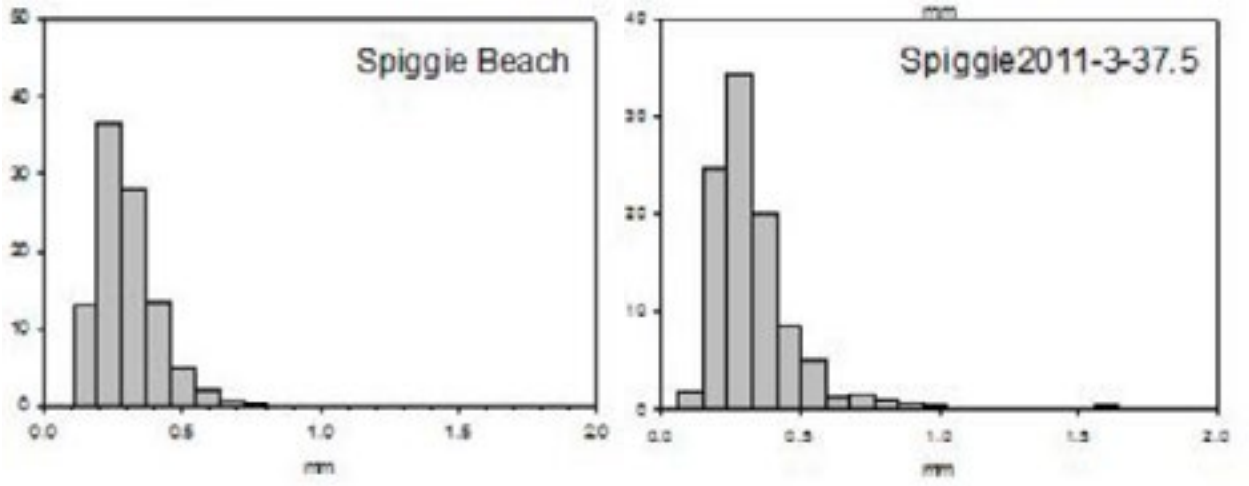

Figure 54a & b: Grain size distribution profiles from the Bay of Scousburgh (a) and the Loch of Spiggie (b). Data were collected by Professor Michael Retelle using a camsizer grain analyzer

Grain Surface Morphology

Overall, grains from the Bay of Scousburgh were angular, with many fresh, fractured surfaces and clear signs of subaqueous transportation. Blocky breakages, conchoidal fractures, and even grinding and crushing features were present on the majority of the Bay of Scousburgh grains, indicating that a significant portion of the sand was recently weathered out of glacial sediments (Bull & Morgan 2006, Mahaney 1990, Krinsley 1968, Whalley & Krinsley 1974). Exposed till deposits on the eastern side of the Bay of Scousburgh provide a potential source for this portion of the sand found in the bay.

This characteristic angularity and freshness is seen again on the Spiggie land bridge surface grains. Many of the surface grains from the land bridge were very angular and displayed fractures with platey edge abrasion (figure 43b). Some grains contained more aeolian weathering textures than others, but almost all contained some fresh fractures associated with more severe aeolian transportation (Marshall et al. 2012). The limited presence of subaqueous impact textures, including star-fractures associated with more intense transportation, indicates that this sand was subjected to some sort of brief, rapid transportation by subaqueous means (Bull & Morgan 2006).

The grains from a depth of 40cm in the land bridge are more weathered than the surface grains, with extensive impact textures which indicate a longer and more severe transportation history. The subaqueous features appear to be overlain by the aeolian textures, establishing a temporal relationship between these two transportation stages. Following the energy regimes put forth by Marshall et al. (2012) (Figure 18), the aeolian textures on the land bridge grains suggest moderately-intense wind transportation after deposition by subaqueous means. These deeper grains are still very angular, and may have also been recently derived from a glacial sediment. The decrease in weathering as one moves up to the surface from depth suggests that the exposed till was being intensively weathered during the period of deposition, with fresher quartz grains being deposited on older, more weathered grains. All of the grains from this location, though, appear fresher and more angular than grains from the Quendale area.

The quartz grains from the Loch of Spiggie share the angularity observed at the Bay of Scousburgh and the Spiggie land bridge (figures 46a - f). Extensive subaqueous textures appear on some of these grains, while others display more fractured surfaces. Aeolian textures also appear on many of the grains, but to less of an extent than observed at the Bay of Scousburgh and the Spiggie land bridge. The mixture of fractures and extensive weathering surfaces suggests that the Loch of Spiggie grains were subjected to rapid and violent transportation during storm events, when the intensity and velocity of transportation can impart such intense and extensive features (Costa et al. 2012).

Summary

Previous work undertaken by Jennifer Lindelof (2012) showed an absence of gyttja under the sand units in the Loch of Spiggie. The sand unit found in the cores showed influence from a marine environment and was located over a coarse-grained diamicton with marine signatures (Lindelof 2012). These observations indicate that the Loch of Spiggie was open to a marine environment prior to the land bridge forming. The results from this study agree with these indications, suggesting a series of events where a land bridge formed from storm washover, creating the sand unit in the Loch of Spiggie in the process.

The physical analysis results agree with the mineralogy results, strongly suggesting a connection between the sand found in the Bay of Scousburgh, the Spiggie land bridge, and the Loch of Spiggie. The characteristic angularity of the Bay of Scousburgh grains is seen across all of these locations, but the stress of transportation imparted unique textures on the quartz grains. Grains from depth in the Spiggie land bridge display subaqueous impact features overlain by aeolian textures, while the surface grains contain a higher ratio of aeolian textures.

Grains from the Loch of Spiggie sand unit show more subaqueous impact textures than other locations, and appear to have undergone rapid, violent subaqueous transport.

These patterns observed in the grain surface morphology, combined with the slight fining observed in the grain size analysis, points towards a local deposition model consisting of one or more large-scale storms that relocated sand from the Bay of Scousburgh into the Loch of Spiggie, forming the land bridge as it did so. In areas with low, uniform backbeach elevations, or where a shallow inlet exists, strong storms can produce washover that penetrates hundreds of meters inland (Morton & Sallenger 2003). The distance and volume of penetration can increase when the wind direction and the angle of wave approach are both directed onshore.

The angular nature of the grains observed througout the Spiggie area add weight to this theory. A storm of high magnitude would erode the till outcrops located at the Bay of Scousburgh on a large scale and would impart chipping and fracturing features on grains during transportation (Bull and Morgan 2006, Costa et al. 2012, Krinsley 1968). It is unlikely that all, or even the majority, of the grains in the Spiggie area were recently eroded out of glacial sediments, but glacial signatures can be seen on grains throughout the sample sites. It is likely, though, that every grain experienced turbulent transportation during this strong storm event, leading to the overall angular nature of the grains found in this area. The grains in the Loch of Spiggie display textures indicating rapid, intense subaqueous transport (Figure 46b), agreeing with the proposed theory of intense storm action (Costa et al. 2012). If included in a large-scale washover, these grains would have been subjected to transportation of hundreds of meters in a matter of minutes (Morton & Sallenger 2003). The aeolian textures observed on the surface of some of these grains (Figure 46d & f) may have been derived during this turbulent transportation, when they may have briefly been exposed to strong, storm-driven winds at the surface. Further supporting this theory are the grain size analysis results for this area, which do not show a significant decrease in grain sizes or sorting between the Loch of Spiggie and the Bay of Scousburgh (Figure 54a & b). A large-scale storm would have the energy required to transport every grain size observed at the Bay of Scousburgh for a considerable distance, and the slight fining observed in the Loch of Spiggie is the extent of grain size distribution changes we would expect to see.

The land bridge separating the Loch of Spiggie from the Bay of Scousburgh shows signs of prolonged deposition. The grains at depth contain more weathering features, including subaqueous features, than the grains at the surface (Figures 43e - g), indicating that they experienced longer, or more intense, transportation before deposition. The subaqueous features from the grains at depth were likely derived from the initial sand invasion event, the strong storm which resulted in a large-scale movement of sediment onshore. The overlying aeolian textures suggest that following the initial deposition above sea -level, these grains were then subjected to aeolian transportation. The extent of the aeolian textures indicates a prolonged period of surface habitation for these grains before their eventual burial. The surface grains from the land bridge display fresher textures than these deeper grains (Figure 43a), indicating that their deposition happened more recently. The initial sand bridge formed during the first sand invasion event likely acted as a barrier onto which waves would break (Elger et al. 2001). This new dynamic, with a closed inlet, likely created a coastal system similar to what we observe today, with a collection of sand in the form of a foredune that backs the beach. As time progressed and further storms hit the area, this sand most likely accumulated on the land bridge, eventually resulting in the formation that we observe today. The decreased weathering we observe in the surface grains reflect this potential series of events. Subsequent storms could have further eroded the till outcrops observed near the Bay of Scousburgh, and the limited subaqueous textures observed on the surface grains indicates that the grains were then transported as washover onto the foredune area (Morton & Sallenger 2003). Aeolian processes then carried the grains to their current locations on the land bridge, leaving overlying aeolian textures on the grains (Figures 43a - f).

Quendale Area

Grain Size Analysis

A clear decrease in grain size and increase in sorting is evident in a transect from the Bay of Quendale to the Loch of Brow (Figures 55a-c). These two trends support the notion of strong winds blowing sand north from the Bay of Quendale, with the finer component ultimately reaching the Loch of Brow. The Quendale transect displayed decreasing sorting with distance inland, but this appears to be caused by the presence of a large hill at the end of the transect (Figure 56). The dunes of the Quendale Links increase in size at the base of this hill, suggesting that it acts as a catchment for sand. Regular winds, which were persistent and strong during the Little Ice Age (Bigelow et al. 2005) likely transported sand north across the Links to the base of this hill, where the increased slope negated the continued transportation of the sediment. Storm events, with stronger winds, could have picked this sand up from the base of the hill and deposited it in large volumes on the Broo archaeological site, located on the western flank of the hill. At the Broo archaeological site there are multiple observed organic horizons that separate the sand into several layers. Each of these layers, with a notable exception to be mentioned, show similar mean grain sizes and sorting values. The organic horizons and lack of variance with depth indicate that the total volume of sand at the site was deposited by a series of intense storms as opposed to a single storm. Similar organic horizons are seen at the Loch of Brow, but are fewer in number than those seen at the Broo site. A maximum of three horizons are present in the Loch of Brow cores, but this number is only seen in one of the cores (Lindelof 2012). Others have one, or zero, organic horizons, indicating that the sand unit in the loch is derived from only two or three major storms. The sand in the Loch of Brow is fine and very well sorted, suggesting that it is the fine component of a larger sand sample which was blown farther than the rest of the sample. The sand unit was present in every core taken from the Loch of Brow except for the core from the western side (Figure 57) (Lindelof 2012). This adds weight to the proposed hypothesis of a Quendale origin for the sand unit, as sand coming from the Bay of Scousburgh would have surely been deposited in larger volumes in the western portion of the Loch of Brow.

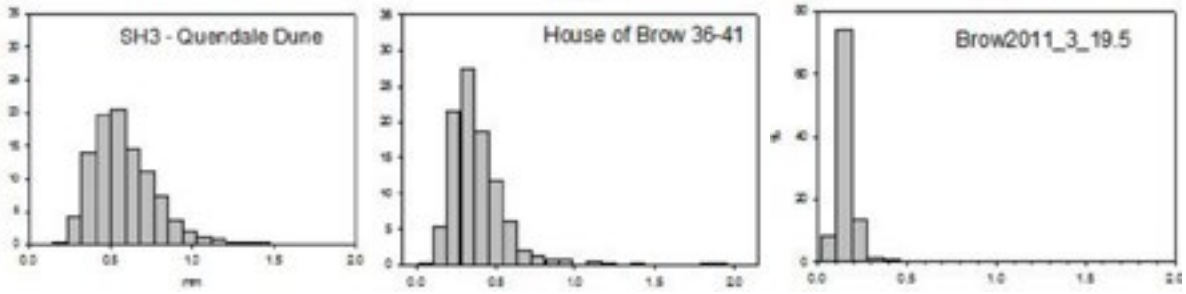

Figure 55a-c: Grain size distribution profiles from the foredune backing the Bay of Quendale (a), the Broo site (b), and the Loch of Brow (c). Data were collected by Professor Michael Retelle.

Grain Surface Morphology

The Quendale transect grains displayed almost entirely aeolian textures (Figures 31a - e). A general trend of increased aeolian weathering with distance inland confirms that the Quendale Links were formed from sand originating in the Bay of Quendale, with sand found further inland having experienced more time travelling in an aeolian dune environment. Grains from the Broo site displayed similar aeolian textures, but contained some more recent fractures. Marshall et al. (2012) showed that conchoidal fractures and blocky breaks can result from

Figure 56: A view from the third stop of the Quendale Transect looking north. The Broo site is located in the approximate center of this photo, on the western flank of the hill. Note the increased dune size at the base of the hill.

intense aeolian transport with grains impacting at velocities of more than 10 m/s (Figure 18). The freshness of the fractures observed on the Broo grains indicates that they were subjected to this intense aeolian transport directly before deposition and burial, after which they were only subjected to minor physical weathering. Many of the grains from the Broo site, including those from deeper layers such as B-6, displayed limited amounts of chemical weathering in the form of silica dissolution and precipitation. This observation, along with the observed organic horizons separating the sand layers, suggests that enough time passed between the deposition of each sand unit for vegetation to form on the surface. Organic acids leaching downward from this vegetation would create a more acidic environment below it, resulting in the dissolution and subsequent precipitation of silica on the surface of quartz grains (Bull and Morgan 2006, Hellend et al. 1997, Krinsley 1968). This vegetated cover must have been short lived, though, as the chemical weathering is limited on the observed grains. Once the vegetation died after being covered by another layer of blown sand, the unit below it increased in pH, eventually becoming neutral enough to halt the dissolution of silica.

Figures 49c - f show that quartz from the Loch of Brow display textures associated with powerful aeolian transport . The majority of the grains show a predominately weathered, aeolian texture interupted by fresh fractures which were likely formed during intensive aeolian transport (Bull and Morgan 2006, Costa et al. 2013, Marshall et al. 2012, Krinsley 1968). The lack of subaqueous features indicates that the grains were covered by other sand

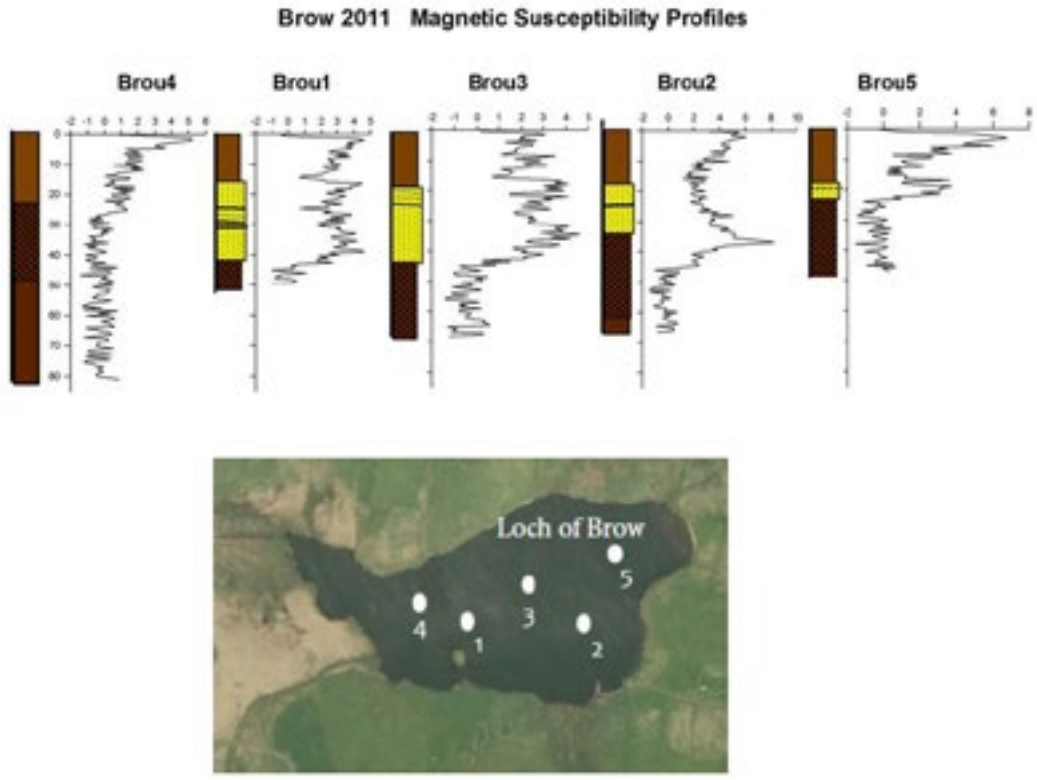

Figure 57: Magnetic susceptibility profiles of cores collected from the Loch of Brow. The yellow portion of the cores is a sand unit with thin organic horizons (black lines). Data were collected by Professor Michael Retelle.

shortly after deposition, limiting their exposure to subaqueous transportation. Figure 49a shows a grain that experienced intensive fracturing, while figure 49c shows a grain that experienced virtually no fracturing, but these grains are not representative of the entire sample. Despite their non-representative nature, these grains still support the notion of intense aeolian transportation. The angular nature of the grain in figure 49a makes it more susceptible to fracturing (Figure 18), which can explain the severity of the fracturing observed (Marshall et al. 2012). The non-fractured grain in figure 49b is entirely covered with a platey, aeolian texture, supporting the conclusion of aeolian transport, despite not displaying characteristics of intensive aeolian movement.

Summary

Lindelof (2012) showed that the sand unit in the Loch of Brow is surrounded by an upper organic rich unit and a lower gyttja unit. Geochemical results showed a strong terrestrial signature in the organic unit, suggesting that the Loch of Brow was never exposed to a marine environment (Lindelof 2012). The mineralogical and physical analyses performed in this study indicate that the sand from the Loch of Brow can trace its provenance to the Bay of Quendale

Mineralogically, the sand found at the Bay of Quendale, the Quendale Links, the Broo archaeological site, and the Loch of Brow are similar. All are missing the accessory minerals unique to the Bay of Scousburgh, as well as the peak that differentiates the Loch of Spiggie from the Loch of Brow. The physical evidence mentioned in this discussion confirms the hypothesis that the inland sand invasion responsible for the formation of the

Quendale Links and the burial of the Broo site happened in stages. Additionally, results from the grain size analyses and grain surface morphology studies further confirm the hypothesis that the sand unit in the Loch of Brow originated in the Bay of Quendale.

Local and Regional Implications:

Local

This study indicates that the coastal changes observed in the Spiggie and Quendale areas were the result of different processes. The sand invasion in the Spiggie area appears to be the result of a high-magnitude storm that produced extensive, thick washover. This washover deposited a sand unit in the Loch of Spiggie that was then covered by organic rich silt. Simultaneously, a low-lying sand bridge was deposited that separated the Loch of Spiggie from the Bay of Scousburgh. Subsequent, smaller storms deposited more sand onto this land bridge, eventually building it to its current form.

The Quendale area appears to have experienced more regular, small-scale storms. These storms gradually transported sand to the base of a hill, which they could not climb. A series of stronger storms blew these sands up the hill, depositing the majority of the sand on the Broo site and transporting the finer portions to the Loch of Brow. Observed chemical textures on Broo grains suggest that these stronger storms were separated by periods of atmospheric stability, allowing a vegetation layer to form on the surface before another strong storm hit, burying the Broo site with a fresh layer of sand.

Recent OSL dating results from Gerald Bigelow and the Scottish Universities Environmental Research Centre constrain the accumulation of sand at the Broo site to a period between the mid-16th century and the mid-18th century (Kinnaird et al., 2014). 14th century sand was dated below the flagstones of the settlement, but the only significant accumulation to occur during the occupation of the site began in the mid-16th century. The sand used to obtain this date was sampled directly above the flagstones, marking the beginning of the sand blows during occupation. The individual layers observed at the Broo site have not been dated, so constructing an exact chronology of the storm sequences is not possible at the moment. The chemical textures observed in the Broo layers, though, suggest that the two hundred year accumulation period for sand at the Broo site likely involved lengthy periods of relief with few storms capable of blowing sand up to the site.

Archaeological evidence points to an abandonment of the Broo site in the early 18th century. The recently calculated OSL ages agree with this, suggesting a short, intense period of sand accumulation around this time (Kinnaird et al., 2014). The physical evidence from the Broo site supports this intense period. Layers B-1B and B-1A (Figures 34a & b) are not separated by an organic layer and contain grains that are coarser and less well sorted than any other layer. Although there are some differences between these layers, they hint at a period of intense storminess with little, if any, stability separating their deposition. No indication of inhabitation is present in these layers, and a thick organic layer overlies them at the surface. The archaeological, dating, and physical evidence points to a brief, intense storm period in the early 18th century that led to the final abandonment and complete burial of the Broo site.

Regional

The constraining OSL ages place the Shetland coastal change events in the peak of the LIA (Lamb 1985, Lamb 1995). Due to its location, adjacent to the North Atlantic Current at 60°N latitude, Shetland is very susceptible to changes in atmospheric circulation. Lamb (1985) proposed a model for the LIA that involved an increased meridional thermal gradient across the North Atlantic, displacing the polar atmospheric and oceanic fronts

south. This displacement increased the number and severity of storms across the north Atlantic, altering coastal morphology across Europe (Clarke et al. 2002, Dawson et al. 2011, Lamb 1995). The sand invasion events in southern Shetland appear to be an example of this LIA coastal change. While the Bay of Scousburgh and the Loch of Spiggie provide evidence of one or two large-scale storms with significant energy, the Bay of Quendale and Broo archaeological site indicate a prolonged stormy period lasting approximately 200 years. The storm event at the Bay of Scousburgh likely occured during this period, as maps from the 17th century show an inlet connecting the Loch of Spiggie to the ocean (Blaeu 1654). The middle of this period, in the mid 17th century, is marked by a dramatic increase in precipitation in the North Sea (Procter et al. 2000). This window of time may be the peak of storminess in the Shetland Islands, a time when the Broo site was further assaulted with sand and the Spiggie land bridge formed. The timing and severity of the coastal change in the Shetland Islands correlate well with the observed atmospheric changes that occured during the Little Ice Age, indicating a causal relationship.

Conclusion

The results of this study confirm our initial hypotheses. The sand responsible for the formation of the Quendale Links and the burial of the Broo archaeological site appears to have been deposited in stages. These stages consisted of storm events followed by periods of atmospheric stability. These periods of stability lasted long enough for a vegetation layer to form on the surface and impart chemical weathering on the underlying sand. When strong storm events blew sand from the Links up to the Broo site, some of the finer sediments were transported to the Loch of Brow, forming a distinctive sand unit with thin organic horizons that can be observed in cores today. During this stormy period, from the mid-16th to the mid-18th centuries, a large-scale storm appears to have created significant coastal change in the Spiggie area. This storm event likely eroded large volumes of sediment out of nearby till deposits, adding sand to the Bay of Scousburgh. The energy produced by this storm was enough to mobilize the sand in the bay and transport it far inland. This washover appears to have covered an inlet that connected the Loch of Spiggie to the ocean, forming a low-lying land bridge consisting of sand. The washover appears as a sand unit in cores from the Loch of Spiggie. The land-bridge progressively built in size as sand was deposited on its bay-facing shore, eventually building a foredune as the terrestrial sand was mobilized by wind. Evidence of this progressive building can be seen in the pattern of increasing weathering with depth, indicating persistent deposition of fresher grains on the surface of the bridge.

There is a large potential for further research in this study area. In order to better establish the pacing of deposition in the Quendale area, dating studies could be performed on individual sand layers observed at the Broo site. Additional dating studies could be performed on the sand units observed in the Lochs of Spiggie and Brow, in order to better establish their depositional history. The Spiggie land bridge has the potential for a number of further studies, including a continuation of the GPR work done by Joe and Alice Kelly and OSL dating that could further constrain the depositional history of the bridge. Additionally, a heavy mineral separation could be performed on sand from the study area in order to establish a concrete mineralogy at the different sample site.

References Cited

Bigelow, G.F., Ferrante, S.M., Hall, S.T., Kimball, L.M., Proctor, R.E., Remington, S.L., 2005, Researching catastrophic environmental changes on northern coastlines: a geoarchaeological case study from the Shetland Islands: Arctic Anthropology, v. 42 (1), p. 88-102.

Blaeu, W.J., 1654, Orcadum et Shetlandiae Insularum accuratissima descriptio: Blaeu Atlas of Scotland, scale not given, 1 sheet. URL: http://maps.nls.uk/view/00000495 (Accessed March, 2014)

Bondevik, S., Mangerud, J., Dawson, S., Dawson, A., Lohne, O., 2005, Evidence for three North Sea tsunamis at the Shetland Islands between 8000 and 1500 years ago: Quaternary Science Reviews, v. 24, p. 1757-1775.

Brown, G.M., 1984a, Sea bed sediments and quaternary geology: British Geological Survey Sheet 60°N - 02°W, scale 1:250 000, 1 sheet.

Brown, G.M., 1984b, Solid geology: British Geological Survey Sheet 59°50'N - 02°W, scale 1:250 000, 1 Sheet.

Birnie, J., Gordon, J., Bennett, K., Hall, A., 1993, The Quaternary of Shetland: Field Guide: Quaternary Research Association, p. 1-126.

Cook, E.R., D'Arrigo, R.D, 2001, A Well-Verified, Multiproxy Reconstruction of the Winter North Atlantic Oscillation Index since A.D. 1400: Journal of Climate, v. 15, p. 1754 - 1764.

Cook, E.R., D'Arrigo, R.D., Briffa, K.R., 1998, A reconstruction of the North Atlantic Oscillation using tree-ring chronologies from North America and Europe: The Holocene, v. 8 (1), p. 9-17.

Costa, P.J.M., Andrade, C., Mahaney, W.C., Marques da Silva, F., Freire, P., Freitas, M.C., Janardo, C., Oliveira, M.A., Silva, T., Lopes, V., 2013, Aeolian microtextures in silica spheres induced in a wind tunnel experiment: Comparison with aeolian quartz: Geomorphology, v. 180, p. 120-129.

Costa, P.J.M., Andrade, C., Dawson, A.G., Mahaney, W.C., Freitas, M.C., Paris, R., Taborda, R., 2012, Microtextural characteristics of quartz grains transported and deposited by tsunamis and storms: Sedimentary Geology, v. 275, p. 55-69.

Dawson, A.G., Dawson, S., Ritchie, W., 2007, Historical Climatology and Coastal Change Associated with the 'Great Storm' of January 2005, South Uist and Benbecula, Scottish Outer Hebrides: Scottish Geographical Journal, v. 123 (2), p. 135-149.

Dawson, A., Elliott, L., Noone, S., Hickey, K., Holt, T., Wadhams, P., Foster, I., 2004, Historical storminess and climate 'see-saws' in the North Atlantic region: Marine Geology, v. 210, p. 247-259.

Dawson, S., Dawson, A.G., Jordan, J.T., 2011, North Atlantic climate change and Late Holocene windstorm activity in the Outer Hebrides, Scotland: Scottish Archaeological Internet Report 48, p. 25 - 36.

Dawson, S., Smith, D.E., Jordan, J., Dawson, A.G., 2004, Late Holocene coastal sand movements in the Outer Hebrides, N.W. Scotland: Marine Geology, v. 210, p. 281-306.

Dawson, S., Dawson, A.G., Edwards, K.J., 1998, Rapid Holocene relative sea-level changes in Gruinart, Isle of Islay, Scottish Inner Hebrides: The Holocene, v. 8 (2), p. 183-195.

Flinn, D, 1983, Glacial meltwater channels in the northern isles of Shetland: Scottish Journal of Geology, v. 19, n. 3, p. 311-320.

Folk, R.L., 1974, Petrology of sedimentary rocks: Austin, TX, Hemphill Publishing Co. p. 41-52.

Hoppe, G., 1972, Ice Sheets around the Norwegian Sea during the Würm Glaciation: The Norwegian Sea Region: Its Hydrography, Glacial and Biological History, Ambio Special Report n. 2, p. 25-29.

Johnstone, G.S., 1978, Southern Shetland, Drift Edition: Geological Survey of Great Britain (Scotland) Scotland Sheet 126 and parts of 123 & 124, scale 1:63 360, one sheet.

Jordan, J.T., Smith, D.E., Dawson, S., Dawson, A.G., 2010, Holocene relative sea-level changes in Harris, Outer Hebrides, Scotland, UK: Journal of Quaternary Science, v. 25 (2), p. 115-134.

Karpuz, N.K., Jansen, E., 1992, A high-resolution diatom record of the last deglaciation from the SE Norwegian Sea: Documentation of Rapid Climatic Changes: Paleoceanography, v. 7 (4), p. 499-520.

Kenig, K., 2006, Surface microtextures of quartz grains from Vistulian loesses from selected profiles of Poland and some other countries: Quaternary International, v. 152, p. 118-135.

Krinsley, D., Margolis, S., 1968, A study of quartz sand grain surface textures with the scanning electron microscope: Transactions New York Academy of Sciences, p. 457-477.

Lindelof, J.A., 2012, Using Sedimentary and Geochemical Proxies for Little Ice Age Climate Change Reconstructions, South Mainland Shetland, Honors Thesis presented to the Faculty of the Department of Geology, Bates College, unpublished.

Long, A.J., Woodroffe, S.A., Dawson, S., Roberts, D.H., Bryant, C.L., 2009, Late Holocene relative sea level rise and the Neoglacial history of the Greenland ice sheet: Journal of Quaternary Science, v. 24 (4) p. 345-359.

Long, D., Smith, D.E., Dawson, A.G., 1989, A Holocene tsunami deposit in eastern Scotland: Journal of Quaternary Science, v. 4, p. 61-66.

Luterbacher, J., Xoplaki, E., Dietrich, D., Jones, P.D., Davies, T.D., Portis, D., Gonzalez-Rouco, J.F., von Storch, H., Gyalistras, D., Casty, C., Wanner, H., 2002, Extending North Atlantic Oscillation reconstructions back to 1500: Atmospheric Science Letters.

Mahaney, W.C., 1990, Macrofabrics and quartz microstructures confirm glacial origin of Sunnybrook drift in the Lake Ontario basin: Geology, v. 18, p. 145-148.

Marshall, J.R., Bull, P.A., Morgan, R.M., 2012, Energy regimes for aeolian sand grain surface textures: Sedimentary Geology, v. 253, p. 17-24.

McKirdy, Alan, 2010, Orkney and Shetland: A Landscape Fashioned by Geology, Perth, Scottish Natural Heritage.

mindat.org - the mineral and locality database, used for multiple mineral references, URL: http://www.mindat.org/ (Accessed February - March, 2014).

Mykura, W., Flinn, D., May, F., 1976, British Regional Geology: Orkney and Shetland: Edinburgh, Her Majesty's Stationery Office, p. 149.

Narayana, A.C., Mohan, R., Mishra, R., 2010, Morphology and surface textures of quartz grains from freshwater lakes of McLeod Island, Larsemann Hills, East Antarctica: Current Science, v. 99 (10), p. 1420-1424.

Peach, B.N., Horne, J., 1879, The Old Red Sandstone of Shetland: read before the Royal Physical Society

Proctor, C.J., Baker, A., Barnes, W.L., Gilmour, M.A., 2000, A thousand year speleothem proxy record of North Atlantic

climate from Scotland: Climate Dynamics, v. 16, p. 815-820.

Ross, E.R., 2000, X-ray diffraction basics: Crain's Petrophysical Handbook, http://www.spec2000.net/09-xrd.htm

Sorrell, L., 2013, Investigation of Historic Coastal Sand Inundation, Shetland UK, Master's Thesis, University of Maine, unpublished.

Surge, D., Barrett, J.H., 2012, Marine climatic seasonality during medieval times (10th to 12th centuries) based on isotopic records in Viking Age shells from Orkney, Scotland: Palaeogeography, Palaeoclimatology, Palaeoecology, v. 350-352, p. 236-246.

Tisdall, E.W., McCulloch, R.D., Sanderson, D., Simpson, I.A., Woodward, N.L., 2013, Living with sand: A record of landscape change and storminess during the Bronze and Iron Ages Orkney, Scotland: To appear in Quaternary International.